Kwame Nkrumah University of Science and Technology, Kumasi

COLLEGE OF SCIENCE

DEPARTMENT OF PHYSICS

INTEGRATED GEOPHYSICAL CHARACTERIZATION OF MUNICIPAL SOLID WASTE DISPOSAL SITES IN THE KUMASI METROPOLIS

BY

DAVID DOTSE WEMEGAH

JUNE, 2015

INTEGRATED GEOPHYSICAL CHARACTERIZATION OF MUNICIPAL SOLID WASTE DISPOSAL SITES IN THE KUMASI METROPOLIS

By
David Dotse Wemegah
B.Sc. Geology and Physics (Combined Major), M.Sc. (Geophysics)

A Thesis Submitted to the Department of Physics, Kwame Nkrumah University of Science and Technology in partial fulfilment of the requirements for the award of the degree

of

DOCTOR OF PHILOSOPHY
(Geophysics)

College of Science

June 2015

DECLARATION

I hereby declare that this submission is my own work towards the award of the Ph.D and that, to the best of my knowledge, it contains no material previously published by another person or material which has been accepted for the award of any other degree of the university, except where due acknowledgement has been made in the text.

David Dotse Wemegah	....	....
(Student)	Signature	Date

Certified by:

Prof. Aboagye Menyeh	....	....
(Supervisor)	Signature	Date

Prof. Sylvester Kojo Danuor	....	....
(Supervisor/	Signature	Date

Head of Department)

ACKNOWLEDGEMENT

I am so much grateful and thankful to God for how far he has brought me. I wish to express my sincere thanks to my local supervisors Prof. Aboagye Menyeh and Prof. Sylvester Kojo Danuor, the head of Physics Department, Kwame Nkrumah University of Science and Technology, for their support toward the successful completion of this work. To all my colleagues in the department, especially Dr. Leonard Kofitse Amekudzi and Dr. Kwasi Preko, I appreciate all the encouragement you gave me throughout the period of this work.

I am highly indebted to my Danish supervisor Prof. Esben Auken for the opportunity given me to join his research term, the Hydrogeophysics Group at the Department of Geoscience, Aarhus University to carry out this research. I acknowledge Prof. Gianluca Fiandaca for his support of taking me through the principles of spectral induced polarization, lesson on data collection and the use of his DCIP code for inverting the IP data. Gianluca the long times we spent in the office trying to make sense out of the data will always be remembered. To all the staffs at the HGG, the deputy head Prof. Anders Vest Christensen, the project secretary Karen Engell Dalsgaard, the computer programmers and all the students in the group especially my Indian friend Pradip Kurma Maurya, I am so grateful for your friendship and companionship during my period of stay in Aarhus.

I wish to thank the field crew that helped me during the period of the data collection, especially Daniel Manu-Marfo, Benjamin Boadi and Abubakar Sadick Dauda. I am also grateful to Takyi Kyeremah, the head of Newmont Ghana Gold Limited, Geophysics, for giving me their Geometrix Magnetometer for this research.

I am also grateful to DANIDA for giving me the opportunity to pursue this programme under the Building Stronger University (BSU) scholarship. To the BSU KNUST steering committee, I appreciate all the effort and support you have given to the BSU 1 group to make sure we finish the programme on time.

Finally, I wish to thank my wife for being there for me during the difficult times in this work. Too my children Sena and Selorm who always asked if I am working anytime they call me and their little sister Senyo, I love you. I am also grateful to my siblings Samuel, Vincent, Grace and Kenneth and my mother Patience for their inspiration and moral support.

ABSTRACT

Full wave spectral time-domain induced polarization, magnetic susceptibility and ground base magnetic datasets were acquired to map and characterize both engineered (Dompoase Landfill) and unengineered (Ohwim and Kwame Nkrumah University of Science and Technology municipal solid waste disposal sites) located in the Kumasi Metropolis. These geophysical datasets were selectively applied and integrated to help in full characterization of the waste disposal sites in terms of waste thickness, pollution plume mapping and the geological model development of the sites. In addition, a total of six boreholes were drilled around the sites to help in correlating the observed geophysical signatures with the waste thickness and the lithostratigraphic sequence in order to help in interpretation and characterization of the sites. The study was carried out with the aim of determining the risk posed by the waste deposit to the quality of soil and the groundwater system which is now becoming the main means of potable water supply in the metropolis due to the erratic supply supply and the inability of the Ghana Water Company (GWC) to supply water especially to new developing settlements in the metropolis. The intrinsic Cole-Cole IP parameters such as chargeability, resistivity and relaxation time as well as the normalized chargeability distributions, together with the magnetic results, aided in a full characterization of the wastes (vertical and lateral distribution), associated pollution plumes and for developing the geological model of the sites. The KNUST site was characterized using Cole-Cole parameters namely resistivity and chargeability as well as normalised chargeability and magnetic datasets. In particular, a clear contrast in resistivity and polarization effect between the saprolite layer and the granite bedrock, the main lithological units of the area aided in the development of a geological model of the site. Furthermore, it was found that the KNUST waste deposit is characterized by a low-chargeability and low-resistivity signature, and that the low-resistivity area spreads out from the waste deposit into the permeable saprolite layer, indicating the presence of a leachate plume which was mapped to be in the range of 5 to 30 m thick. A mapped fracture zone within the granitic bedrock linked to the pollution plume with the potential of aiding in leachate percolation of groundwater by serving as a conduit for infiltration of the leachate was also mapped. Similarly, the Ohwim Waste Disposal Site was mapped with the magnetic, magnetic susceptibility and full wave spectral time-domain induced polarization. These methods helped in determining the waste thickness and the extent of the pollution plume as well as the geological model of the site. The waste recorded high magnetic anomaly, low resistivity and high normalized chargeability. The geological model of the site was developed by using the strong chargeability signature it produced. Furthermore, the Dompoase Landfill survey which was planned mainly to determine and monitor possible pollution plume around the waste, produced some intriguing result. The magnetic and the magnetic susceptibility results aided in the full mapping of the lateral extent of the waste as well as the channel of the released effluent from the treatment sewage pond, showing the high ferromagnetic iron content of the leachate. The strong IP effect in terms of chargeability and normalized chargeability as well as the low resistivity signature associated with the plume helped in mapping the plume around the catchment area of the waste. The controlled nature of the waste disposal at the Dompoase landfill makes it a possible resource for the production of natural gas. The research provides a cost effective means of monitoring and characterizing municipal solid waste site in the Kumasi Metropolis. It provides a full outline of the solid waste disposal sites investigated and also provides the information needed for assessing the future impact of the waste on the water quality in the area, and the need for designing risk-mitigation actions in these sites. The impact of waste disposal sites on the quality of the environment as shown by this work calls for a review of national policy in the waste site management with focus on reduction of the impact of the waste on the ecosystem.

TABLE OF CONTENT

CONTENT **PAGE**

LIST OF TABLES

TABLE **PAGE**

LIST OF FIGURES

FIGURES **PAGES**

LIST OF ACRONYMS

WMD-KMA	Waste Management Department of Kumasi Metropolitan Authority
NESP	National Environmental Sanitation Policy
EDL	Electrical double layer
IP	Induced polarization
DCIP	Direct current induced polarization
TDIP	Time domain induced polarization
K	Geometrical factor
∇V	Potential difference
I	Current
t	Time
V	Potential
V_0	DC potential
FE	Frequency effect
PFE	Percentage frequency effect
MF	Metal factor
ρ^*	Complex electrical resistivity
σ^*	Complex electrical conductivity

ω	Frequency,
$\sigma\,'$	Real component and
σ''	Imaginary component of the conductivity
σ'_{bulk}	Complex bulk electrical conductivity
σ'_{surf}	Complex surface electrical conductivity
m0	Chargeability
NM	Normalized Normalized Chargeability
ρ	Resistivity
ρ_a	Apparent resistivity
τ	Relaxation time
C	Frequency factor
ξ	Complex resistivity
χ	Magnetic susceptibility
κ	Mass specific susceptibility
A(x, y, z)	Analytical Signal derivative in *x*, *y* and *z* directions
RTP	Reduction to the pole
θ	Wave number direction
H	Ambient magnetic field strength
I	Magnetic inclination
D	Magnetic declination.
GPS	Global positioning system
TMI	Total magnetic intensity
UTM	Universal Transvers Mercator
WGS	World Geodetic System
GRF	Geomagnetic Reference Field

CHAPTER 1: INTRODUCTION

1.1 Introduction

Environmental pollution caused by municipal solid waste disposal sites is of major concern to both environmental scientists and the citizenry. These waste disposal sites inevitably generate pollutants that reach the surroundings, such as soil, groundwater resources, and even the ambient air. This is caused by the environmentally unacceptable disposal of solid waste and improper maintenance of these sites such as the non-usage of impermeable lining systems to prevent the infiltration of the leachate into the ground. This poses a serious pollution threat to groundwater, downstream surface water and soil leading to an adverse impact on the environment, public health and property (Wemegah *et al*., 2014). The problem caused by municipal solid waste can be attributed to weak waste management policies.

In many parts of the world, municipal solid waste is disposed in landfills (Morris and Barlaz, 2011), and even though waste management policies have considerably evolved in the last decades (e.g., Butt *et al*., 2008) many landfills worldwide were (and are still) designed without any kind of capture system underneath, leading to percolation through the waste and into the underlying geological layers and aquifer systems (Christensen *et al*., 1993; Kjeldsen *et al*., 1998a; Kjeldsen *et al*., 1998b; Christensen *et al*., 2001; Poulsen, 2002).

Landfills without leachate collection systems thus provide a high risk to the ecosystems and to human health. In the past, this was not considered as much of a problem because of the availability of large unused parcels of land and abundant natural resources such as water. The ever increasing population in the urban areas due to rural-urban migration, especially in the developing worlds, has put pressure on land use, demand for potable water and increase waste generation. There are also cases of redefinition of land use, where areas which were once considered not to be suitable for habitation, such as land used as waste disposal sites, have been occupied by people, disregarding the risk of these sites on public health and livelihood (Wemegah *et al.*, 2014, 2015). The pollutants originating from unengineered landfills pose health risk to the people who are exposed to them and sometimes lead to death. The effects on quality of life caused by the intake of pollutants from industry and domestic wastes have been reported (e.g Dolk and Vrijheid, 2003; Moore *et al*., 2011). These pollutants tend to accumulate in the soil and finally leach into the groundwater system which is becoming the main source of potable water for most communities due to the ever increasing pollution of surface water (Patel *et al*., 2011; Barthiban *et al*., 2012) and drying of surface water due to climate change. These problems are mostly compounded by the improper management of these sites especially in a developing country like Ghana because of lack of capital investment, poor laws and improper enforcement of existing laws.

In order to improve the situation in some of these areas, there is the need to monitor and determine the impact of these sites on the quality of the environment and give the appropriate remedy to the situation at hand. For large areas, it is very expensive to gain information on the landfill characterization using only drillings. Thus, having a fast, cheap and nondestructive mapping technique allowing coverage of the whole area of interest is a huge benefit. Although the mapping of the waste body is a target itself (for instance for the recognition and delineation of buried and forgotten landfills), it is also very relevant to identify eventual pollution plumes and to assess the geology below the waste, in order to detect potential pollution threats.

Landfill leachate is saline, rich in organic matter, and electrically conductive. These make the application of geophysical techniques, and particularly the electrical method, very useful tools for the visualization of landfill impacts in the shallow subsurface. The main competitive advantages of the geophysical methods are that they are minimally-invasive, inexpensive and fast while still providing good resolution at the field scale (Chen *et al*., 2012). Methods such as magnetics, magnetic susceptibility and time spectral induced polarization surveys are particularly well suited for these purposes. In a developing country like Ghana where there is no waste separation before disposal, the municipal waste often contains domestic ferrous materials which produce strong magnetic anomalies that are helpful in delineating the lateral extent of the waste deposit (e.g. Gibson *et al*., 1996; Marchetti *et al*., 2002; Wemegah *et al*., 2014). On the other hand, induced polarization has recently emerged in a variety of environmental applications linked to the characterization of waste sites, ranging from the detection and mapping of contaminants (e.g. Vanhala, 1997; Kemna *et al*., 2004; Sogade *et al*., 2006; Flores Oroszco *et al*., 2011, 2012; Johansson *et al*., 2014), to the geological discrimination (e.g. Schmutz *et al*., 2010; Gazoty *et al*., 2012b) and the landfill delineation (e.g. Carlson *et al*., 2001; Leroux *et al.*, 2010; Gazoty *et al*., 2012a,b; Wemegah *et al*., 2014).

The health risk and the effect on the quality of livelihood caused by municipal solid waste disposal sites calls for comprehensive approach to the assessment of the impact of waste disposal sites on the environment. Most researches in Ghana are based mainly on hydrochemical and geochemical analyses (e.g. Khanal, 2007; Denutsui *et al*., 2012) in determining the level of environmental impact caused by this practice. These analyses depend on samples which are picked from selected location from the sites and may not give a true picture of the overall level of pollution in the areas. This study used the capability of geophysics to determine the environmental threat posed by three municipal solid waste disposal sites in the Kumasi Metropolis. This was done by mapping the waste and its associated pollution plume as well as the lithostratigraphic units of the area. The areas of the site that are at high risk from possible effect of the plume were outlined. Some recommendations were also given to help control some of these sites in order to reduce their impact on the environment.

1.2 Problem Statement

The environment has over the years faced adverse natural and anthropogenic challenges including overpopulation, rapid loss of biodiversity, global warming and waste management. Urban managers in developing countries, in particular, face an enormous array of problems. Some of the most important ones are poor housing, unemployment, land degradation, and waste management with the range of problems requiring immediate attention constantly increasing.

Environmental pollution from solid waste landfilling (SWL) is of major concern in recent times due to the poisonous chemicals or pollutants generated from these sites that end up in the environment. These activities pollute the fragile ecosystems by modifying their quality to such an extent that subsequent use becomes restricted (Beatriz *et al.*, 1998). This can cause adverse impacts on the environment and to public health and property (Wildung and Zachara, 1981).

Increasing the amount of municipal solid waste (MSW) emanating from residential, commercial and industrial areas, together with changing nature of waste over time, have led to the degradation of the quality of the environment especially in urban areas.

Environmentally sound management and increasing difficulty in treating organic waste is of major concern in these cities. Available statistics indicated that the Kumasi Metropolis generates about 1,500 metric tons of solid waste per day with Waste Management Division (WMD) of Kumasi Metropolitan Assembly, the agency responsible for waste management and its partners collecting about 80% of the solid waste generated in the metropolis (Obeng *et al.*, 2009). The rest of the wastes are therefore left uncollected for days or end up in drains and rivers in the communities. The enactment of the pay-as dump policy has greatly improved the waste collection in the municipality in recent times.

The collected wastes are disposed off at landfills, most of which are open and uncontrolled solid waste disposal sites. This is the most common waste disposal system in Ghana. Most of these waste landfills are improperly designed due to their low capital investment, thus allowing for environmental pollution in those areas.

The health risk and the effect on the quality of livelihood due to this practice calls for comprehensive approach to the assessment of the impact of waste disposal sites on the environment. This work therefore adopted integrated geophysical approach in monitoring municipal solid waste disposal sites in the Kumasi Metropolis. This approach is considered suitable because it is non-invasive, cost effective and provides a large amount of data with big area coverage. In addition, this work provides insight into the extent of pollution caused around waste disposal sites in the Kumasi Metropolis and its potential impact on the soil and groundwater quality.

1.3 Objectives

1.3.1 Main Objective

- The research seeks to characterize municipal solid waste disposal sites in the Kumasi Metropolis using integrated geophysical techniques

1.3.2 Specific Objectives

- The project involves two-stage processes:

– Determination of the level of soil pollution around the waste deposit sites.

- Determination of the level and extent of soil and groundwater pollution in the catchment area of the waste disposal site.

1.4 Project Description and Scope of Study

Geophysical methods namely time-domain spectral induced polarization, magnetic and magnetic susceptibility methods were employed in the mapping of the two unengineered municipal solid waste disposal sites and one engineered landfill site located in the Kumasi Metropolis. The research was conducted after full consultation with all stake holders in the waste management in the metropolis as well as the chiefs who are the custodians of the land on which the waste disposal sites are located. The integration of datasets from these geophysical methods aided the full characterization of the municipal solid waste (MSW) disposal sites. Magnetic susceptibility and the analytical signal of the magnetic datasets helped in the mapping of the lateral extent of the waste while the five intrinsic parameters of the spectral time domain induced polarization data obtained by inverting the IP data using the inversion algorithm developed by Fiandaca *et al*. (2013) aided in the development of models of the waste, plume and geological setup of the research sites.

1.5 Literature Review

Geophysical methods have played major role in revealing the various phenomena occurring within the interior of the Earth. These methods employ the physical properties of a medium that distinguishes it from its hosting environment. These properties include variation of pore fluid conductivity of rocks and soil as employed in resistivity and electromagnetic surveys, variation of polarization effect caused by clay, the presence of biofilm within waste produced by microbial activity in the waste as well as pore fluid salinity as employed by induced polarization method. Similarly, the magnetic susceptibility of a medium as employed by the magnetic method depends on the amount of magnetic mineral mainly magnetite content in a rock or the amount of ferrous metal and other high heavy metal (Mg, Nickel etc) composition from household battery cells and car batteries in municipal solid waste. Similarly the variations in the density of the medium are employed in seismic and gravity exploration. Geophysical researchers therefore depend on these phenomena to help distinguish a material of interest from the hosting environment by relying on the property that distinguishes it from the hosting environment for geophysical investigations.

The applications of these methods include mineral exploration (Ferre *et al*., 1999; Sandrin and Elming, 2006), exploration for groundwater (Kirsch *et al.,* 2003; Gyau-Boakye and Dapaah-Siakwan, 2004; Okrah *et al*., 2013) detection of ancient artifacts (Wynn, 1986; Gaffney *et al*., 2002), monitoring and detection of environmental contaminants (Vanhala, 1997; Splajt *et al*., 2003; Yenigula *et al*., 2005; Gazoty *et al*., 2013; Wemegah *et al*., 2014) and geological characterization (Jørgensen *et al*., 2003; Boadi *et al*., 2013, Graham *et al*., 2013; Christiansen *et al*., 2014). All these are possible because of the distinct geophysical signatures that are associated with these phenomena which make it possible for them to be discriminated and mapped from their host formations. Also, the general nondestructive, in situ nature of the geophysical field methods have made them preferable means of revealing the hidden Earth in recent years and leading in the scientific and the industrial applications when it comes to the understanding of the Earth.

Geophysical monitoring of landfill has piked up in recent years due to their reliability and the increase in the awareness of the impact and health risk the landfills pose to mankind. Many researchers employed methods including magnetics (e.g. Marchetti *et al*., 2002; Jordanova *et al*., 2008; Rucker, 2010; Wemegah *et al*., 2014, 2015;), induced polarization (e.g. Sogade *et* *al*., 2006; Flores Orozco *et al*., 2012; Gazoty *et al*., 2012b; Gazoty *et al*., 2013), resistivity (e.g. Zume *et al*., 2006; Dahlin *et al*., 2010), ground conductivity (e.g. Hackworth, 1996; Buselli and Lu, 2001; Pettersson and Nobes, 2003) and ground penetrating radar (e.g. Daniels *et al*., 1995; Splajt *et al*., 2003) for the survey. The results from these surveys were useful in mapping the thickness, lateral extent and the associated plume of the waste as well as developing geological models of the landfills and their catchment area.

The current advances in geophysical tools development, enhancement and inversion software development (e.g. Fiandaca *et al*., 2012; Fiandaca *et al*., 2013) have made time domain spectral induced polarization one of the important methods in landfill studies in recent years. This method is simple and robust when applying standard multi-channel acquisition systems and the approach of dealing with optimized acquisition parameters (Gazoty *et al*., 2013) makes it possible to get reliable data in order to extract the spectral content contained in the TDIP signal.

Wemegah *et al*. (2014, 2015) employed induced polarization method coupled with magnetic survey in mapping and characterizing some municipal solid wastes in the Kumasi Metropolis. In these works the methods aided in the mapping of both the lateral and the vertical extent of the waste. The extent of the associated plume, its flow direction and geological model of the sites were also developed. Vanhala and Peltoniemi (1992) and Atekwana *et al*. (2004b) applied the spectral induced polarization method in hydrocarbon contaminated soil study. The results from these research and others (e.g. Atekwana *et al*., 2004a; Carlson and Mayerle, 2009; Flores Orozco *et al*., 2011) have identified the biofilm production associated with the microbial activities during biodegradation of the waste to be the main cause of the IP effect produced by the contaminant. Angoran *et al*. (1974) and Slater *et al*. (2006) performed laboratory studies of the effect of metal composition in soil on spectral induced polarization and reported that the metal content of the waste plays a role in the IP effect that is associated with it.

The conductivity of the pore fluids of soil plays a great role on the IP effect as used in mapping municipal solid waste landfills. Olorunfemi and Griffiths (1985) and Barker (1990) reported that the IP effect increases proportionally with increasing salinity of medium to a concentration beyond which the IP effect decreased. They also noted that the concentration at which this occurs depends on the type of soil.

The use of the Cole-Cole model in the spectral induced polarization has provided additional advantage in that it provides other parameters (relaxation time and frequency factor) in addition to resistivity and chargeability to help in decision making. One important parameter in this case is the relaxation time. Several researchers have found an inverse relation between the hydraulic conductivity (hence, grain size) and porosity and relaxation time (e.g. Olhoeft, 1985; Vanhala and Peltoneimi, 1992; Vanhala, 1997; Binley *et al*., 2005). Wemegah *et al*. (2014, 2015) used this property in distinguishing between highly porous saprolite weathered soils from highly consolidated granitic bedrock in the development of geological model in a catchment area of a waste disposal site. The integration of the intrinsic Cole-Cole parameters therefore produces a better resolution of induced polarization data.

Similarly, magnetic and magnetic susceptibility surveys have found role in the mapping and monitoring of waste containing ferrous metal. In environmental monitoring, the magnetic susceptibility gives a measure of the amount of the ferrous metal and heavy metal composition in the soil. Adriano (1986) reported that magnetic susceptibility gives a qualitative estimation on the degree of ferrous metal in municipal solid waste. The magnetic susceptibility measurement therefore serves as proxy for determining the heavy metal composition in environmental study. This is because magnetic particles and heavy metals from waste from industrial and domestic processes are produced together and either form separate particles or the former may incorporate the latter into their atomic lattice or absorb them into their surfaces. This genetical relationship between magnetic particles and the heavy metal makes it possible to use magnetic measurements as a proxy for chemical methods in assessing heavy metal loadings in soil (e.g. Hanesch and Scholger, 2002; Schmidt *et al*., 2005; Klučiarová *et al*., 2008; Canbay, 2008, 2010). It has also played a major role in the mapping of municipal solid waste due to its high ferrous metal content (Barrows and Rocchio, 1990; Jordanova *et al*., 2008; Wemegah *et al*., 2014, 2015).

Furthermore, magnetometric surveys detect the surface effects and local disturbances to the Earth's magnetic field that can be caused by buried ferromagnetic objects. The magnetometry therefore is one of the most used methods in environmental monitoring and generally considered to be effective, rapid and precise for the identification of buried ferromagnetic masses (Marchetti, 2000). Tyagi *et al.* (1983) performed a laboratory controlled field tests in which the strength of magnetometry in determining buried drums at various depths were tested. Similarly, Marchetti *et al*. (1998) and Marchetti and Settimi (2011) applied magnetics survey in the identification of buried mass of ferromagnetic material such as buried drums. The application of magnetic survey in the mapping of MSW was also documented. Wemegah *et al*. (2014, 2015) applied the magnetometric survey in the mapping of the lateral extent of municipal solid disposal site in a developing country like Ghana where waste separation is not a practice. Gilkeson *et al*. (1986) describe a magnetic survey of a series of landfill trenches that had been used to dispose off steel drums. In this work distinctive pattern of magnetic highs were found over the trenches and lows over the intertrench corridors. This helped in the identification of the positions and the removal of this drums which posed risk to the quality of the groundwater system. Barrows and Rocchio (1990) reported that surveys involving the use of effective susceptibility in the determination of ferrous metals of a material are limited by demagnetization. In this case, the magnetic field variations associated with the ferrous metal will be due to the configuration (depth of burial and geometry) of the magnetized material rather than its concentration.

1.6 Organization of Thesis

Chapter one gives the general introduction to the work, the aim and scope of work and also pertinent literature review of previous work on the subject. Chapter two looks at the various aspects of the waste management and the existing policies in the Kumasi Metropolis and the country at large. Chapter three discusses the theoretical background of the various geophysical methods employed in this study. Chapter four looks at the study area, its location, climate, vegetation and its general geological setup. Chapter five discusses the various methods and processes employed in the data collection for the work. Chapter six discusses the geophysical result from the KNUST municipal solid waste disposal site and its implication to the environment. Chapter seven discusses the geophysical result from the Ohwim municipal solid waste disposal site and its implication to the environment. Chapter eight discusses the geophysical results from the Dompoase Landfill detailing various polluted areas and its implication to the environment. Finally, chapter nine gives a summary, conclusion and recommendation of the work.

CHAPTER 2: MUNICIPAL SOLID WASTE MANAGEMENT

2.1 Municipal Solid Waste

Municipal solid waste (MSW) is a solid waste produced by households, commercial entities and institutions. Gershman *et al*. (1986) stated that the wastes are highly heterogeneous and are influenced by socio-geographical factors. The managements of MSW have great effect on the quality of the environment. Municipal solid waste management (MSWM) over the years has been undertaken with many drivers worldwide. The major component of MSWM in recent time includes concerns of environmental health protection, human safety, resource conservation and the reduction of, as much as possible, the environmental burdens of waste management (McDougall and Hruska, 2000).

The ever increasing populations in the urban areas due to rural-urban drift had led to increasing waste generation rates. Also changing lifestyles of people, development and consumption of products with materials that are less biodegradable have led to the diverse challenges for MSWM in various cities of the world (Asase *et al*., 2009, Fobil *et al*., 2010). The major problem facing urban city in the developing world is the management of the waste generated leading to city-wide filth and systemic deterioration in urban environmental conditions as well as a general decline in aesthetic beauty of towns. The level of environmental condition also depends on the socio-economic state of people within these communities. Songsore (1992, 1998) on work on the assessment of the environmental problem and health status of Accra indicated that areas that accommodate people with the lowest educational standards and the lowest incomes have the poorest facilities in terms of water, sanitation and housing.

The problem of MSWM systems are mainly common in the developing countries often characterized by inadequate service coverage, operational inefficiencies of services, limited utilization of recycling activities, inadequate management of non-industrial hazardous waste and inadequate landfill disposal (Zurbrügg and Schertenleib, 1998; McDougall and Hruska, 2000). In Ghana the problem of MSWM is attributed mainly to factors such as rapid urbanization, inadequate funds, bad attitudes, negligence, institutional challenges and in some cases corruption (Cofie *et al.,* 2003).

2.2 Waste Management Policies

Generally, waste management in developed countries have strong goal of reducing the impact of the waste on the quality of the environment. The sound environmental management of waste is enforced by most developed countries in recent years (Wilson, 2007) due to the effect it can cause on the quality of livelihood if not well managed. The major components of the sound environmental waste management policies involve utilizing sanitary landfills, waste treatment and processing, energy and material recovery options. One important policy that is in existence today is the United State of America‟s Environmental Protection Agency (EPA) is the Municipal Solid Waste Management Policy enacted in 1989. The main agenda of this policy involves the concept of integrated waste management, in which municipal solid waste is reduced or managed through several different practices, which can be tailored to fit a particular community‟s needs. The hierarchical order of MSWM as contained in this document is (US EPA, 2006):

- source reduction, including reuse of products and on-site composting of yard trimmings,
- recycling, including off-site composting,
- combustion with energy recovery,
- disposal through landfilling or combustion without energy recovery.

Whereas the enacting and enforcement of strong and adequate legislation both from the national and city levels has led to a great success in the waste management in the developed countries, they are non-existent or not well enforced in the developing world. In these countries, waste disposal is uncontrolled and waste treatment, processing, energy and material recovery are rare or non-existence. According to Johannessen and Boyer (1999), the design and optimization of solid waste management technologies and practices that aim at maximizing the yield of valuable products from waste, as well as minimizing the environmental effects are rarely considered in the African region. In areas where some policies were put in place, the enforcement and adherence is poorly done.

If the success made by developed countries is anything to go by as a guide in waste management in developing countries, there is the need for the enactment of a comprehensive national waste management law, backed by the requisite regulatory framework in terms of the bye-laws by Metropolitan Authorities. The success of any such policies needs a great change in attitude of the citizenry and the full enforcement of the laws by the agencies.

2.2.1 Ghana National Environmental Sanitation Policy

General waste management in Ghana is vested in the Ministry of Local Government and Rural Development (MLGRD) which supervises the Metropolitan, Municipal and District Assemblies (MMDAs). The MMDAs are responsible for the collection and disposal of solid waste through their waste management departments (WMDs).

The Ghana National Environmental Sanitation Policy (NESP) was developed in 1999 by the Ministry of Local Government and Rural Development (MLGRD) which is vested with responsibility of creating and coordinating sanitation policy, issuing guidelines on sanitation services and their management, and for supervising the National Environmental Sanitation Policy Coordinating Council (Republic of Ghana, 1999). This was formulated in consultation with a variety of agencies with vested interest in this sector. The sanitation issues targeted in this policy included solid and liquid waste, industrial and hazardous waste, stormwater drainage, environmental and hygiene education, vectors of disease and disposal of the dead (Republic of Ghana, 1999). The policy sought to improve the situation by strengthening the institutional structures and arrangements at the local government levels to improve service coverage and introduce cost recovery. The policy strategy included (MLGRD, 1999):

- formal establishment of environmental sanitation as a sub-sector within the national development programme;
- rationalization of institutional objectives and functions at all levels, including delineation of responsibilities and the establishment of inter-agency linkages;
- development and strengthening of the community‟s role in environmental sanitation;
- development of human resources and strengthening institutional structures for managing environmental sanitation;

- assigning delivery of a major proportion of environmental sanitation services to the private sector through contract, franchise, concession and other arrangements; and
- adoption of cost recovery principle in the planning and management of environmental sanitation services.

The major shift in the waste management practices in the country as included in this policy is the involvement of the private sector with finance coming from the people using the pay-asdump or the house to house collection of waste and the change of the role of the WMD from that of direct service provision to supervision and monitoring of activities of private contractors. Despite this shift, WMD is mandated to provide 20% of the sanitation services. The pay-as–dump policy which is included in this has helped in the cost recovery, as it shifted the cost of collection to the citizenry.

2.3 Waste Generation in the Kumasi Metropolis

The waste generated within Kumasi Metropolis is mainly household waste. It is estimated that households generate the highest amount of waste, followed by markets, then industries with the least from institutions such as schools, hospitals etc. The yearly rate of waste generation in the municipality is estimated to be increasing at 15% (WMD-KMA, 2008). The domestic solid waste generation in the municipality was 600 tons per day in 1995 (Post,
1999), this increased to 1000 tons per day in 2005; and by 2008 it was 1,200 tons a day, and 1,500 metric tons of waste per day in 2010 (WMD-KMA, 2008, 20012). The Subin Submetropolitan area that has a land cover of 8.5 km^2 (the second smallest in the metropolis) is the highest waste generating area in the metropolis. This is attributed mainly to the presence of the largest market, the Kumasi Central Market in the area.

The bulk of the domestic waste generated in the municipality is organic which contributes to about half of the waste collected. The WMD estimates that paper, plastics, metals and rubber constitute about 8% of total household waste (WMD-KMA, 2010). Table 2.1 details the percentage of the various domestic waste fractions generated in the metropolis in 2009.

Table 2.1 Composition of Municipal Solid waste in 2009 (WMD-KMA, 2010).

Material	Percentage of Municipal Solid Waste
Biodegradable	47%
Paper	3.1%
Plastic	3.5%
Glass	0.6%
Metal	0.6%
Inert, ash, debris	44.6%
Total	100%

The high proportion of organic waste generated makes the use of compositing as a means of reducing the volume of waste deposited in landfill in the municipality and the country at large a possibility. This can help increase the lifespan of most of these landfills thereby reducing the hassle of locating land for creating new landfill as there is scarcity of land for waste disposal within the country in recent times.

The major industrial waste in the municipality is generated by Guinness Ghana Bottling Company, Coca Cola Bottling Company, the Kumasi Abattoir which generate about 1,510 m^3 of effluent daily (KMA and MLGRD, 2006) and the Cudbury Cocoa Processing Company. Other enterprises such as automobile repairers in the various parts of the metropolis generate various quantities of waste although this has greatly improved in recent times due to the processing of ferrous metals in the country. Sawmills also generate significant amount of waste (Fobil *et al*., 2010).

2.4 Waste Collection and Management in the Kumasi Metropolis

Before the enactment of the NESP in 1999, sanitation services were provided by the Waste Management Department (WMD) of the Kumasi Metropolitan Authority (KMA). In this arrangement the WMD supervises the design and construction of public sanitation facilities, collect waste in the metropolis with the help of private companies sub-contracted to collect household waste in which the department has supervisory responsibility (Ketibuah *et al.*, 2005). The financing of the activities of the department was borne by the KMA (Vodounhessi, 2006) which was not adequate as the department had no financial autonomy making it difficult for the department to fully function. The key constraint in the provision of improvement on environmental sanitation in the metropolis was therefore attributed to the weak institutional structures and lack of financial resources.

Attempt to address some of these weaknesses in the municipal solid waste management (MSWM) system of the country led to the enactment of the NESP 1999 which has cost recovery as one of its major objectives. This was based on the pay-as-you-dump scheme and housing-to-house waste collection schemes using private public partnership (Post, 1999; Obeng *et al*., 2009). Awortwi (2004) noted that this policy has greatly improved waste collection and sanitation in the metropolis.

In order to fulfil the cost recovery in the municipal solid waste management as contained in the NESP (199) pay-as-you-dump policy was introduced. In this system the collection of the waste and its management in the metropolis is based on two systems. These are the house-tohouse (curbside) solid waste collection and communal solid waste collection. The communal collection system (pay-as-you-dump) involves the location of metal containers (skips) at designated sites known as transfer stations, which are shared by a number of houses within that community. The communal waste collection system consists of 124 containers placed throughout the metropolis. The households participated in the communal collection system by paying between GH¢ 0.2 to GH¢ 0.5 per load. Generally, poor households depend on this means of service. The full skips are transported and emptied at the final disposal site by skip loading trucks (WMD-KMA, 2010; Asare *et al*., 2009) who were paid an amount GH¢ 100 by the one in charge of the stations. The major private service providers in the municipality are the Zoomlion Waste Geoup, Freko FD Limited, Asadu Royal Waste and J Owusu Stanley Waste Management Ltd who also double as the manager of the Dompoase Landfill.

The house-to-house collection is based on a monthly payment by the households to a private waste collector who picks up the waste twice a week (WMD-KMA, 2010; Obeng *et al.,* 2009). Obeng *et al.* (2009) have stated that patronage of the house-to-house collection services has increased from 2.1% of the population in 1999 to 20.8 per March 2004. It was also observed that, between 2001 and 2004, the amount recovered through house-to-house collection services by private operators increased from 26.5 per cent of the WMD‟s expenditure to 68.6 per cent. The growth of house-to-house collection services therefore implies the growth and the success of cost recovery within the metropolis (Obeng *et al.,*
2009).

In order to meet the 20% of sanitation service provision as stipulated in the National Environmental Sanitation Policy (NESP), the WMD provides communal waste collection service in some communities in the metropolis (Obeng *et al*., 2009; WMD-KMA, 2010). In this system the WMD lifts the waste in these communities and uses the money generated as part of its internally generated funds to help service their truck and other administrative expenditures. Despite the success chalked in this regard, waste collection in the metropolis the recent years increase between 40 to 50% in the price of the lifting cost in the house-tohouse collection is affecting this gain. Most households in the low income groups are withdrawing from the use of this service as they see it to be too expensive to continue.

2.4.1 Waste Treatment and Disposal

Although most household waste generated in the metropolis is organic, recycling and composting are not widely practiced. Some residents and a few enterprises salvage such materials as plastic bottles, metals and bags, and some people re-use items like plastic bottles to store different types of liquids, but recycling is still not officially part of solid waste disposal management. Recycling clearly needs to be given heightened consideration as a means of reducing the volume of waste sent to the landfill.

2.4.1.1 Landfill

Municipal waste sanitary landfill is a method of disposing of refuse on land without creating hazards to public health where harm to the environment is prevented, and through restoration of land used for that purpose (Bagchi, 1994). This is done by confining the waste to the smallest practical area using engineering, to reduce it to the smallest practical volume, and covering it with a layer of soil at such frequent intervals as may be necessary (Zanoni, 1972). The landfills have the aim of preventing environmental impact from the waste. The landfill can either be a hole in the ground, or built on the surface of the ground. The design of the landfill includes containment of leachate and gas, daily cover for the working surface, run-off and run-on diversions to decrease potential surface and groundwater pollution. It is composed of two separate segments: 1) synthetic foundation protective layer which helps to prevent the infiltration of the effluent into the groundwater system and 2) drainage layer which helps in the collection of the leachate from the waste deposit. Furthermore, the necessary measuring setups are put in place to monitor any possible pollution from the site (Williams, 2005). Despite these measures landfills continue to pose threat to the quality of environment and livelihood. The environmental impact of the landfill leakage, particularly on groundwater quality, has been reported regardless of an ideal site selection and a monitoring network design (e.g. Mikac *et al*., 1998; Riediker *et al*., 2000; Yenigül *et al*., 2005).

2.4.1.2 Dompoase Landfill

The main site for the disposal of collected solid waste in the Kumasi Metropolis is the Dompoase Sanitary Landfill. The sanitary landfill is constructed on a hundred acre land which became operational in 2004. The operation of the landfill is done by J Stanly Waste Management Limited with supervision of KMA-MWD. The landfill treats both solid waste and sewage (WMD-KMA, 2008) mainly from domestic septic tanks. The government bears 95% of the landfill management cost. Post (1999) estimated that prior to the construction of the landfill two-thirds of residential waste was disposed in open lots or on the banks of natural streams. Uncollected waste was routinely dumped in open spaces, in drains or was burned. The enactment of good environment policies in the metropolis has seen the collection of over 90% of waste from the municipality which ends up on the landfill site.

CHAPTER 3: THEORETICAL BACKGROUND

3.1 Electrical Resistivity

The electrical resistivity of a material is a measure of how well the material retards the flow of electrical current through it. Properties that affect the resistivity of a soil or rock include porosity, water content, composition (clay mineral and metal content), salinity of the pore water, and grain size distribution. For instance clayey material is characterized by a low resistivity, because water can diffuse between the mineral grains and thereby increase the specific surface area, which supports the surface conductivity (Kirsch, 2006). Resistivity varies tremendously from one material to another. For example, the resistivity of a good conductor such as copper is in the order of 10^{-8} Ωm, the resistivity of an intermediate conductor such as wet topsoil is approximately 10 Ωm, and the resistivity of poor conductors such as sandstone is approximately 10^{8} Ωm (Herman, 2001). The electrical resistivity method can therefore be used for detecting and distinguishing between subsurface materials. The capability of the method in mapping different soil types is dependent on the electrical contrast of the soil and their heterogeneity. Hence the electrical resistivity of the soil can be considered as a proxy for the variability of soil physical properties (Banton *et al*., 1997).

3.1.1 Basic Theory

In general, the electrical resistivity survey method involves two current electrodes, A (source) and B (sink) for ejecting current into the ground and two potential electrodes for measuring the potential difference points (M and N). The surveying is based on the principle that the distribution of electrical potential in the ground around a current-carrying electrode depends on the electrical resistivity and distribution of the surrounding soils and rocks. The apparent resistivity of the ground is computed from this set of arrangement. The current pattern and equipotential surfaces for a homogenous and isotropic ground is shown in Figure 3. 1.

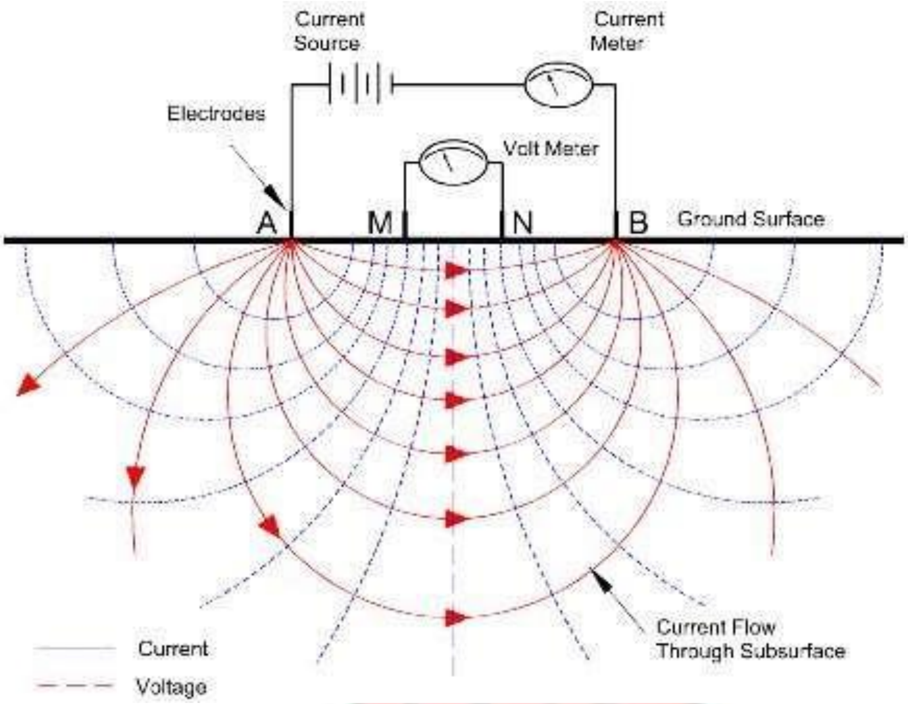

Figure 3. 1 Electrical current and potential field in a homogenous ground, A and B are current electrodes and M and N potential electrodes.

The measured potential due to such arrangement is given by:

$$\nabla V = \frac{\rho I}{2\pi}\left(\frac{1}{|AM|} - \frac{1}{|BM|} - \frac{1}{|AN|} + \frac{1}{|BN|}\right) \quad (1)$$

where $|AM|$, $|BM|$, $|AN|$ and $|BN|$ denote the distances between current and potential electrodes, ∇V the measured potential difference and I the injected current. The apparent resistivity (ρ_a) of such system is computed as:

$$\rho_a = \frac{\nabla V}{I} 2\pi \left(\frac{1}{|AM|} - \frac{1}{|BM|} - \frac{1}{|AN|} + \frac{1}{|BN|}\right)^{-1} = \frac{\nabla V}{I} K \quad (2)$$

where K is the geometrical factor, which depends on the geometry of the chosen electrode configuration.

3.2 Induced Polarization (IP)

Induced polarization response is the degree to which the subsurface is able to store electrical charge attributed to the presence of interfaces at which local charge concentration gradients result in a delayed voltage response in Earth materials upon current stimulation (Schön, 1996). The polarization is caused by the movement of free and bound ions in the neighbourhood of the interface between the ionic solution and the solid conductive or ionexchange-competent (clay and some organic material, biofilm) particles. The composition of the medium (rock) and defects in the crystal structure of the composing minerals are the factors controlling the IP effect.

3.2.1 Origins of Induced Polarization (IP) response

The IP response is mainly due to the surface phenomenon that occurs in the interface between two media of different conductivity leading to a charge buildup on the surfaces of these media. This effect is a function of the lithology, nature and structure of the pores, liquid saturation level of the rock and pore fluid properties (salinity, and state of ions in the fluid). The mechanisms that give rise to IP effect include electrical double layer, membrane polarization, electrode polarization, pore necking and pore fluid salinity (Renolds, 1997; Vanhala, 1997; Sogade *et al*. 2006; Kemna *et al*., 2012).

3.2.1.1 Electrical Double Layer (EDL)

Electrical double layer is formed when defects in the crystalline structure of mineral grains leads to the accumulation of charges on the surfaces of these particles. The charged particle surfaces attract charges of opposite polarity to form a diffuse layer next to the fixed layer forming the electrical double layer (EDL). In rock formation the EDL is formed at the boundary between the mineral particles (solid phase) and the pore water (liquid phase). The negatively charged surface of the rock attracts cations from the electrolyte to form electrical double layer

(Figure 3.2). According to Sogade *et al*. (2006) the double layer presents capacitive impedance to current passage across the solid interface. The property that controls the IP effect in such a medium is the cation exchange capacity which is a function of the product of the surface charge density and the specific surface area of the solid phase (Bolt and Bruggenwert, 1978; Olhoeft, 1985; Vanhala, 1997; Sogade *et al*., 2006). Thus the polarization effect is associated with the electrochemical charge migration and accumulation in the electrical double layer at the mineral–fluid interface of soils and rocks (Weller *et al*., 2010; Kemna *et al*., 2012).

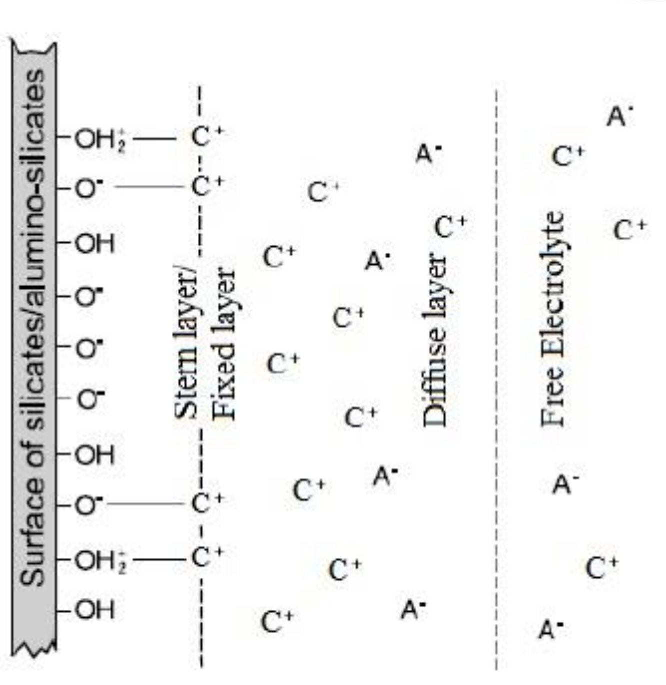

Figure 3.2 Sketch of electrical double layer model (Modified from Leroy and Revil, 2009).

When an external electric field is applied to such a medium there is a displacement of the charge buildup along the double layer as shown in Figure 3.3. The redistribution of the charges back to the EDL state is what is observed as the decaying potential in the medium in the absence of the external field.

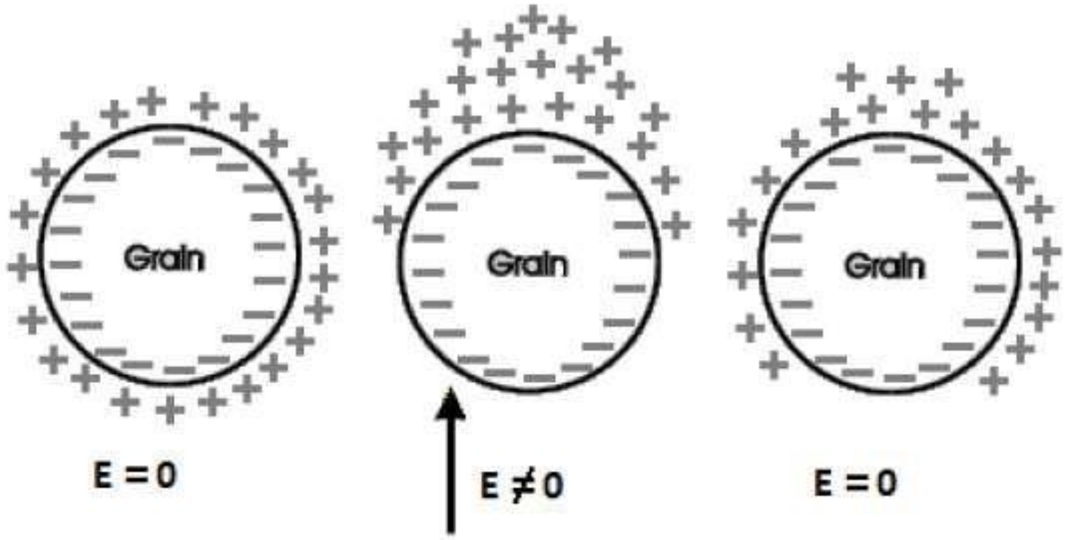

Figure 3.3 Polarization effect on EDL as observed on a grain fluid interface.

3.2.1.2 Membrane Polarization

Membrane polarization is caused by the accumulation of anions at clay blockages that form at pore throats. It is as a result of the interface impedance that results when the diffuse layer in some portion of a normal conducting pore path block the path, thereby selectively allowing the passage of ions of certain size and polarity, reducing the mobility of charge carriers and causing charge buildup (Sogade *et al*., 2006). Reynolds (1997) suggests that membrane polarization is attributable to the constriction of the pores due to the presence of clay and clay coated sand grains with high specific surface area (Figure 3.4). It occurs due to the difference between the ion transport numbers in large and narrow pores (Marshall and Madden, 1959; Vinegar and Waxman, 1984). The distribution of the fine grains/clay affects the constriction of the pore channels which block movement of ions upon application of voltage. In this case, negative ions will tend to leave the constricted zone while positive ions will increase their concentration causing a development of a potential difference across the blocked path resulting in electrical polarization (Boadu and Seabrook, 2000). The IP effect in such a medium is determined by the ratio of the cation-to-anion mobility through the clay membrane (Marshall and Madden, 1959).

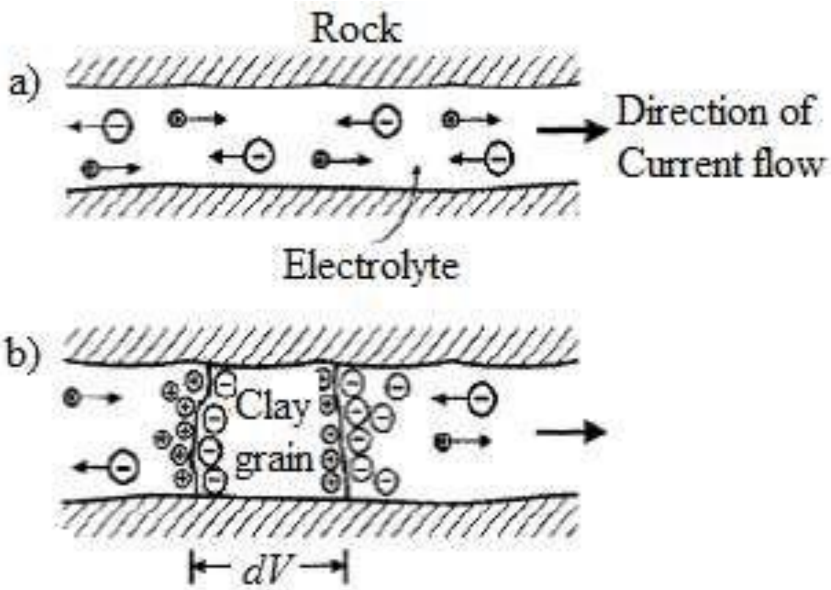

Figure 3.4 Schematic diagram of membrane polarization a) electrolyte with free flow ions b) block of the flow path in the pore of rock by a clay grain (After Renolds, 1997).

3.2.1.3 Electrode polarization

Electrode polarization is the result of the interface impedance that results when electronically conductive grain, blocks a channel in a pore or a small fracture. The mode of current conduction changes from ionic to metallic at the mineral electrolyte interface (Figure 3.5), and current is carried across the interface either capacitively via the double layer or by charge-transfer reactions (Dias, 2000).

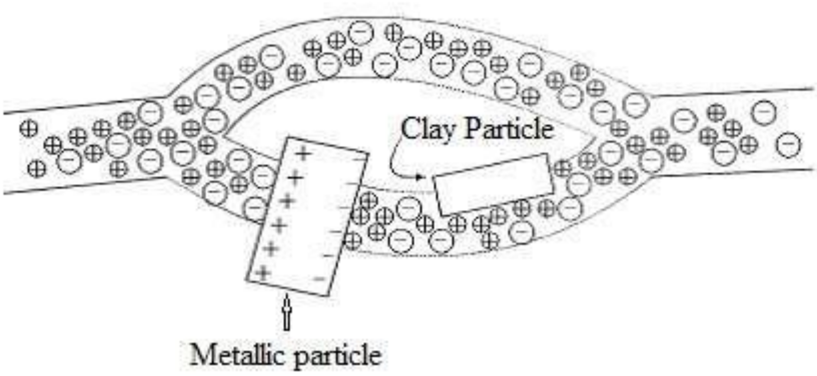

Figure 3.5 Schematic diagram of rock electrical polarization (After Dias, 2000).

3.2.1.4 Pore fluid salinity

The ionic concentration of the pore fluid has effect on the distribution of the grains surface hence, affects induced polarization. The polarization effect increases directly with increasing pore fluid salinity till the concentration reach a value beyond which the effect is reduced (Olorunfemi and Griffiths, 1985; Barker, 1990). This is caused by a decrease in the thickness of the electrical double layer with increasing salinity, since the ion concentration in the free electrolyte is higher and thus the ions are not at the disposal for the electrical double layer. The concentration at which the decrease occurs is a function of the rock type and structure of the connected pore (Buselli and Lu, 2001).

3.2.2 Basic Induced polarization theory

The IP effect manifests itself as a residual voltage following termination of an applied current or as a frequency-dependent resistivity. Induced polarisation measurements are therefore performed either in the time domain, frequency domain or complex resistivity.

3.2.2.1 Time Domain IP

The time domain IP (TDIP) method measures the residual voltage decay induced in the Earth material when an external applied field is turned-off after a time interval of application. A measure of the magnitude of the IP effect in the time domain is the chargeability, M (e.g., Schön, 1996) which determines the magnitude of the polarization storage relative to the conduction loss (Keller, 1959; Lesmes and Frye, 2001). When the current is turned off, the voltage drops to a secondary level, V_s, and then decays with time during the relaxation period. This decay curve is the target of the time domain IP method, because it is characteristic of the medium in terms of initial magnitude, slope and relaxation time (Figure 3.6). The signal $V(t)$ along the decay is usually integrated over number of time windows or gates, for the computation of the chargeability M, which is expressed as (Schön, 1996; Slater and Lesmes, 2002):

$$M = \frac{V_s}{V_0} = \frac{1}{V_0[t_{i+1} - t_i]} \int_{t_i}^{t_{i+1}} V(t)dt \qquad (3)$$

The potential $V(t)$ is integrated in the time window $[t_i, t_{i+1}]$, then divided by the duration of the window and by the DC potential V_0, which is the measured voltage at the time of application of the current. The schematic diagram of the induced polarization decay curve is shown in Figure 3.6. The unit of chargeability is millivolts per volt (mV/V).

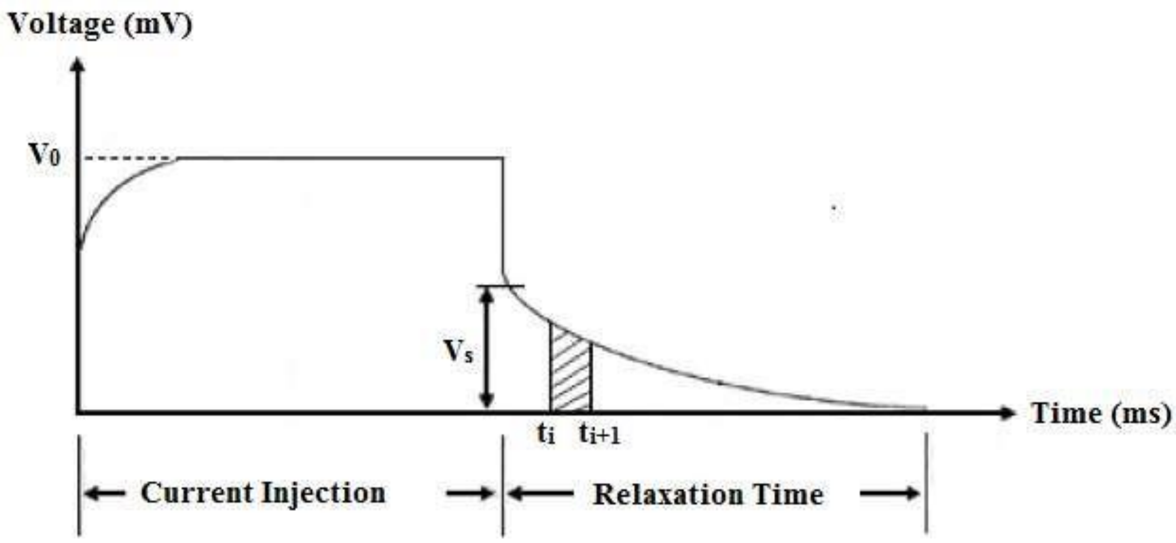

Figure 3.6 Schematic diagram of the induced polarization phenomena.

3.2.2.2 Frequency-Domain IP

The frequency domain IP is determined based on the resistivity response of a medium at two different frequencies. The IP effect is computed in terms of frequency factor or percentage frequency factor and metal factor (Telford *et al*., 1990).

Frequency effect (*FE*) is defined as

$$FE = \frac{(\rho_{dc} - \rho_{ac})}{\rho_{ac}} = \frac{\rho_{dc}}{\rho_{ac}} - 1 \qquad (4)$$

where ρ_{dc} and ρ_{ac} are apparent resistivities measured at dc and very high frequency. This phenomenon is also expressed as percentage frequency effect (*PFE*) (Telford *et al*., 1990; Slater and Lesmes, 2002).

$$PFE = \frac{(\rho_{dc} - \rho_{ac})}{\rho_{ac}} x100\% \qquad (5)$$

The metal factor (*MF*) which was suggested by Marshall and Madden (1959) is a pore fluid resistivity normalization of the frequency domain IP parameter. It is given as (Telford *et al*., 1990; Lesmes and Fry, 2001):

$$MF = 2\pi x10^5 \frac{(\rho_{dc} - \rho_{ac})}{\rho_{ac}\rho_{dc}} = 2\pi x10^5 \frac{FE}{\rho_{dc}} \qquad (6)$$

3.2.2.3 Complex Resistivity

In complex resistivity measurement the phase shift between injected current and voltage drop is used to quantify the polarization effect. The phase shift is a property of the material. The IP effect in this case is described in terms of complex electrical resistivity, ρ*, or complex electrical conductivity, σ*.

$$\sigma^*(\omega) = \frac{1}{\rho^*(\omega)} = \sigma'(\omega) + i\sigma''(\omega) \quad (7)$$

where ω is the frequency.

The investigation of complex conductivity dependence on ω is often referred to as spectral induced polarization (SIP). The measurements are usually recorded as conductivity ($|\sigma|$) or resistivity ($|\rho|$) magnitude and a phase angle, υ, both being related to the conduction and storage mechanisms:

$$|\sigma| = \frac{1}{|\rho|} = \sqrt{\sigma'^2 + \sigma''^2} \quad (8)$$

$$\varphi = tan^{-1}\left(\frac{\sigma''}{\sigma'}\right) \quad (9)$$

For small phase angles, which are typically observed in nonmetallic environments, the phase is equal to the ratio of the imaginary conductivity (σ'') to the real conductivity (σ') (Slater and Lesmes, 2002) expressed as φ:

$$\varphi = tan^{-1}\left(\frac{\sigma''}{\sigma'}\right) \cong \left(\frac{\sigma''}{\sigma'}\right) \quad (10)$$

The conductivity depends on intrinsic properties of the sample or the medium. The lowfrequency capacitive properties of a sample depend on the electrochemical surface phase, whereas the low-frequency conductive properties of the sample depend on the bulk conduction and surface conduction mechanisms.

Pelton *et al*. (1978) defined the chargeability in terms of the bulk conductivity (σ'_{bulk}) and a surface conductivity (σ'_{surf}). If the bulk conductivity is much greater than the surface conductivity, the chargeability is proportional to the ratio of the surface conductivity to the bulk conductivity effects:

$$M \propto \frac{\sigma'_{surf}}{\sigma'_{bulk} + \sigma'_{surf}} \cong \frac{\sigma'_{surf}}{\sigma'_{bulk}} \quad (11)$$

3.2.3 Normalized Chargeability (*NM*)

The concept of normalized IP which is directly related to the complex surface conductivity parameter $\sigma'_{surf}(\omega)$ of the Earth material was proposed by Keller (1959). The normalized chargeability is a parameter that quantifies the magnitude of surface polarization. It is a property of the surface conductance of the soil (Slater and Lesmes, 2002; Danhlin *et al*., 2010) rather than the pore fluid. The normalization of the chargeability helps to isolate the surface conductivity effects especially at high solution conductivity. The normalized chargeability is independent of the bulk conduction effects and is much more sensitive to the surface chemical properties of the material (Lesmes and Frye, 2001). The normalized chargeability (*MN*) is defined as the ratio of the chargeability to the magnitude of the resistivity:

$$MN = \frac{M}{\rho_a} = \sigma M \quad (12)$$

The normalized chargeability is related to the surface chemical properties and very sensitive to changes in geochemical and microstructural parameters. It is therefore more effective for characterizing geochemical and lithological variability (Lesmes and Frye, 2001).

3.3 Inversion Theory

The full IP decay data were inverted using the 2-D DC/IP inversion algorithm developed by Fiandaca *et al*. (2013) and incorporated into the Aarhus Workbench and its inversion kernel AarhusInv (Auken *et al*., 2014) to get the spectral content of the decay. The inversion code takes into account the current waveform and filter characteristic of the instrument in the forward computations, allowing for a quantitative interpretation of the IP parameters (Fiandaca *et al*., 2012). This gives access to the spectral information contained in the IP decays, retrieved in terms of the Cole-Cole model (Pelton *et al*., 1978; Cole and Cole, 1941).

The inversion Cole-Cole parameters including direct current (DC) resistivity (ρ), chargeability (m_0), the relaxation time (τ) and the frequency factor (C) were based on the complex resistivity (ξ) equation:

$$\xi(\omega) = \rho\left[1 - m_0\left(1 - \frac{1}{1 + (i\omega\tau)^C}\right)\right] \tag{13}$$

where ω is the frequency and *i* is the imaginary unit.

The parameters describe different physical properties of the subsurface, m_0 describes the magnitude of the polarization effect and τ indicating in the frequency domain, the position of the phase peak (Gazoty *et al*., 2013). Pelton *et al*. (1978) and Luo and Zhang (1998) showed that m_0 and τ depend on the quantity of polarizable elements and their size, respectively.

Binley *et al*. (2005) observed a strong inverse correlation between τ and pore throat size as well as the surface area to pore volume ratio. It can therefore serve as means of distinguishing lithological units based on their hydraulic properties. The *C* on the other hand depends on the size distribution of the polarizable elements (Vanhala, 1997; Luo and Zhang, 1998).

3.4 Electrode Array

The electrode array employed for this survey is the gradient array. Gradient array is an electrode configuration especially designed for multi-channel acquisition, which means that many data points can be measured concurrently for each current injection. The fieldwork time is thus reduced, while maintaining a high data density (Dahlin and Zhou, 2006). Another important aspect of the gradient array is that it is specifically designed to minimize the disturbance caused by electrode polarization. This is done by keeping the time interval between the moment an electrode was used to transmit current and the moment it was used for measuring the potential, as long as possible (Dahlin *et al*., 2000). Figure 3.7 shows a sketch of the measuring sequence with the gradient array.

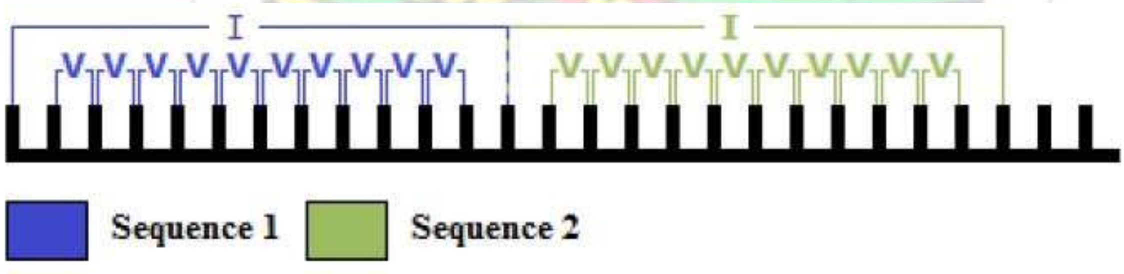

Figure 3.7 Measuring sequence with the gradient array. V refers to the potential measured between two electrodes and I the current injected into the ground by two electrodes.

3.5 Magnetic Susceptibility (χ)

Magnetic susceptibility of a volume of material is a measure of the induced magnetic moment of that material and it is a function of the amount of magnetic materials (magnetite for rocks and ferrous metal (MSW), contained within it. Quantitatively, magnetic susceptibility is a measure of how magnetizable a substance can be in the presence of a magnetic field, and it is expressed as the ratio of magnetization (*M*) to magnetic field (*H*) (Telford *et al*., 1990). It is a dimensionless quantity.

$$\chi = \frac{M}{H} \quad [\,] \qquad (14)$$

Mass specific susceptibility (κ) on the other hand is the induced magnetic moment of the unit mass of material obtained as the ratio of the magnetic susceptibility to the bulk density of the material ρ. It has a unit of m^3/kg.

$$\kappa = \frac{\chi}{\rho} \qquad (15)$$

The magnitude of the magnetisation acquired by rocks is proportional to the strength of the Earth's field, in their vicinity. Magnetic susceptibility measurement can provide a rapid estimate of the magnetic content of the rock. This measurement can be interpreted to reflect lithological changes, degree of homogeneity and the presence of alteration zones in the rock mass (Verduzco *et al*., 2004). In environmental study such as landfill mapping, magnetic susceptibility depends on the presence of ferrous metal composition of the waste.

3.6 The Magnetic Method

Magnetic surveys looks for variations in the magnetic field of the Earth that are caused by changes in the subsurface due to differences in the magnetic properties of near-surface rocks that is caused by inherent properties of the rock. The magnetic properties of rocks are either acquired by induced magnetization due to the effects of the Earth‟s present magnetic field or remanent magnetization obtained by the effect of the Earth‟s magnetic field when the rock last cooled down (O‟Reilly, 1984; Reeves, 1989). The strength of the magnetization is a function of the composition of iron oxides in the rock. The main iron oxides responsible for this effect in rocks are the ferrimagnetic minerals such as magnetite and maghemite. The main sources of these minerals in the soil are (i) parent rock material from which the soils are developed; (ii) in situ formation by pedogenetic processes (iii) aeolian deposition of dust (iv) anthropogenic processes such as industrial fly ashes (v) Flood deposition.

The interpretation of magnetic anomalies in environmental study consists of contribution from anthropogenic and lithogenic influences (Magiera *et al*., 2006) with high magnetic anomaly attributed to the anthropogenic source (Hanesch and Scholger, 2002). This is because the anthropogenic pollution is accompanied by a release of magnetic fractions into the soil. Similarly municipal solid waste containing high proportion of ferrous metal and industrial wastes containing strongly magnetic fraction also enhance magnetic response of the top-soil. These make the use of magnetometry as a proxy for environmental pollution measurement possible (Jordanova *et al*., 2008). Proton magnetometers can detect buried ferrous metals, in a properly designed magnetometry survey (e.g. Jordanova *et al*., 2008). Ferrous metals create variations in the local magnetic field which may be detected by the magnetometer. The intensity of the magnetic response is directly proportional to the mass of the ferrous object and inversely proportional to the cube of the source distance.

$$\text{Intensity of response} = \frac{\text{mass}}{\text{distance}^3} \tag{16}$$

This makes magnetic survey a very useful tool in waste disposal sites detection since it is sensitive enough to detect relatively small masses of ferrous materials at depth (Blasting, 1987).

3.6.1 Magnetic Data Processing

The effect of remanent geomagnetic field on magnetic anomaly obtained at points of low latitudes makes interpretation of magnetic field data at low magnetic latitudes difficult. This effect where areas of high magnetic susceptibility are depicted with low magnetic anomaly and vice versa is attributed to the influence of the geomagnetic field. This effect is removed by the application of reduction to the pole or analytical signal. These filters help to remove north-south components of noise and magnetic effects that is associated with magnetic data collected at low latitude where magnetic causative bodies magnetized in directions different from the inducing field (Nabighian, 1984; MacLeod *et al.*, 1993; Aziz *et al*., 2013). Figure 3.8 shows the change in the anomaly direction of the magnetic intensity at different magnetic inclinations.

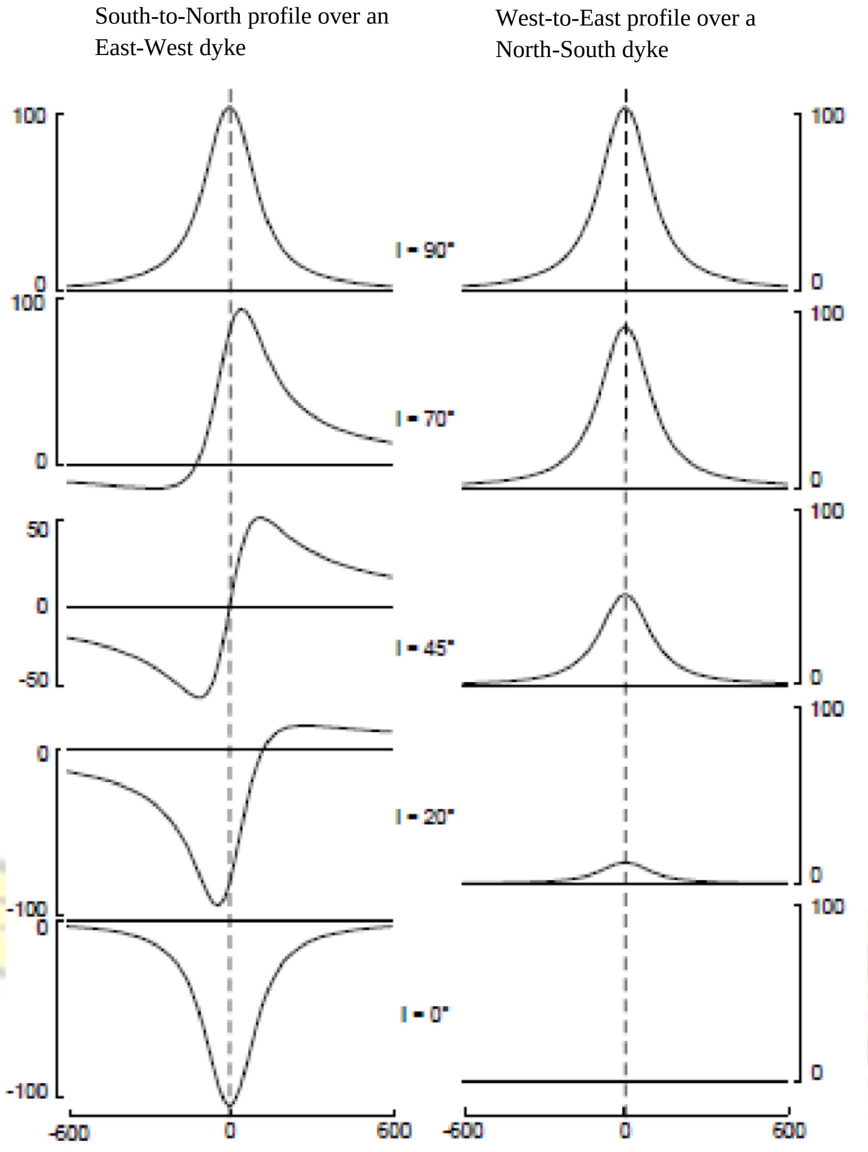

Figure 3.8 The shape of total magnetic field profiles over a vertically dipping dyke depends on the direction of the dyke (After MacLeod *et al.*, 1993).

3.6.1.1 Analytical Signal

The amplitude of the Analytic Signal is defined as the square root of the squared sum of the magnetic derivatives in the *X*, *Y* and *Z* directions (Nabighian, 1972, 1984; Roest *et al*, 1992; Aziz *et al*., 2013). It is a form of reduction to the pole (MacLeod *et al*., 1993) used to remove the effect of the geomagnetic field on magnetic data collected at low magnetic latitude. The analytical signal is able to determine the location of the causative sources of the magnetic anomalies, where its maxima are mainly positioned over the edges of the sources, regardless of their magnetization direction (Roest *et al*., 1992; MacLeod *et al*., 1993; Aziz *et al*., 2013). The transform is devoid of the effect of the direction of the Earth"s magnetic field thus the inclination and the declination of the Earth magnetic (Nabighian, 1972; MacLeod *et al.*, 1993). The magnitude of the Analytical Signal *A(x, y, z)* is given as:

$$|A(x,y,Z)| = \sqrt{\left(\frac{dT}{dx}\right)^2 + \left(\frac{dT}{dy}\right)^2 + \left(\frac{dT}{dz}\right)^2} \qquad (17)$$

where *T* is the total magnetic field intensity and *x, y* and *Z* are the direction of the derivative.

The amplitude of the 3-D analytic signal of the total magnetic field produces maxima over magnetic contacts regardless of the direction of magnetization. Also the distance between inflection points of analytic signal anomalies can be used to determine the depth to sources.

3.6.1.2 Reduction to the Pole

The goal of reduction to the pole is to take an observed total magnetic field map and produce a magnetic anomaly that would result if the magnetization and ambient field were both vertical (had an area been surveyed at the magnetic pole) (After MacLeod *et al.,* 1993). Nabighian *et al.* (2005) reported that the RTP operator becomes unstable at lower magnetic latitudes because of a singularity that appears when the azimuth of the body and the magnetic inclination both approach zero. If all the observed magnetic field of a study area is due to induced magnetic effects, pole reduction can be calculated in the frequency domain using the following operator (Grant and Dodds, 1972):

$$\mathrm{L}(\theta) = \frac{1}{[\sin(\mathrm{I}) + \mathrm{i}\cos(\mathrm{I})\cos(\mathrm{D}-\theta)]^2} \qquad (18)$$

where θ is the wave number direction, I is the magnetic inclination and D is the magnetic declination.

CHAPTER 4: STUDY AREA AND SITES DESCRIPTION

4.1 Study Area

4.1.1 Location

The study was conducted in the Kumasi Metropolis in the Ashanti Region. The region has a land size of 24,390 sq.km, which is about 10.2% of the land area of Ghana. It lies approximately between longitude 0.15^o to 2.25^o and latitude 5.50^o to 7.40^o N and shares boundaries with the Brong Ahafo to the north; Central Region to the south, Eastern Region to the east and to the west with Western Region.

The metropolis is situated within (636,000, 756,000) and (671,000, 728,000) in the World Geodetic System (WGS) 84, category Universal Transverse Mercator (UTM) zone 30 North, with total land surface area of 254 km^2. The area lies on portions of the Survey of Ghana 1: 50,000 scale series topographic maps sheets 0602A4 and 0602C4. It is located in the middle belt of the country about 270 km from the national capital Accra.

4.1.2 Climate and Physiography

The area falls within the transition zone with climatic condition categorized as sub-equatorial and has two main seasons, namely the rainy and the dry seasons. The rainy season is divided mainly into two, the major season starting from April reaching the peak around June and the minor season starts from September to November. The average annual rainfall in the area is 1282.30 mm. The average humidity is around 85% within most part of the rainy season and around 60% in the dry season. The dry season normally starts from November or December to February and attains a peak in January. The humidity in this time is generally low and visibility generally poor especially at the peak of the dry season, due to prolonged dry season and dusty north-east trade winds that blow across the country during the period. The mean monthly temperature is in the range of 25^oC – 32^oC with average annual temperature about 29^oC.

Topographically, the area is generally flat with topography ranging between 250 to 350 m above mean sea level. The area has few rounded hills which are mainly batholithic granitic rocks intrusions.

4.1.3 Vegetation

The study area falls in the main forest belt of the country and was once called the Garden City of West Africa due to the many tress and green areas that are in the city. The vegetation in the area is broadly classified into two: Semi deciduous forest and Guinea Savanna woodland. Currently, the vegetation in most part of the metropolis has been cleared for residence accommodation. The main forest reserve in the area is the Owabi Forest Reserve Sanctuary which is also under threat from encroachment in recent years.

4.1.4 Hydrology

The hydrogeology of the area consists of a dual aquifer system corresponding to the surficial geology and the basement rocks. The 0 to 30 m thick overburden of the Precambrian basement of the area forms the shallow aquifer and includes the surficial sediments and the weathered basement rocks (saprolite layer) (Wemegah *et al*., 2014; Erdelyi, 2010; KankamYeboah *et al*., 2003). The groundwater flow in the lower aquifer on the other hand is controlled by fault zones in the basement granitic bedrock and quartz veins of bedrock. The groundwater stored in the two aquifers is hydraulically connected and are the only source of subsurface water supply (Kortatsi, 1994; Erdelyi, 2010) and are in recent times serving as the main source of potable water supply to households in the metropolis due to the erratic supply of water from the Ghana Water Company and the ever increasing pollution of surface water networks in the metropolis due to human activities.

The study area also exhibits dense drainage system that shows trellis patterns (Figure 4.1). The major rivers in the area are the river Offin to the west and the river Sisa to the centraleast part of the metropolis. These rivers flow mainly from north to south and have various tributaries which are second and third orders with few higher orders. The most important of these tributaries are Owabi River which has the Owabi Dam, water treatment station that supplies potable water to most part of the metropolis. Other rivers which are important to this work are the Anyinasu and Anomakosa both of which are tributaries of river Owabi and carry leachate from the Ohwim waste deposit site. The river Oda into which the effluent from the Dompoase landfill site flows and the river Kentinkrono which is in the catchment area of the KNUST waste deposit site are second order tributaries to river Sisa and river Wiwi respectively (Figure 4.1).

4.1.5 Demographics

The Kumasi Metropolis is the second most populous metropolis in Ghana with a population of 1,170,270 in 2000 increasing to 2,035,064 in 2010 according to the Population and Housing Census of Ghana (GSS, 2012; GSS, 2002). The metropolis has ten submetropolis namely Asawase, Asokwa, Bantama, Kwadaso, Manhyia, Nhyiaeso, Oforikrom, Suame, Subin and Tafo.

4.1.6 Economic Activities of the inhabitants

Kumasi is the second largest city after Accra, and has the largest markets and transport stations in Ghana. The metropolis has relatively lower industrialization as compared with other bigger cities (Accra, Tema and Takoradi) in the country. The informal sector accounts for about 70% of the labour force. People in this sector are mainly involved in trade, driving, apprenticeship jobs such as sewing, carpentry, mason, and shoe-making. The traders who form the highest percentage of the informal sector sell food stuffs and other goods ranging from locally manufactured to exotic and imported used products. The level of education among these workers is relatively low, greater part, about 78%, stopping after senior secondary schools, while a considerable number of 4% do not even have basic education at all (Fobil *et al*., 2010).

4.2 Research Sites

The research sites were selected taking into consideration the geographical location, economic activities in the area, and also the feasibility of carrying out the geophysical surveys devoid of interference from noise such as electrical powerlines, residential settlement etc. In all, three sites were selected and used in this work. Two main categories of waste deposit sites were investigated. These are unengineered waste deposit sites which include the KNUST and Ohwim Waste Deposit Sites and the Dompoase Landfill site which is on engineered waste disposal site.

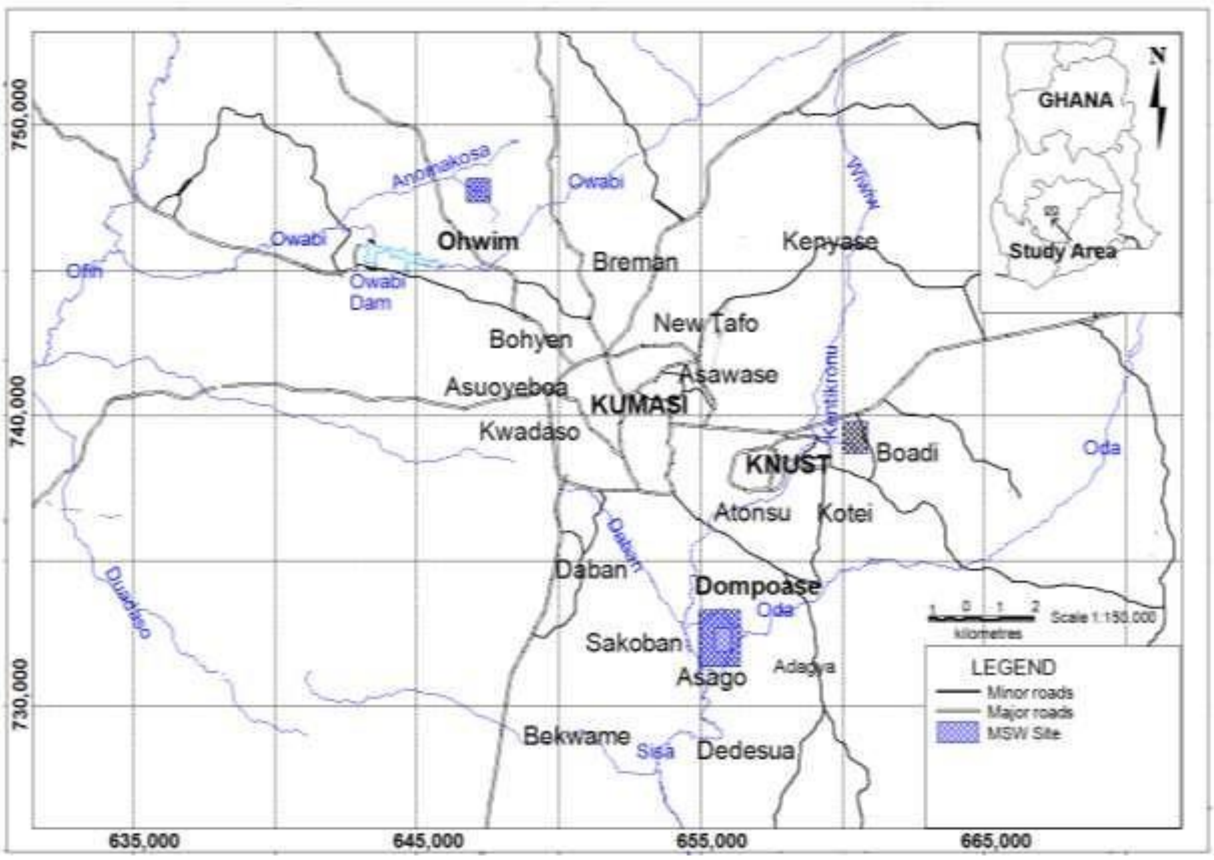

Figure 4.1 Map of Kumasi Metropolis showing the study sites.

4.3 Geological Setting

The important role the crustal geology plays in the interpretation of geophysical data cannot be over emphasised. This is because the geophysical result is greatly influenced by the rock and their physical properties. This section therefore reviews the general geology of the study area by considering the various rock types in the area and lithostratigraphic units obtained from drill borehole during the course of this research work.

4.3.1 Birimian Supergroup

The Early Proterozoic Birimian Supergroup of Ghana consists of NNE-SSW trending alternations of coeval parallel sequences of volcanic and sedimentary assemblages called belts and basins units respectively (Leube and Hirdes, 1986; Leube *et al*., 1990). This division which is considered as the accepted division of the formation was arrived at over a period of disputes (Taylor *et al*., 1992) on the stratigraphic and chronological relation in the interpretation of the two units (e.g. Tagini, 1971; Hottin and Quedraogo, 1975; Kesse, 1985; Leube *et al*., 1990; Milesi *et al*., 1992; Sylvester and Attoh, 1992).

The Birimian basin rocks are predominantly metasedimentary units which consist mainly of volcanoclastic, flysch-type turbidite wackes, argillitic rocks and chemical sediments with felsic to intermediate protolith (Hirdes *et al*., 1992; Sylvester and Attoh, 1992; Davis *et al*., 1994) which are isoclinally folded (Hirdes *et al*., 1988; Allibone *et al*., 2002). The volcanic belts consist of basaltic flows, andesitic to dacitic pyroclastic rocks and lavas, volcanogenic turbidites, and manganiferous cherts (Leube *et al*., 1990), which have been widely affected extensively by compressive deformational events which probably occurred around 2.1Ga and is expressed by a penetrative foliation and metamorphosed to predominantly greenschist

(Sylvester and Attoh, 1992) with some areas reaching amphibolite grade (Milesi *et al.*, 1992; Griffis *et al.*, 2002). The formation hosts most of the supergenic gold deposits which are controlled by a NE-SW oriented megashear (Sylvester and Attoh, 1992).

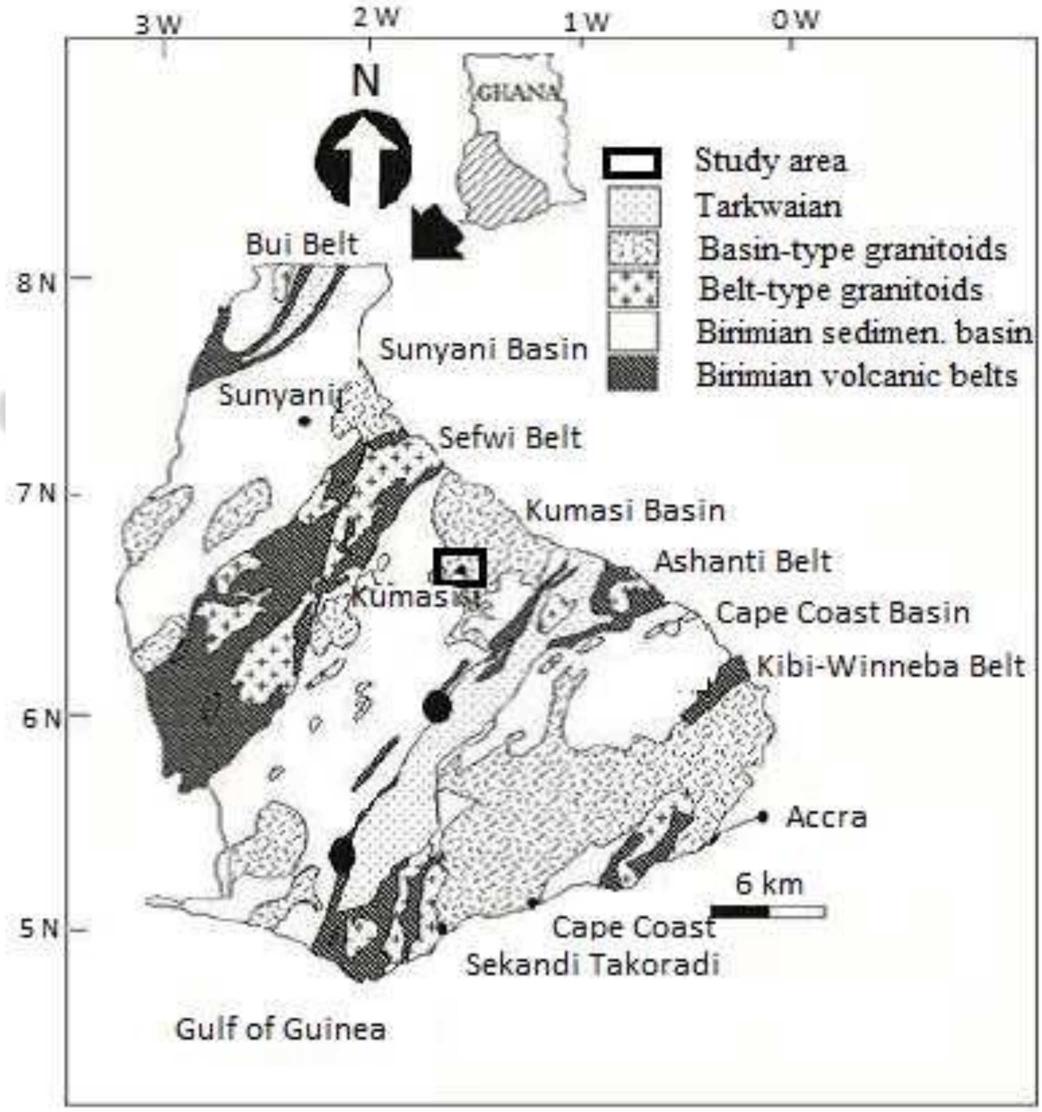

Figure 4.2 Geological Map of Southern Ghana (Modified from: Taylor *et al*., 1992; Leube *et al*., 1990).

4.3.2 Granitoids

The Birimian rocks are intruded by two main granitoid units, namely the basin type granitoids in the metasedimentary basins which are mostly batholitic in nature (Sylvester and Attoh, 1992) and the belt type granitoids in the volcanic belt (Hirdes *et al*., 1988). The intrusion events took place in time intervals of 2180 - 2170 Ma and 2116 - 2088 Ma, respectively (Hirdes *et al*., 1992).

The basin granitoid which is batholitic in nature tends to coincide with the central axes of the sedimentary basins (Leube *et al*., 1990). The rock types in this group include quartz, diorite, tonalite to trondhjemite compositional types, granodiorites, admallite and granites which are sometimes characterised by weak foliations. Biotite is the main ferromagnesian mineral identified in this rock and is mostly accompanied by muscovite (Leube *et al*., 1990). The belt granitoids are mostly elongated and often unfoliated plutonic bodies. These granitoids consist of quartz, diorite, tonalite and trondhjemite, granodiorite, admallite and to a minor extent, granites. These granitoids are characterised by the mafic mineral hornblende, varying amount of biotite and plagioclase as the major feldspar mineral.

4.3.3 Local Geology

The study area is within the Kumasi Basin which is bounded by the Ashanti Belt on the south-east and the Sefwi Belt to the north-west. It is largely dominated by very thick sequences of poorly exposed Birimian Metasediments and small to very large granitoid complexes of the basin type (Griffis *et al*., 2002) refer to as the Kumasi Granitoid Complex (Kesse, 1969, 1972). The basin sediments are tightly folded with steeply dipping folds and NE trending axial planes. Regional faults, parallel to the NE structural fabric, are evident in many areas and more intense folding and fault systems appear to be concentrated along the margins of the basins and belts.

4.3.4 Stratigraphic Units

The stratigraphic classification of the rocks identified from drilled samples obtained during the course of the work included two main units namely thick saprolitic weathered layer overlaying granitic bedrock. The saprolite is rich in clay with composition decreasing with depth. The bedrock was found at depths ranging from 25 to 30 m.

CHAPTER 5: MATERIALS AND METHODOLOGY

5.1 Introduction

The mapping of the waste involved the use of methods that are sensitive to the waste composition and/or the ionic concentrations of the effluent hence they had the ability to discriminate the waste from the host formation. The methods employed in this work included magnetic susceptibility, ground magnetics in both the total magnetic intensity and the gradiometry mode and the spectral induced polarization surveys. These surveys were carried out with the state of the art instruments which helped in getting good quality data which is critical in helping arrived at the goals of the research. Furthermore, the integration of these datasets gave a better mapping of the waste as the various ambiguities that are associated with any one of the methods are compensated for in this approach.

5.2 Site Reconnaissance and Site Selection

Site selection for the survey was done after a visit to the various solid waste disposal sites in the Kumasi Metropolis with the help of staff of the KMA-WMD to determine the MSW sites that have the possibility of being studied using the proposed geophysical methods. The selection was done after the consideration of the level of noise in the catchment area that could affect the geophysical data quality. Other factors considered in the site selection were availability of land area around the waste to enable complete traversing of the waste and accessibility to the site. In all ten sites were visited from which four were selected initially for the start of the work and later reduced to three in the course of the research due to unavailability of land space around the site to enable effective geophysical data collection.

5.3 Magnetic Susceptibility Survey

The magnetic susceptibility survey was conducted using the Bartington MS2 Magnetic Susceptibility System. The instrumental setup comprises a handle with an integral electronics unit and an extension tube to which a search loop MS2D was connected (Figure 5.1 and Figure 5.2). The loop allows the bulk susceptibility of a circular area approximately 200 mm diameter to be measured. It helps in the rapid assessment of the concentration of ferrimagnetic materials in the top 100 mm depth of the land surface and requires a consistent contact with the sample surface for good results (Dearing, 1999). The probe has a dimension of 208 mm diameter by 90 mm height and operates at a frequency of 0.958 kHz. It has a measuring period of 0.6 s for measuring with sensitivity of 1x 10^{-6} range and 6 s for 1x 10^{-7} SI. The inducing magnetic field produced around the tip of the circular loop by this probe is toroidal in shape with varying sensitivity with depth across the base of the loop. The depth response of the probe decreases exponentially with depth and varies from 50% at a depth of 15 mm to about 10% at a depth of 60 mm. Lecoanet *et al*. (1999) reported that sensitivity of the probe for environmental monitoring is strongly influenced by the thickness of grass layer, humidity, etc. This limits the use of this method in monitoring landfills in areas that are grown with thick grass vegetation or having thick layer of soil cover.

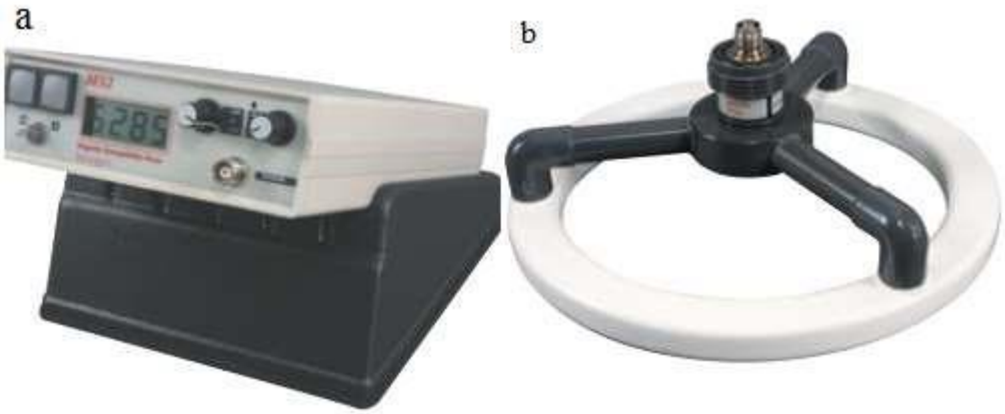

Figure 5.1 The measuring equipment a) MS2 magnetic susceptibility meter b) MS2D loop sensor.

5.3.2 Field Procedure

The magnetic susceptibility of the investigated areas was conducted using a profile separation of approximately 15 to 25 m and station separation of 5 m. The system was operated as follows:

- The sensor was connected to the meter (Figure 5.2) and then switched on and set with measuring sensitivity of 10^{-6} using the SI unit mode.
- The system was then allowed for about 10 minute to get into thermal equilibrium with the environment.
- The sensor was then initialized by zeroing it after holding it in the air about 100 cm high.
- The air reading was taken by holding the sensor in the air at the start of the measurement on a profile and after every five readings to help compensate for the instrumental drift over the period.
- The sensor was then placed onto the required surface at every 5 m station location and the magnetic susceptibility value taken. The global positioning system (GPS) locations of the data points were taken using a handheld Map6 Garmin GPS.

- At the end of the survey, the sensor was again held in the air and the final air reading taken. The interpolated air reading corresponding to a particular data picked time was used to adjust for drift in the measurement sequence.

Figure 5.2 Magnetic susceptibility data acquisition using the MS2D sensor.

5.3.2 Data Processing

The corrected magnetic susceptibility data and the corresponding coordinates of the data points were inputted into an excel document and imported into Geosoft to create a Geosoft Database. The gridding of the data was done using minimum curvature algorithm at onequarter (1/4) the profile spacing. This gridding algorithm substantially increased the smoothness and resolution of the datasets (Geosoft Inc., 1996), providing useful information on the detail outline of the waste deposit (e.g. Wemegah *et al*., 2014).

5.4 The Magnetic Survey

The magnetic survey which measures the variation of the magnetic intensity of the Earth was conducted in the total magnetic intensity (TMI) mode and the gradient mode. The instruments used for the survey were

- The Geometrics Magnetometers G856 and G858 with sensitivity of 0.1 nT, owned by Newmont Ghana Gold Limited were used for the measurement of the total magnetic intensity. The setup consists of two units, one for the establishment of the base station for measuring the diurnal variation in magnetic field. The second unit (rover) for measuring the total magnetic field of the survey site. The handheld Map6 Garmin GPS was used in collecting the coordinates of the data points.
- The GSM -19TGW v7.0 Gradiometer, owned by the Department of Physics KNUST was used in the collection of the data in the gradiometric mode. The setup consists of a magnetometer unit, two consoles and the in-built GPS unit.

5.4.1 Field Procedure

5.4.1.1 Base Station

The base station for monitoring diurnal variation of the geomagnetic field during the period of the survey was set at point (660436E, 739098N) for the KNUST site survey and the Ohwim and Dompoase base stations set at (656090E, 732700N). These areas were selected by visual inspection to make sure they were devoid of magnetic influence. Series of reconnaissance magnetic data were then collected in the areas to get a point of sound uniform magnetic anomaly where the base stations were established. The base station magnetometer was setup in the morning before the start of the survey during the period of the survey. This was done by orienting the console in approximately E-W direction to reduce the influence of the Earth N-S magnetic field on the data. The necessary tuning was done at this stage in order to determine the point of good signal for the survey. The system was setup to collect data at every 4 s over the period and removed after the survey was concluded at the end of the day.

The data were used to remove the effect of the diurnal variations from the measured data.

5.4.1.2 Total Magnetic Field Measurement

The mobile or the rover magnetometer was then setup and tuned to determine the good signal strength. The sensor was oriented in approximately E-W direction during the data collection. The orientations of the profiles were set in order to traverse the whole waste with lengths varying from 300 m to 800 m. The data collection was done using a station separation of 5 m. The profile separations used also varied from 15 m to 30 m with higher data density collected over the waste deposit. The handheld GPS was used to determine the coordinates of the data collection points. At the end of the survey the datasets (base data and the filed data) were downloaded and the diurnal correction done using the MagMap2000 software package. Furthermore, the GPS locations of data points and the diurnally corrected magnetic data were merged and the data loaded into Geosoft database for further processing.

5.4.1.3 Magnetic Gradiometry Field Measurement

The gradiometry survey was carried out using the GSM-19TW Proton Precession Magnetometer with sensitivity of 0.05 nT. The gradiometry setup was mounted as shown in Figure 5.3. The two sensors were mounted with separation of 56 cm and the GPS antenna mounted on the top sensor also at a separation of 56 cm from it. The in-built GPS in these instruments was used to determine the geographic coordinates during the data collection. The measurement of the two magnetic fields by the two sensors for determination of the magnetic gradient is done concurrently. The survey was also carried out with a station separation of 5 m on profile lengths varying from 300 m to 800 m. Similarly, the profiles separation used varied from 15 m to 30 m. All profiles layout in the survey were done to fully traverse the waste deposit and to extend at least 100 m away from it in both directions. This helped to get a distinct anomaly in the data that enabled the discrimination of the waste from the host formation.

Figure 5.3 a) The console, two sensors with GPS option b) magnetic gradiometer setup mounted on a backpack.

5.4.2 Data Processing

The data processing involved two main stages, the pre-data processing which involved the downloaded data and carrying out the necessary corrections such as spike removal and diurnal corrections on the data. The second stage involved the creation of the Geosoft database and interpolation and the application of the necessary enhancement filters to the data.

The following software was for downloading and pre-data processing the data:

- Magmap for the Geometrics instrument
- GEMLink v5.3 for the GSM -19TGW v7.0 Gradiometer

The corrected data obtained from these software packages were imported into Geosoft to create a Geosoft database for further processing and enhancement by the application of various filters, namely reduction to the pole, analytical signal, upward continuation, vertical and horizontal derivatives.

The datasets were projected to the Universal Transverse Mercator (UTM) World Geodetic System (WGS 84) coordinate system with category member of zone 30N. They were then gridded at a grid cell size of 0.25 of the profile separation using the Geosoft Oasis Montaj software (Oasis Montaj, 2006). This helped to increase the data density over the study area.

5.4.2.1 Data Reduction

The Geomagnetic Reference Field (GRF) was computed for the surveyed area, at that time of the year, using Geosoft Oasis Montaj software (Oasis Montaj, 2006). The results of the ambient magnetic field strength (*H*), inclination (*I*) and declination (*D*) were H = 32,383 nT, I = -13.51^{o}, and D = -3.82^{o}, respectively. These parameters were used in the application of reduction to the pole filter on the data in order to remove the effect of the geomagnetic field on the data. Similarly, analytical signal derivative as a form of reduction to the pole (Nabighian, 1972, 1984; Roest *et al*., 1992; Li, 2008) was applied to the data to remove the effect of the geomagnetic field. These were important because the study area is located at a point of low magnetic latitude. This derivative therefore helped to transform the magnetic data such that points of low magnetic susceptibility record low magnetic signature and vice versa.

5.5 Full WaveTime Domain Spectral Induced Polarization

The time domain spectral induced polarization survey was conducted using SyscalPro owned by the Aarhus University, Aarhus Denmark. The instrument uses 10 channels for potential measurement during the data collection. The survey was performed using gradient array (Dahlin and Zhou, 2006) because of its efficiency on a multi-channel acquisition system, the low geometrical factor, how it minimizes the effect of electrode polarization (Dahlin *et al*., 2002; Gazoty *et al*., 2013) and also yields a high image resolution (Dahlin and Zhou, 2004). The data sampling was done using 4 s current turn on-and-off. The data were acquired using 20 gates, approximately log-sampled between 10 and 800 ms using 3 stacking in each acquisition. The electrode spacing used in the survey was 5 m, with profile lengths ranging from 300 m to 800 m.

5.5.1 Data Collection

The multi-electrode systems which consist of 81 stainless steel electrodes which serve as both current and potential electrodes, spaced at 5 m apart were implanted into the ground along the profile. The electrodes were connected to the instrument using cables which were connected to the electrode using jumpers. The instrument controls the switching unit, current waveform etc. A full layout consists of four cables with a length of 100 m each, forming a total of 400 m on a full spread. Profiles that were longer than 400 m were surveyed by the principle of roll-along where the first cable from a full layout was moved to connect to the fourth cable at the end of measurement and data collected. This procedure was repeated till the whole length of the line is surveyed as shown in Figure 5.4.

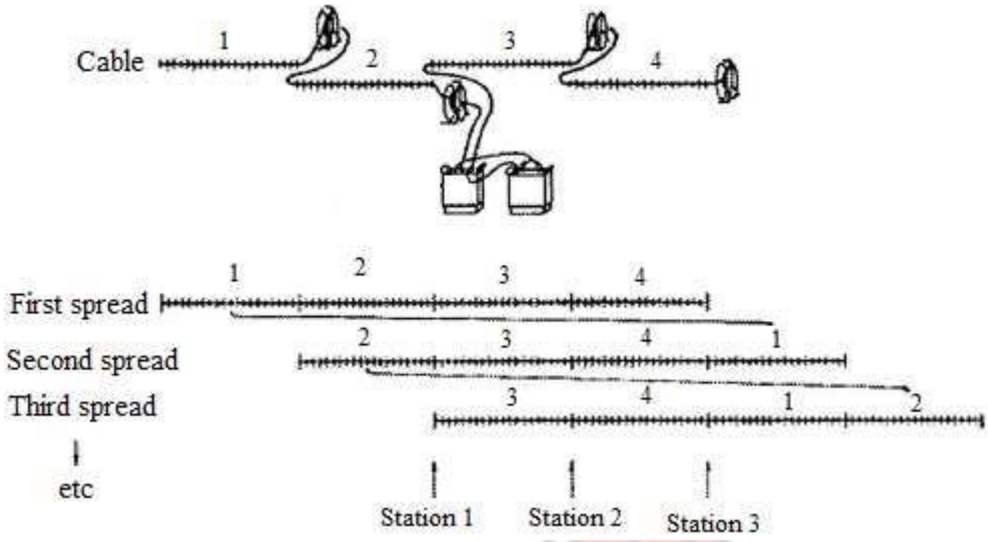

Figure 5.4 Roll-along measurement system used for acquisition of DCIP field data (Modified from Van Overmeeren and Ritsema, 1988).

During data collection the electrodes function as both current and potential electrodes. When measuring, two electrodes function as stationary current electrodes, injecting current across eleven potential electrodes (ten channels). The switching unit within the measuring instrument assigns which electrodes are used as current and potential electrodes, respectively. For each current injection 10 potential measurements are measured, before another two electrodes are assigned as current electrodes and ten new potential measurements are measured. The electrode selection sequence is written to leave enough time between the time when an electrode is used as a current and the time that it will be used as a potential electrode. The measurement continues in this manner until the chosen protocol has finished.

5.5.2 Data Processing and Inversion

The DCIP datasets were processed by first importing the data into Aarhus Workbench (Auken *et al*., 2009) which enables the display of the data in a GIS environment. The data were then processed to remove bad decay (outlier) from the datasets (Auken *et al*., 2014).

Figure 5.5 shows typical IP decay curves from IP survey with 20 gates. The blue curves are smooth decay curves used in the inversion of the data while the gray curves are noisy IP decay curves that are deleted before the inversion of the data. The noisy curves could be due to the noise in the data that can be attributed to poor electrode contact, galvanic coupling (Viezzoli et al., 2008), electrode polarization etc.

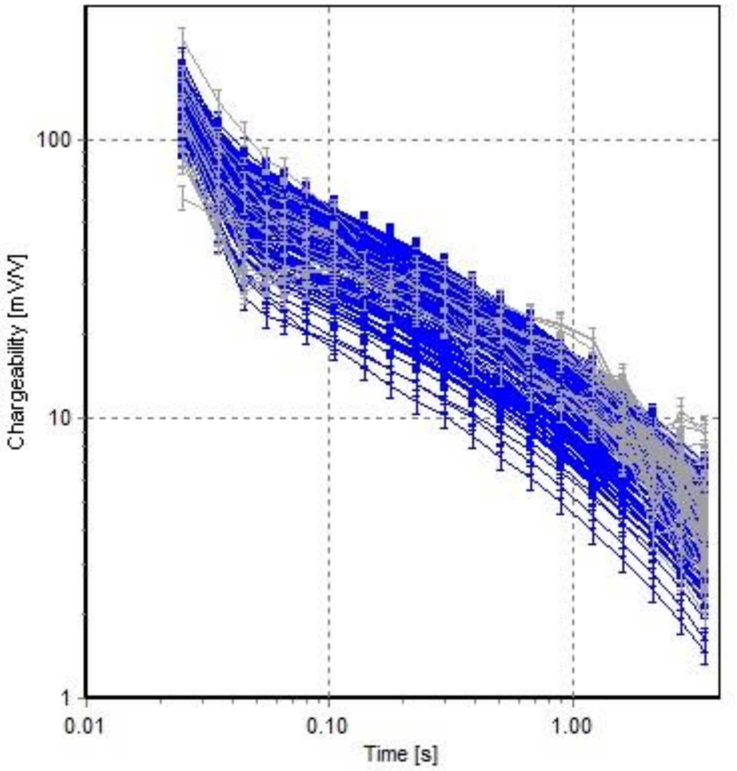

Figure 5.5 Decay curve of IP inversion, blue curves are smooth IP curves while the gray curves are deleted noisy IP curves.

The full IP decay data were inverted using the 2-D DC/IP inversion algorithm developed by Fiandaca *et al*. (2013) and incorporated into the Aarhus Workbench with its inversion kernel AarhusInv (Auken *et al*., 2014). In these inversion algorithms, the transmitter waveform, in terms of duration of current pulses and stack size is accurately modelled, as well as the effect of filters sometimes present in the acquisition instruments.

Filter characteristic specifically calibrated for the SyscalPRO IP/Resistivity instrument (used in data acquisition) was used in the inversion of data in this work. The forward computation, allows for a quantitative interpretation of the spectral IP parameters (Fiandaca *et al*., 2013). This gives access to the spectral information contained in the IP decays, retrieved in terms of the Cole-Cole model (Pelton *et al*., 1978). The intrinsic IP parameters obtained in this inversion included direct current (DC) resistivity (ρ), chargeability (m_0), the relaxation time (τ) and the frequency factor (*C*). Also produced at the end of the inversion are the residual of the model parameter which helped to determine whether the model fits the data. The misfit of the DC and the IP parameters were also calculated and displaced along the profile which gives an idea of how well the data is fitted along profile. The standard deviation on the DC and IP data was computed using 2% and 10% relative values, respectively, plus a noise floor of 1 mV (Gazoty *et al.*, 2013).

CHAPTER 6: KNUST MUNICIPAL SOLID WASTE DISPOSAL SITE

6.1 Introduction

The characterization of the Kwame Nkrumah University of Science and Technology (KNUST) decommissioned solid waste disposal site situated in the Oforikrom Submetropolitan Area of the Kumasi Metropolis was done using three geophysical methods. The methods employed were ground based magnetic survey in both gradiometry and the total magnetic intensity modes and spectral induced polarization surveys. The surveys were conducted in the catchment area of the waste disposal site with the aim of fully characterizing the site. This was done by mapping the waste, its associated plume, the determination of lithological units and any possible geological features that can aid in the infiltration of the leachate into the groundwater system. Two boreholes were also drilled in the area which helped in determining the waste thickness, lithological units in the area. This aided in the correlation of the geophysical signatures that are associated with the waste, geological units of the profiles on which they are drilled and thereby serving as a benchmark for the interpretation of the other data sites collected in the area.

The catchment area has approximate area of 400 x 600 m, with the waste spread to cover an approximate area of 300 x 200 m. The site was operational between 2000 and 2007 before waste disposal at the site was relocated to the Dompoase Landfill site. There is no record on the quantity of waste deposited at the site. Materials deposited at the site are mainly domestic waste from student halls and lecturer‟s residence as well as hospital waste from the main university hospital. The burning of the area for farming by people leaving around Boadi, the closest community to the area had left non-burnable materials (bottles, Figure 6.1b) as the main visible waste remaining on the site. The site was not properly controlled and maintained causing a wide spread of the waste over the whole area.

This research characterized the unengineered and decommissioned Kwame Nkrumah University of Science and Technology (KNUST) waste disposal site by using TD spectral IP and magnetic surveys. Thirteen induced polarization profiles 500-800 m long and twenty two magnetic profiles 600-800 m long were acquired. Also two boreholes were drilled to help in the interpretation of the geophysical datasets. The aim of the research was to determine the effect of this site on the quality of the soil and groundwater, which is the main source of water supply to the KNUST Senior High School and the Teaching Hospital and Veterinary School situated in the area (Wemegah *et al*., 2015).

The results aided in the mapping of the lateral extent of the waste (300 x 400 m) at the main waste site and 100 x 100 m at both northern and the southern ends of the main waste. The vertical extent of the waste deposit was found to be in the range of 3 to 10 m. Similarly, the lateral extent of associated plume of the waste in the area was mapped to be in the range of 6 to 30 m thick. The results also helped in the lithostratigraphic characterization of the site. In all two main lithological units namely the muscovite rich saprolite unit which is in the range of 10 to 32 m thick, hence the depth of the granitic bedrock were mapped. A fracture zone which is considered to be a potential conduit for the percolation of pollution into the groundwater system was also mapped.

6.2 Location of the KNUST Waste Disposal Site

The Kwame University of Science and Technology (KNUST) waste disposal site is situated on the south-eastern part of the KNUST campus. The site is situated in the Oforikrom Submetropolitan area of the Kumasi Metropolis. It is about 7 km from the main campus and 1 km from the agriculture research station of the university. The boundary of the site falls within coordinate 660200-660700 E and 738950-739400 N defined in the Universal Transverse Mercator (WGS84), zone 30N. The waste was deposited in a wetland just behind the KNUST Senior High School with portion of the waste extending into the school as it is frequently spread over the area during its operation. The waste was deposited in the area before the relocation of the school from its former location on the main university campus to its current location in 2010. About 0.5 km south-west from the waste is situated the proposed site for the KNUST Teaching Hospital and Veterinary School of the University, both which are currently under construction.

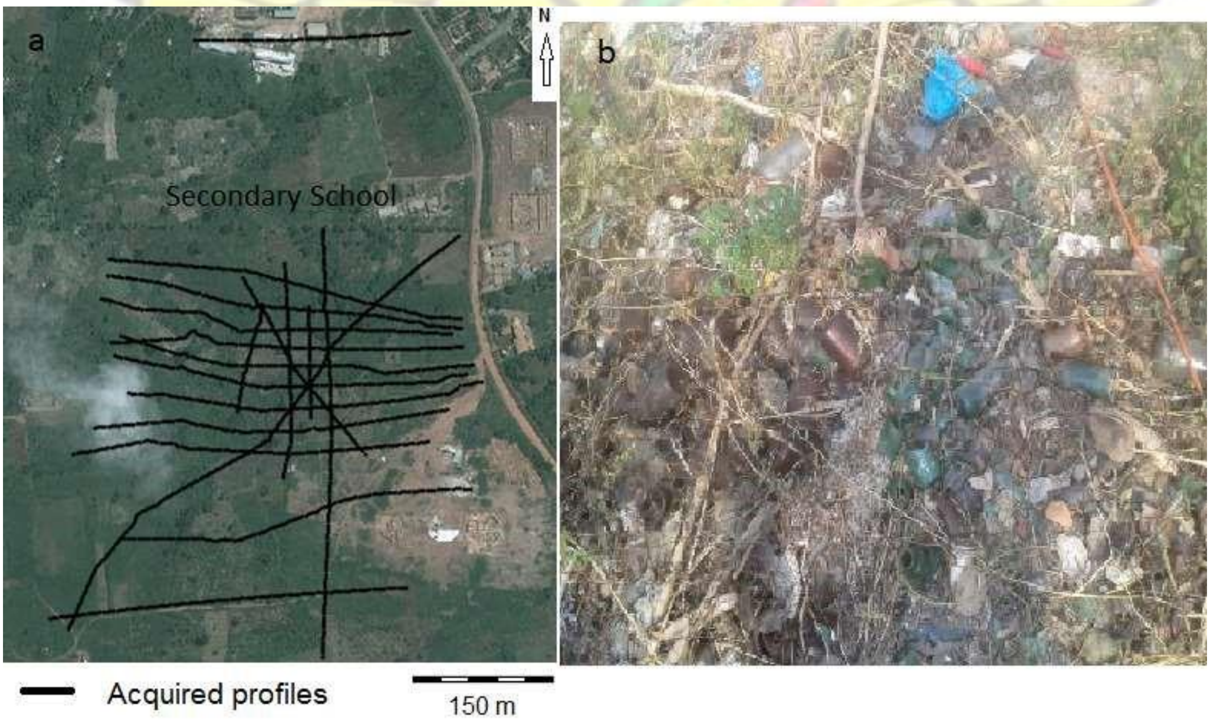

Figure 6.1 a) Satellite Image of study area, b) bottles at the waste disposal site.

Geologically, the area is underlain by a thick layer of saprolite with thickness ranging from 10 to 30 m laying on a basin type granitic bedrock. Hydrologically, the groundwater flows west into the wetland area which is used for vegetable cultivation all year round.

6.2.1 Digital Elevation Map (DEM)

Figure 6.2 is the digital elevation map of the KNUST waste deposal site showing the variation in topography of the area. The topography ranges from 265 to 290 m with the lowest altitude recorded in the north-western corner and the highest altitude recorded in the eastern part of the site. This topographic gradient controls the hydrology of the area with surface and groundwater flowing in the north-western direction. The lowest region (L-L) forms a river channel in which a river which is a tributary of river Kentinkrono flows. The water from this channel is used for irrigation farming by people in the area around Boadi who grow vegetables all year round.

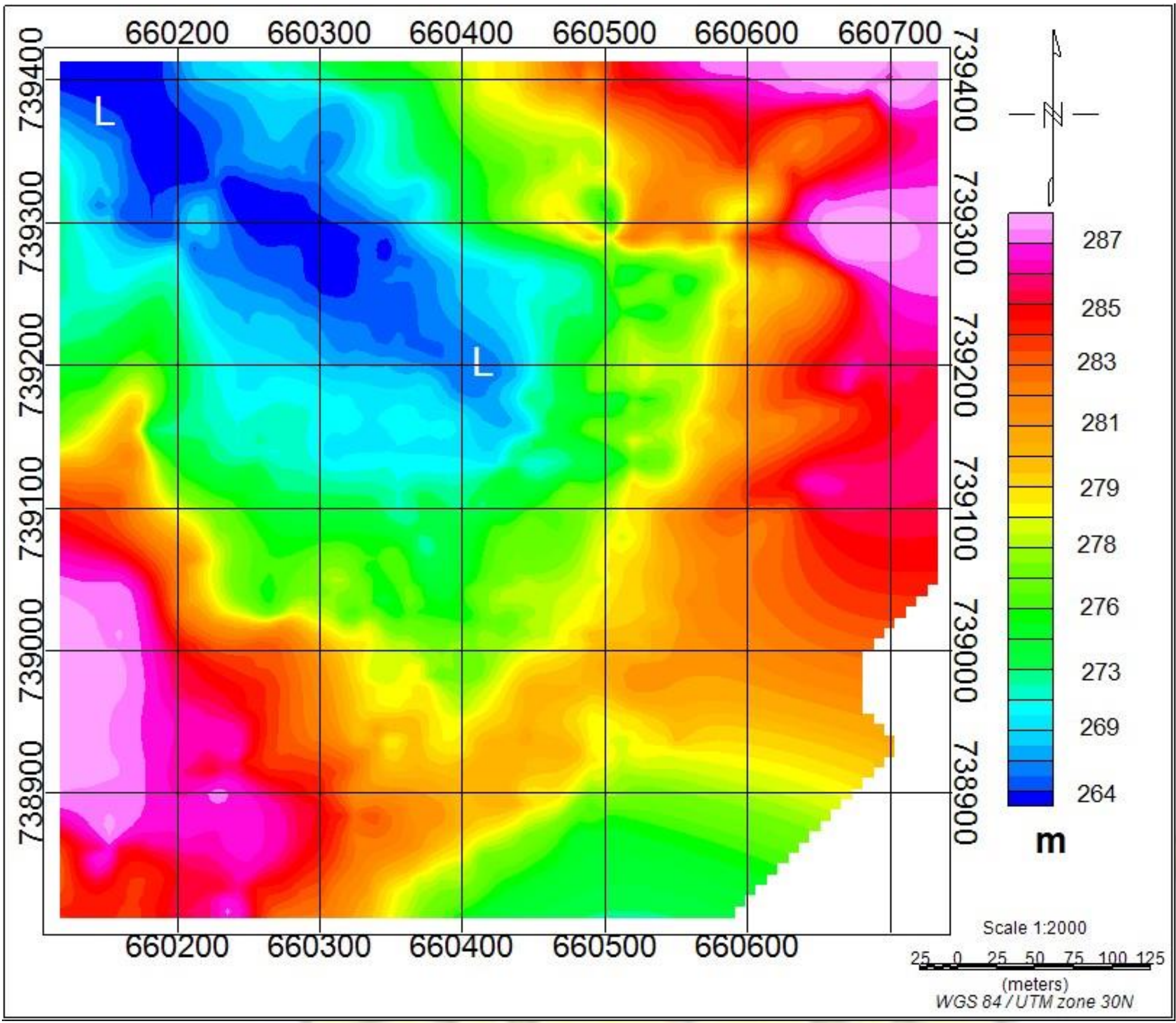

Figure 6.2 Digital elevation map of the KNUST waste disposal site.

6.3 Research Design and Survey Structure

The magnetic survey was conducted in the gradiometry and the total magnetic intensity modes. Both surveys were conducted along 26 profiles with length ranging between 400 to 800 m. The survey covered a total profile length of 10.2 km for each of the modes and was designed to help in the full mapping of the waste deposit.

Furthermore, the spectral TD IP survey was conducted on 18 profiles (Figure 6.1a) with profiles lengths ranging between 500 m and 800 m with total surveyed profile length of 6.9 km. The survey was performed using the gradient array (Dahlin and Zhou, 2006) because of its efficiency on a multi-channel acquisition system, the low geometrical factor, and how it minimizes the effect of electrode polarization (Dahlin *et al*., 2002; Gazoty *et al*., 2013). Most of the profiles were oriented in the west-east direction, with a crossing profile in north-south direction and a diagonal profile in north-eastern direction. These survey directions were chosen so as to traverse the whole waste deposit. The E-W direction was observed to have the shortest distribution of waste hence, the choice of this direction for most of the profiles.

These survey directions were chosen so as to traverse the whole waste deposit. Profile TECD (300 m long) was surveyed inside the school to determine whether the waste was spread as far to that point. The presence of electrical powerline and staff accommodation just behind the wall of KNUST Secondary School did not make it possible for a profile to be surveyed close to the well to determine the extent of the waste in that area.

6.4 Results and Discussion

6.4.1 Magnetic Results

Magnetic data from the site mapped the waste deposit based on its composition of magnetic minerals and the ferrous metal. The magnetic signature of the waste deposit superimposed on the magnetic signature of the crustal geology was obtained after the removal of the regional field from the data. The small nature of the study site with a general homogeneous geological setting, therefore makes the strong magnetic anomaly produced by the ferrous metal which is a major constituent of the waste to be used to map the waste deposit.

6.4.1.1 Total Magnetic Intensity (TMI) Result

Figure 6.3 is the total magnetic intensity map of the area showing the distribution of magnetic signature over the study area. The measured ambient magnetic data of the site is in the range of 31986.7 to 32629.2 nT and the residual magnetic value in the range of -263.943 to 181.705 nT. The TMI map has the effect of geomagnetic field since it is collected at point of low magnetic latitude (MacLeod *et al*., 1993; Fedi and Florio, 2001). This produces an effect where the magnetic signature is not observed vertically above the causative body (kw). The total magnetic intensity map therefore produced no distinct signature that can help in the delineation of the waste due to this effect.

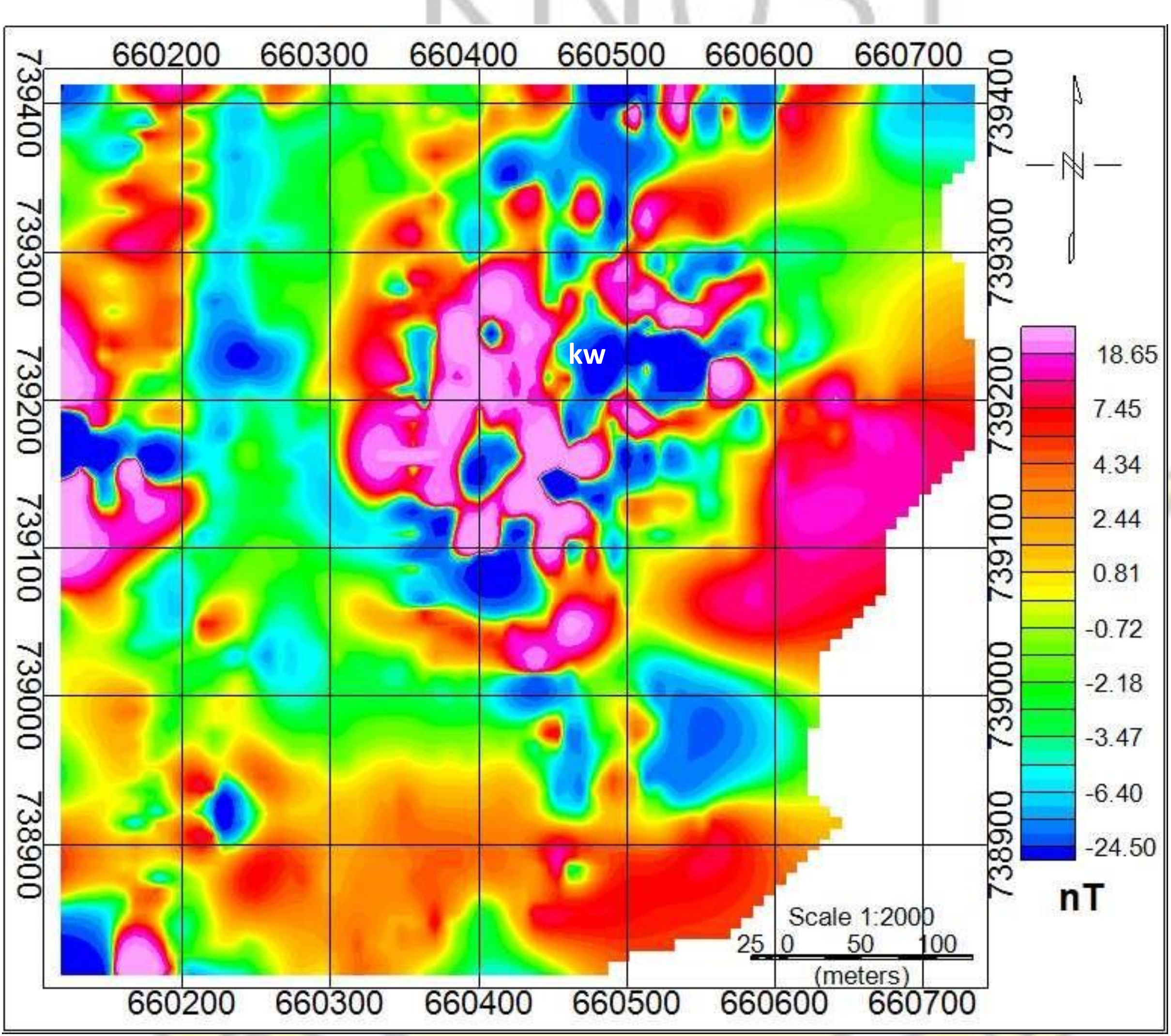

Figure 6.3 Total magnetic intensity map.

In order to remove the effect of the geomagnetic field on the magnetic data, the Analytical Signature which is a form of reduction to the pole (Nabighian, 1972, 1984; MacLeod *et al.*, 1993; Roest *et al*., 1992; Li, 2008; Ansari and Alamdar, 2009) was applied to the TMI map to obtain Figure 6.4. This transform which is devoid of the effect of the direction of Earth magnetic field thus the inclination and the declination of the Earth magnetic (Nabighian, 1972; MacLeod *et al.*, 1993) field produces anomalous high magnetic signature at points labelled kw (Figure 6.4). This high magnetic signature is attributed to the position of the waste and caused by the high ferrous metal composition of the waste.

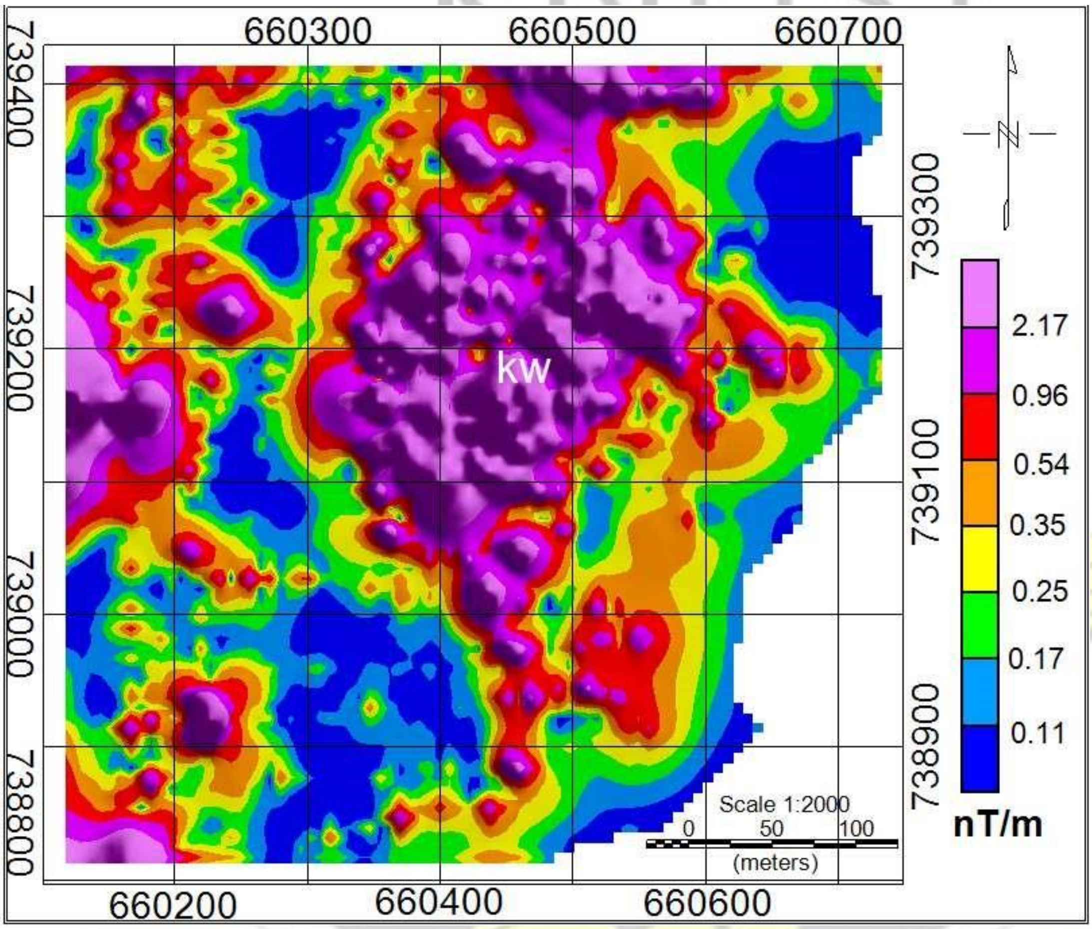

Figure 6.4 Analytical signal derivative map of total magnetic intensity data.

Figure 6.4 is the analytical signal derivative of the total magnetic intensity map. This helped to locate the observed magnetic anomalies directly over the magnetic causative bodies. From the result the waste is delineated with high magnetic signature with value greater than 0.96 nT/m. The position of the waste (kw) is mapped to extend across an approximate area of 300 x 400 m. Furthermore, the erratic distributions of high magnetic signatures in the area are also identified in the western part of the site attributed to the uncontrolled deposition of the waste in the area.

6.4.1.2 Gradiometry Result

The magnetic gradiometry survey which is sensitive in delineating near surface magnetic features was conducted over the study area to obtain Figure 6.5. This image shows the distribution of the magnetic signature over the study area as affected by the geomagnetic field. In this regard, the position of the waste that has high magnetic susceptibility produced low magnetic signature. The measured magnetic gradient values range from -161.16 to 92.78 nT/m in the area. As observed in the total magnetic intensity map (Figure 6.3) there is no distinct magnetic signature in this image that can help in the mapping of the waste.

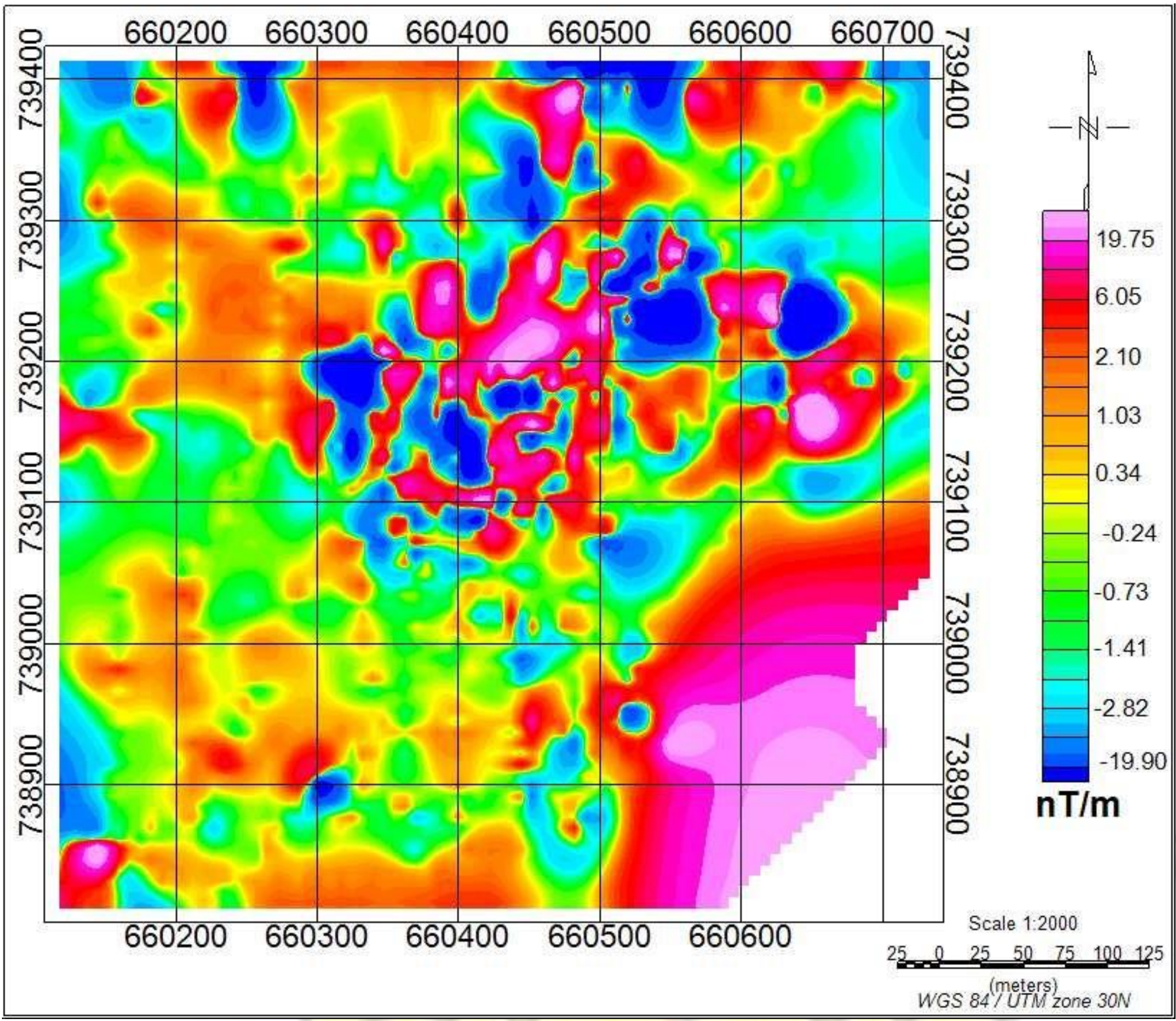

Figure 6.5 Magnetic gradiometry data of the KNUST disposal site.

The analytical signal derivative of the magnetic gradiometry map shows the zones of high magnetic signature representing the position of the waste deposit with magnetic intensities greater than of 0.6 nT/m^2 (Figure 6.6). The main waste is mapped at the central part of the site, with the northern and the western parts of the site recording significant anomalous high magnetic values. This high magnetic signature is attributed to the ferrous metal composition of the waste, mainly from domestic food cans and ferrous metals from hospital waste disposed at the site. Magnetic halo around the main waste can also be identified. The uncontrolled nature of the waste deposition at the site is also evident in the form of various spots of high magnetic anomaly as observed in the various parts of the area.

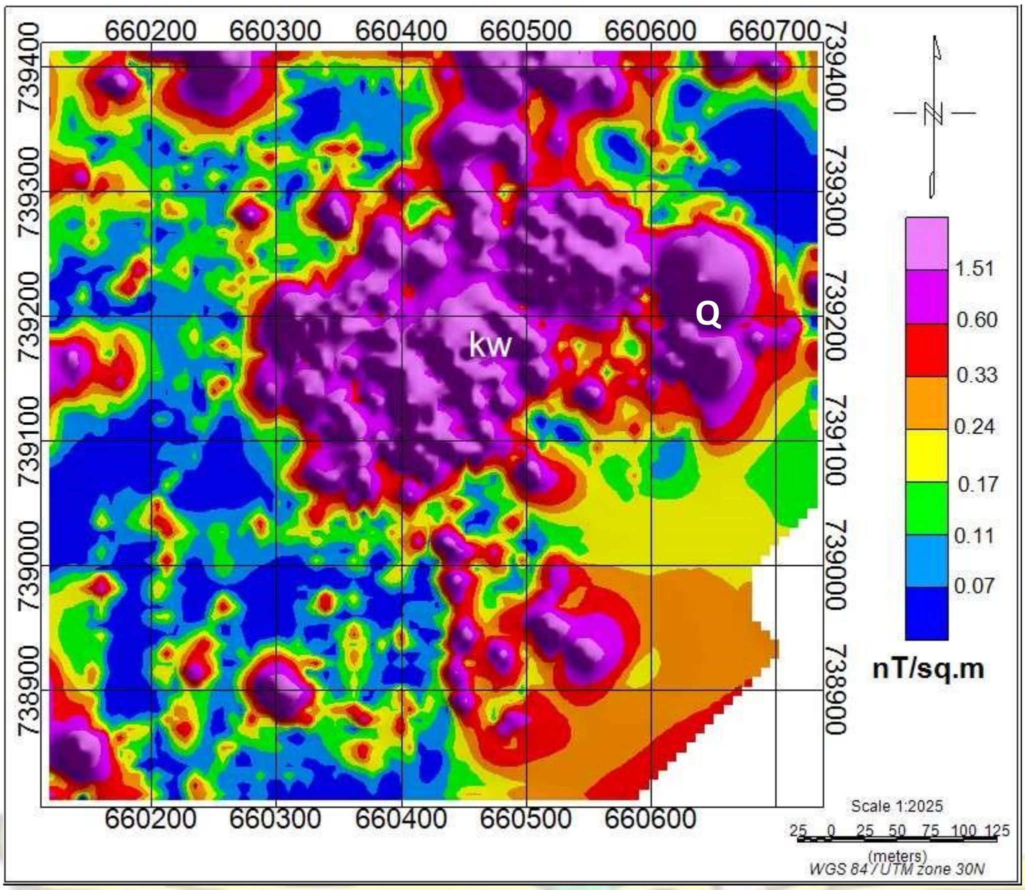

Figure 6.6 Analytical signal derivative of the magnetic gradiometry result.

Generally, both magnetic results show almost the same signature over the area except at the points labelled kw (Figure 6.6) where there is different degree of magnetic anomaly strength. The main identifiable zone in the site is the high magnetic signature area which represents the position of the waste and covering a total area of approximately 300 x 400 m. There are regions of relatively moderate magnetic signature representing a zone in the site where the waste was spread over. Also notable in the area is the erratic distribution of points with high magnetic signatures. This may be attributed to the inhomogeneity in the distribution of the ferrous metal in the waste and disturbed nature of the soil in the site. The uncontrolled nature of the waste deposition at the site is also evident. The deviation in the anomaly at Q (Figure 6.6) as compared to (Figure 6.4) is due to the high sensitivity to nearby magnetic noise sources by the magnetic gradiometry data compared with the TMI data.

6.4.2 Time Domain Spectral Induced Polarization

6.4.2.1 Processing of IP Data

The resistivity and chargeability (gate 5) pseudosections of profile 8 are shown in Figure 6.7 (a and b). The grey data points on the section show bad data points that were deleted from the section. In all about 95% of the data points were maintained for resistivity (Figure 6.7a) while about 87% were maintained for chargeability (Figure 6.7b) for the inversion. Figure 6.7c and Figure 6.7d show the IP decay of the raw data with the deleted data points in grey colour. The bad data points can be caused by poor contact between the electrodes and the ground, couplings, instrument errors or noise of unknown origin.

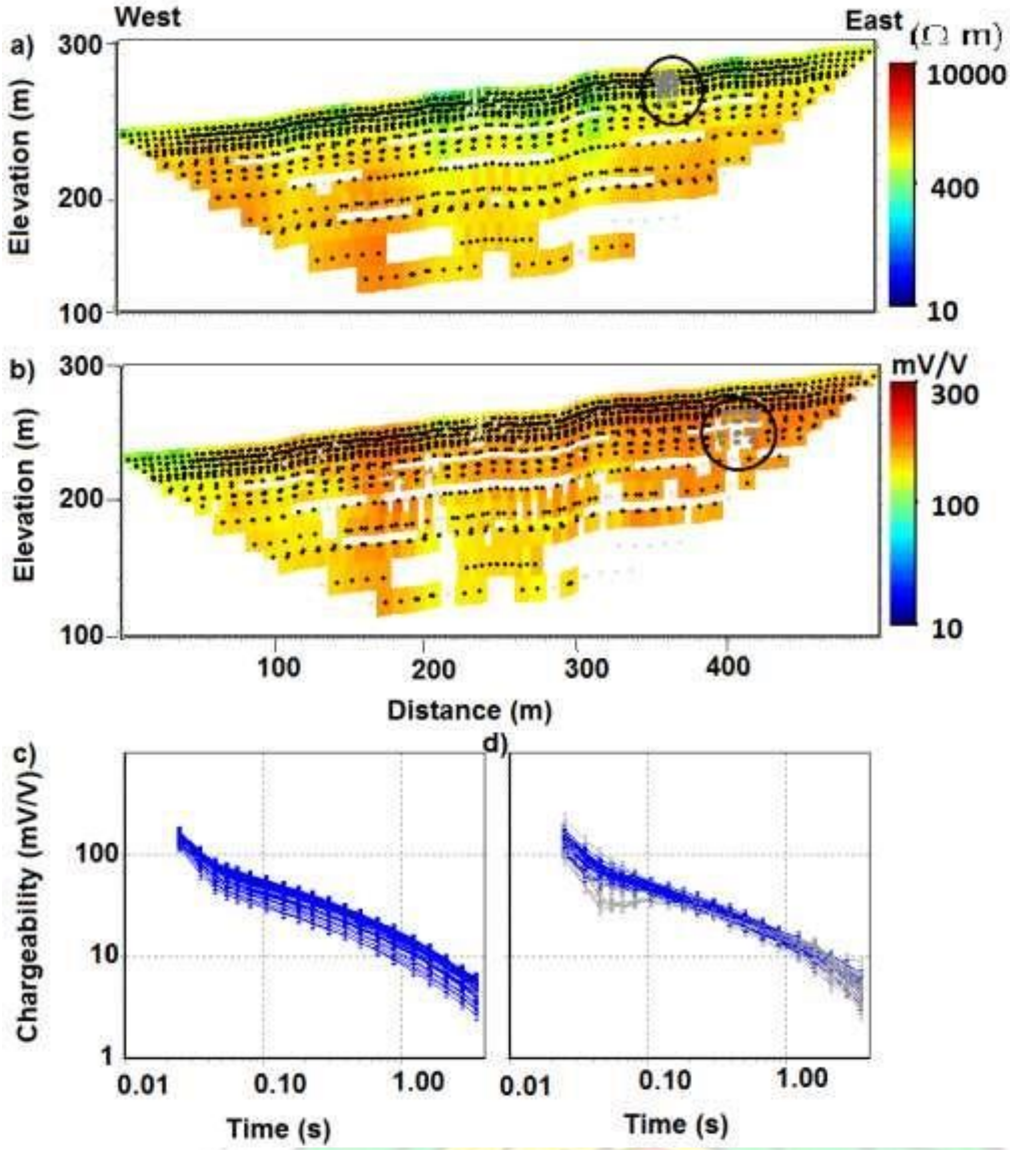

Figure 6.7 Figure 2 Section showing a) resistivity pseudosection, b) chargeability pseudosection of gate 5 c) smooth decay curve picked from the black circle on section a d) smooth decay curves in blue and deleted outlier in gray picked from the black circle on section b

6.4.2.2 Time Domain Spectral Induced Polarization Pseudosections

The inversion results of spectral time domain induced polarization of four profiles are presented in Figure 6.8 (1 and 5) and Figure 6.9 (Profile 10 and 11). The profiles in Figure 6.8 were surveyed across the waste while those in Figure 6.9 did not traverse the waste. The sections a-d (Figure 6.8 and Figure 6.9) represent the spectral induced polarization Cole-Cole inversion parameters, i.e. section (a) resistivity (ρ), (b) chargeability (m_0), (c) relaxation time (τ) and (d) frequency factor (*C*). Furthermore, the normalized chargeability sections (e), computed as the ratio of the m_0 and ρ parameters, and the misfit sections (f) are presented. Also shown on Figure 6.8 are the picked surfaces that were used to generate the waste thickness, plume thickness and the geological models of the area. The boreholes drilled in the course of this study, showing the waste thickness and geological logs were also shown on profiles 5 and 11.

The profile 1 (Figure 6.8a1-f1) located on the edge of the site and shows a distinct reduction of resistivity in the granitic bedrock (*FWZ*) is interpreted as a fractured zone and considered to be a potential threat to groundwater quality; profile 5 (Figure 6.8a2-f2) traverses the main waste and presents anomalous signatures linked to the waste and the resulting pollution plume. Profiles in Figure 6.9 present signatures of the IP parameters that are related mainly to the geology of the area, hence serves as a guide to lithological model development.

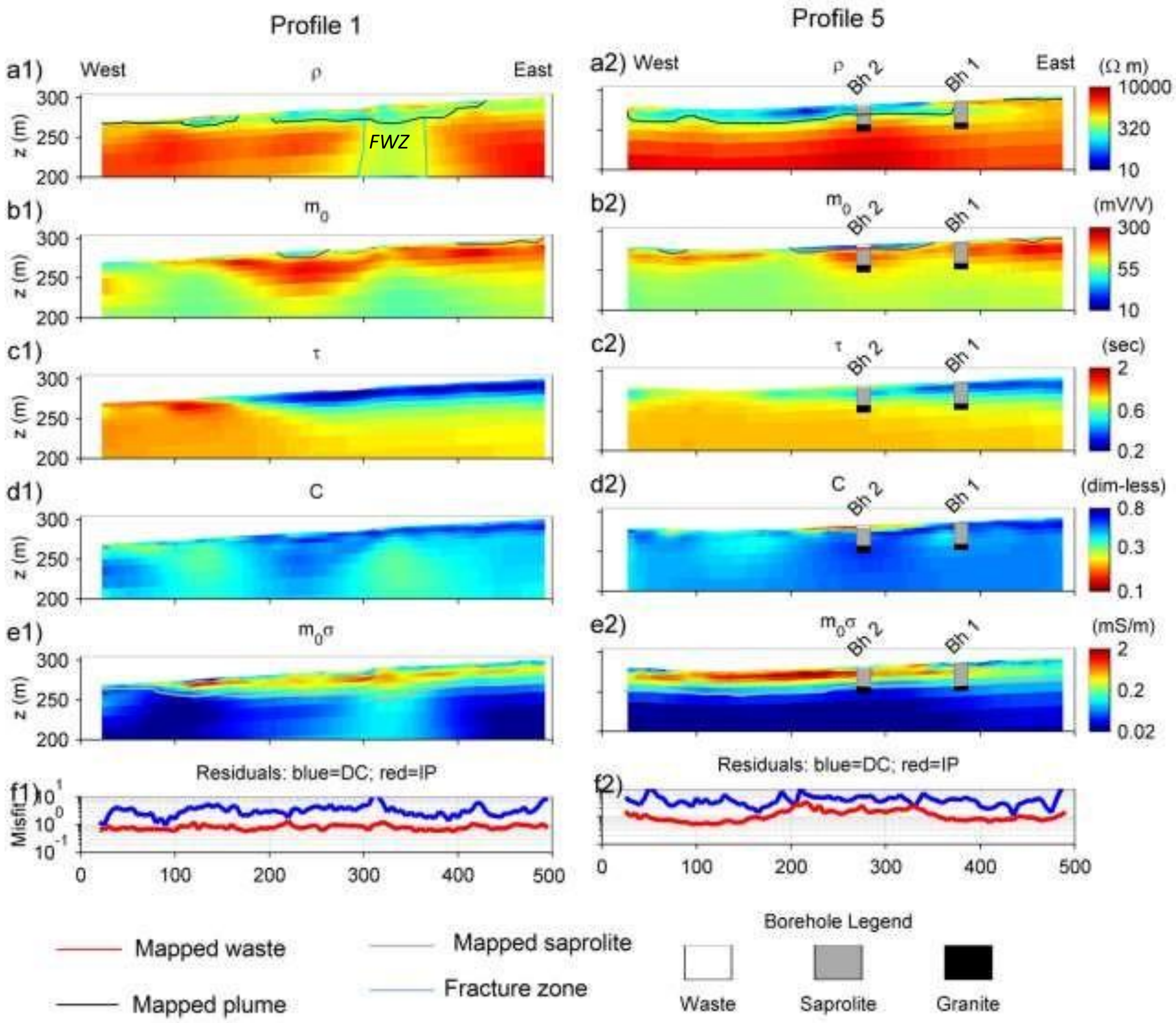

Figure 6.8 Cole-Cole DCIP parameters of profiles 1 (sections 1) and 5 (sections 2) a) resistivity section showing the picked plume bottom b) chargeability section showing the picked waste bottom c) frequency factor section d) relaxation time e) normalized chargeability section showing the picked saprolite granite interface f) misfit of the inversion results.

The resistivity sections (Figure 6.8 a1 and a2) can be categorized into three zones. These are zone 1 with resistivity value less than 140 mΩ, zone 2 with resistivity values in the range of 200–2000 mΩ and zone 3 with resistivity values greater than 2000 mΩ. The low resistivity zone (zone 1) is observed in profile 5 (Figure 6.8a1) with thickness ranging from 9 to 16 m and with thickness ranging from 1 to 28 m on profile 5 (Figure 6.8a2). Zone 2 having thickness between 5 to 30 m (Figure 6.8a1) and thickness between 10 to 35 m (Figure 6.8a2) are also observed to overlay the high resistivity lower layer (zone 3). The zone 2 is seen to reduce considerably in thickness below the position of the low resistivity layer. One of the most prominent features on Figure 6.8a is the down dipping low resistivity zone (FWZ) between the profile length 280 and 380 m. Also observed in this zone (FWZ) is a distorting signature in chargeability section (Figure 6.8b1) and frequency factor section (Figure 6.8d1). These signatures are seen to traverse the entire geological layer and also observed in nearby profiles.

Similarly, the chargeability sections show three main distinct chargeability zones, these are zone one with chargeability value less than 50 mV/V, zone two with chargeability value greater than 100 mV/V and zone three with chargeability values between 50–100 mV/V. This zone has thickness ranging between 1–3 m on profile 1 (Figure 6.8b1) and in the range of 1 to 5 m on profiles 5 (Figure 6.8b2). The high chargeability layer, zone 2 with thickness in the range of 5 to 40 m (Figure 6.8b1) and 10 to 46 m on profile 5 (Figure 6.9b2) were observed.

Furthermore, the relaxation time sections (Figure 6.8c1 and c2) show two zones. Zone one with tau values less than 0.5 and zone two with tau values greater than 0.5. The thickness of zone one ranges between 2 to 30 m on the two profiles (Figure 6.8 c1 and c2). The position of the low conductivity which corresponds in part to the position of decreasing chargeability leads to a general increase in the value of the tau as noted in the western ends of the sections.

Figure 6.8(d1 and d2) are the frequency factor sections of profiles 1 and 5 respectively. Figure 6.8e2 produces value less than 0.3 that seems to correlate with the waste thickness.
These positions coincided well with the position of low chargeability signatures that was used to produce the waste model. The normalized chargeability sections in Figure 6.8(e1 and e2) present two main zones. The high normalized chargeability zone with values greater than 0.2

mS/m that has thickness in the range of 25 to 30 m. Below this zone is a low normalized chargeability zone which has value less than 0.01 mS/m.

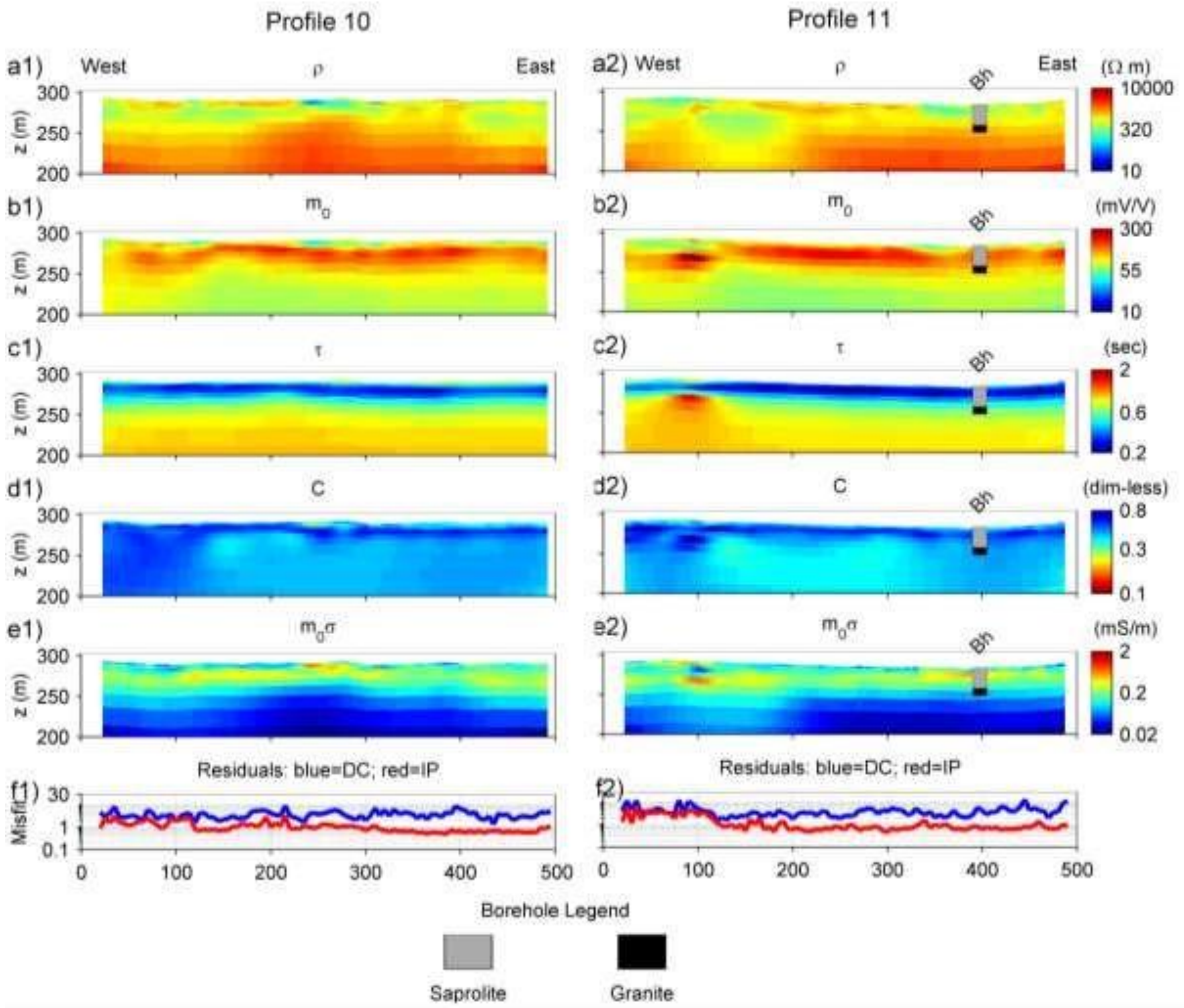

Figure 6.9: Cole-Cole DCIP parameters of profiles 9 (sections 1) and 10 (sections 2) a) resistivity section b) chargeability section c) frequency factor section d) relaxation time e) normalized chargeability section f) misfit of the inversion results.

Figure 6.9 shows the IP Cole-Cole inverted parameter sections of two surveyed profiles which do not traverse the waste. Comparing these sections to Figure 6.8, shows that distortions which were observed in the IP parameter sections at areas of low conductivity (Figure 6.8) which were attributed to increasing pour conductivity (Olorunfemi and Griffiths, 1985; Barker, 1990; Wemegah *et al.*, 2015) were absent in these sections. Comparing the drilled lithological logs to the sections (Figure 6.9b) shows a strong correlation between the saprolite thickness, hence the depth to granitic bedrock with distinct anomaly zones in chargeability, relaxation time and normalized chargeability sections. Generally, high resistivity (>200), low chargeability (<100 mV/V) and high relaxation time (>0.5) signatures are associated with the granitic bedrock. Furthermore, the chargeability section, the relaxation time and normalized chargeability sections (Figure 6.9b, c and e) produced high signature (>100 mV/V), low signature (<0.5) and high signature (0.15 mS/m) respectively which mapped the saprolite. The thickness of this layer also corresponds to the depth of the bedrock which is in the range of 25 to 30 m as observed in the drilled log.

By comparing the borehole logs and the magnetic map with the time domain induced polarization (TDIP) inversions, it is possible to identify several general trends in the distributions of the Cole-Cole parameters, in the exemplary profiles 1 and 5 (Figure 6.8) as well as in the other profiles 10 and 11 (Figure 6.9):

- A significant contrast is present between saprolite and granite in terms of resistivity (ρ), chargeability (m_0) relaxation time (τ). In particular: i) the granite resistivity is at least 50 times higher than saprolite resistivity, except in localized areas where the granite resistivity decreases significantly; ii) the saprolite chargeability (m_0) is about one order of magnitude higher than the granite chargeability, except in the areas of low resistivity, where the contrast is smaller or absent (e.g. Figure 6.8b2); iii) the relaxation time (τ) is smaller in the saprolite layer.
- In the saprolite layer a spatial correlation between low resistivity and low chargeability areas are present (e.g. Figure 6.8a, b and Figure 6.9a, b). Distinct low relaxation time signatures that mapped the saprolite layer are observed in the sections (Figure 6.9e1 and e2) which do not traverse the waste hence devoid of the effect of pore fluid conductivity. Similarly, the normalized chargeability (□m_0) sections show smaller

lateral variability when compared to the (m_0) sections and a higher vertical contrast between saprolite and granite.

- The waste lateral extent mapped by the magnetic survey and the waste thickness measured in the borehole logs correlate with areas of low m_0 and C values.
- The resistivity values in the vicinity of the waste areas in the saprolite layer are significantly smaller than in the zones far from the waste, but the areas of decreased resistivity are bigger than the waste extent, both vertically and horizontally.
- Localized areas of low resistivity are present in the granite layer, with more than two order of magnitude of resistivity contrast (e.g. Figure 6.8a1, from 300 to 360 m along profile 5). These areas are spatially correlated in adjacent profiles.
- The tau sections of profiles that do note traverse the waste (Figure 6.6 e1 and e2) produces low signature which correlates very well with the depth of the saprolite, granite interface as observed in the lithological unit from the drilled log (Wemegah *et al*., 2014, 2015).

The general decreased resistivity values in the vicinity of the waste body, as retrieved by the IP parameters and the magnetic survey, together with the correlation of low resistivity and low chargeability values in the saprolite layer, suggest that the decreased resistivity is due to an increase in the pore fluid conductivity caused by the infiltration of leachate into the soil. In fact, as documented by Lesmes and Frye (2001) and Slater and Lesmes (2002), an increase of the fluid conductivity would imply a reduction of both the resistivity and chargeability values. Consequently, the low resistivity areas can be interpreted as areas polluted by the waste leachate. This interpretation is also corroborated by the thickness of the low resistivity anomalies, which is significantly bigger than the waste thickness, as known from waste site records and confirmed by the borehole loggings. This means that the DC resistivity method alone is not enough for mapping the waste body in this unprotected and unengineered waste site, where the leachate infiltrates from the waste to the porous subsoil. This interpretation of the low resistivity anomalies suggests that the normalized chargeability is the better parameter linked to the site lithology, being less affected than chargeability by the water conductivity.

Low relaxation time produces low signatures that correlated very well with the saprolite thickness. This is due to the fact this parameter is inversely related to the sample pore hence the hydraulic conductivity of the subsoil (Ruffet, *et al*., 1991; Bomer *et al*., 1996; Boadu, 2000; Boadu and Seabrook, 2000). Binley *et al*. (2005) and Revil and Florsch (2010) reported an inverse relation between the characteristic hydraulic conductivity and the relaxation time. The weathered saprolite layer generally has a high porosity as compared with its underlying consolidated granitic bedrock. This distinct difference in the porosity between the two stratigraphic units makes it possible for the relaxation time to be used in mapping these units. It was noted from profiles that traverse the waste deposit that increasing pore conductivity greatly affects this effect hence making it unusable in the mapping of the lithological set up of the area.

Localized areas of low resistivity present in the granite bedrock observed in the northern profiles close to profile 1 (Figure 6.8a1) and some of the southern profiles (Figure 6.1) were interpreted as fracture zones. The Birimian sediment basin which consists of weathered zone of saprolite top layer has various associated fractured zones within the granitic bedrock often containing mylonites which serve as potential aquifer (Wright *et al.,* 1985; Wright and Burgess, 1992). Kortatsi (1994) stated that the fractured zone aquifers normally occur at depth beneath the weathered zone. These zones which are mostly water saturated produce low resistivity signatures as observed and therefore serve as potential aquifer in the area. This signature which was also observed in the adjoining profiles were therefore attributed to the presence of fracture and used in the development of the fracture model of the study area.

Groundwater occurrence is associated with the development of secondary porosity as a result of jointing, shearing, fracturing and weathering. This has given rise to two main types of aquifers; the weathered zone aquifers and the fractured zone aquifers. The weathered zone aquifers usually occur at the base of the thick weathered layer. The fractured zone aquifers normally occur at some depth beneath the weathered zone. Both types of aquifers are normally discontinuous and limited. Due to the sandy clay nature of the weathered overburden, the groundwater occurs mostly under semi-confined or leaky conditions (Kortatsi, 1994).

Contrary to the resistivity distribution, two IP parameters show a signature clearly linked to the waste body. In fact, the waste shows low m_0 and C values, typically below 50 mV/V and 0.2 respectively, which is smaller than the saprolite values. This is different from what is usually reported in the literature, where the waste generally presents high chargeability values (e.g. Slater and Lesme, 2002; Gazoty *et al*., 2012a; Gazoty *et al*., 2012b, Gazoty *et al*., 2013). This may be due to the waste composition and the annual burning of the area, which leads to decreased biological activity in the waste. The effect on IP parameter by bioremediation in waste is reported (e.g. Abdel Aal *et al*., 2004; Atekwana *et al*., 2004a, 2004b). Atekwana *et al*. (2004a) reported that high IP effects are produced in zones where peak microbial populations and activity are known to occur in study of IP effect in petroleum contaminated samples.

6.4.3 Models from IP Inversion Parameters

The chargeability, resistivity and normalized chargeability results were used to map the waste, leachate plume and the saprolite-granite interface respectively. The picking of the interfaces was done using an *ad hoc* tool provided in Aarhus Workbench (Wemegah *et al.,* 2015). The mapping was done by first picking: i) the elevation of the interface corresponding to the low resistivity anomaly (below 140 Ωm) in the resistivity sections (Figure 6.7a1 and a2) to map the plume bottom; ii) the elevation of the interface corresponding to the low m_0 anomaly (below 50 mV/V) in the chargeability sections (Figure 6.7b1 and b2) to map the waste bottom; iii) elevation of the interface corresponding to normalised chargeability (greater than 0.09 mS/m) in the normalized chargeability sections (Figure 6.7e1 and e2) to get the saprolite-granite interface. The picked points were then gridded with the Kriging algorithm to generate the waste bottom, plume bottom and the saprolite bottom (saprolitegranite interface) surfaces. Secondly, the thickness models were obtained by subtracting the gridded surfaces from the digital elevation model of the area.

6.4.3.1 Modelled Waste Thickness

Figure 6.10 presents the mapped waste thickness delineated using the low chargeability areas of the inversion models. From the result, the main waste was mapped in the central position of the site (kw, Figure 6.10) with thickness ranging from 3 to 10 m. The waste mapped in the western boundary of the site is the area where the waste was spread to, from the main deposit site. The waste mapped at northern part of the site extended into the KNUST Senior High School, this is also observed in the magnetic data (Figure 6.4 and Figure 6.6). The lateral extent of the mapped waste mapped from the IP data (Figure 6.10) is in agreement with the magnetic results, but with a little reduction in the area covered. The smaller lateral extension of the waste mapped by IP is probably due to the different sensitivity of the two methods to thin waste layers: the IP inversions cannot resolve waste thickness significantly smaller than the electrode spacing which is the case at the edges of the waste.

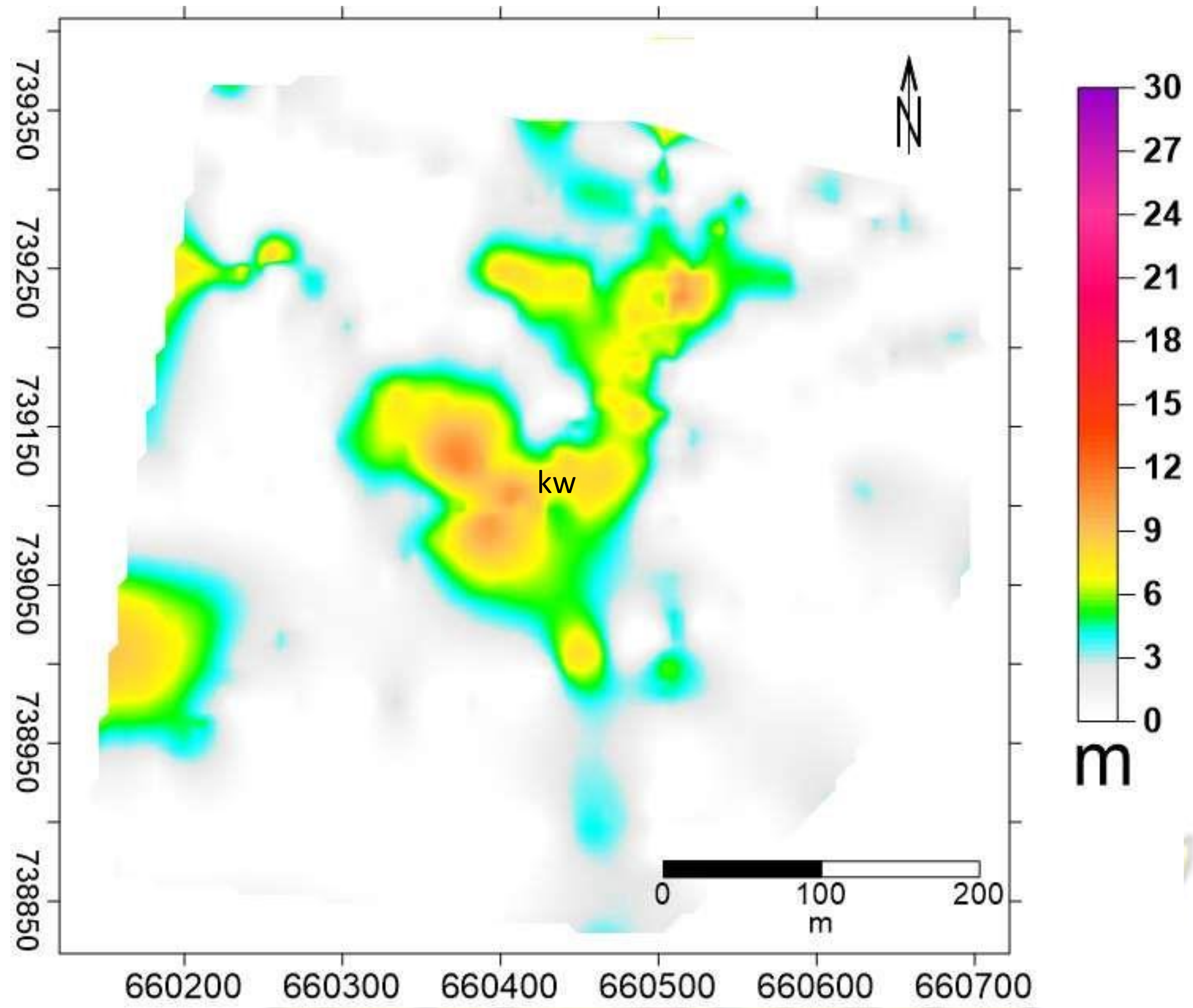

Figure 6.10 Delineated waste thickness mapped from chargeability sections.

6.4.3.2 Modelled Saprolite Thickness

Figure 6.11 shows the saprolite thickness derived from the normalized chargeability sections. The thickness of the saprolite is generally homogeneous in the study area, with the thickness around 26 m, except in the north-western part of the site, where it thins to about 10 m, and in the south-western part, where it reaches values greater than 30 m. The thinner area corresponds to the zone of low elevation (Figure 6.2) which is a position of a river channel.

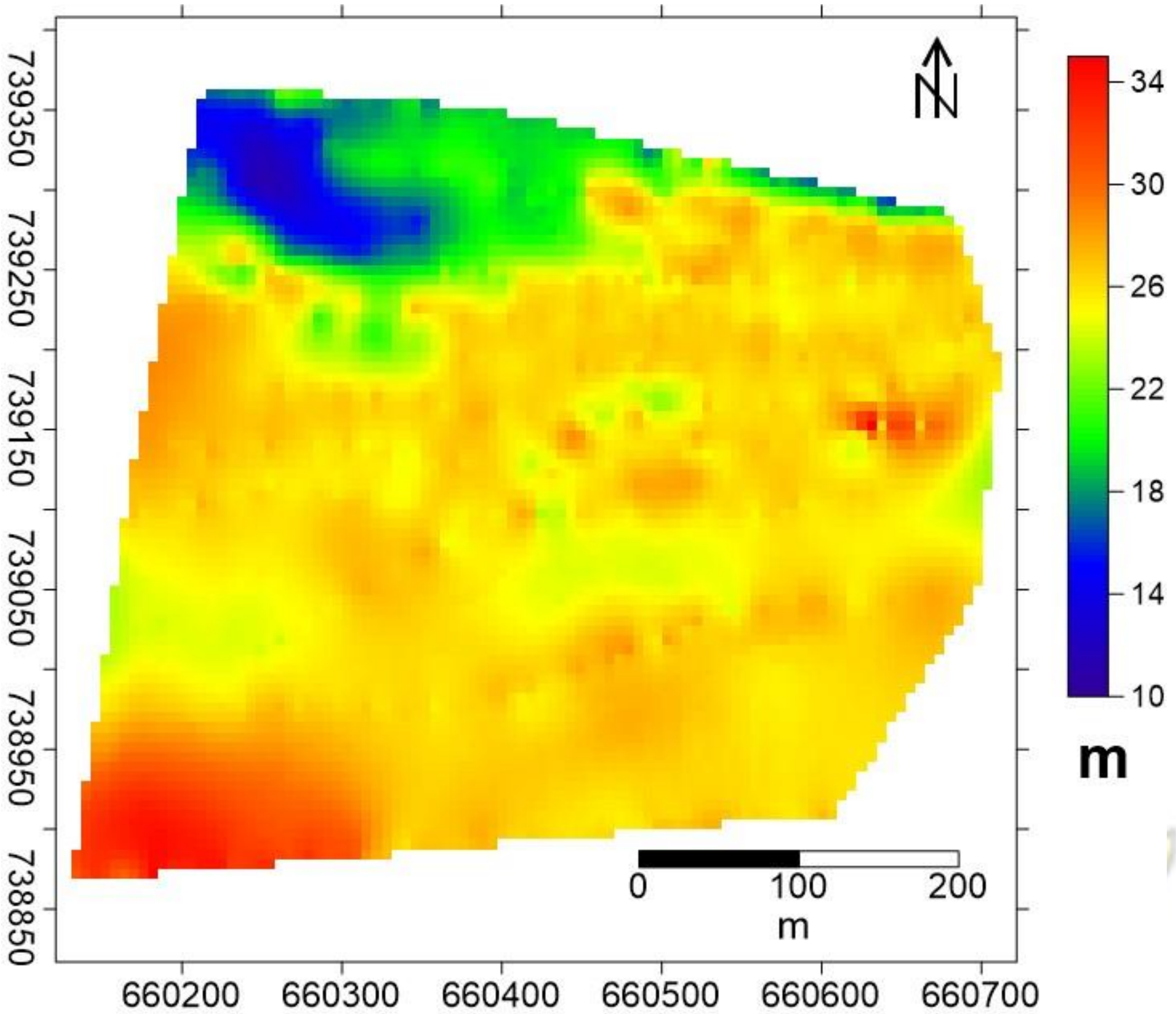

Figure 6.11 Modelled saprolite thickness map.

6.4.3.3 Modelled Pollution Plume Thickness

Figure 6.12 presents the map of the pollution plume thickness showing the distribution of pollution plume associated with the waste. The plume shows a bigger lateral and vertical extension than the waste body, as evidenced by comparing the waste thickness map of Figure 6.10. The greatest plume thicknesses (> 20 m) were mapped below the main waste (Figure 6.6 and Figure 6.10) at the central and north-eastern section of the study area. Significantly noted is the wide plume distribution in the low laying area in the north-western section of the site attributed to the leachate flow through river channel which is a tributary to river Kentikrono, used for vegetable cultivation in the area. This poses a health risk as poor quality of water used in growing crop can lead to contamination of foods which when consumed and can lead to food poison. Also superimposed on this map are the two fractured zones (black), obtained from the low resistivity anomalies in the granite bedrocks.

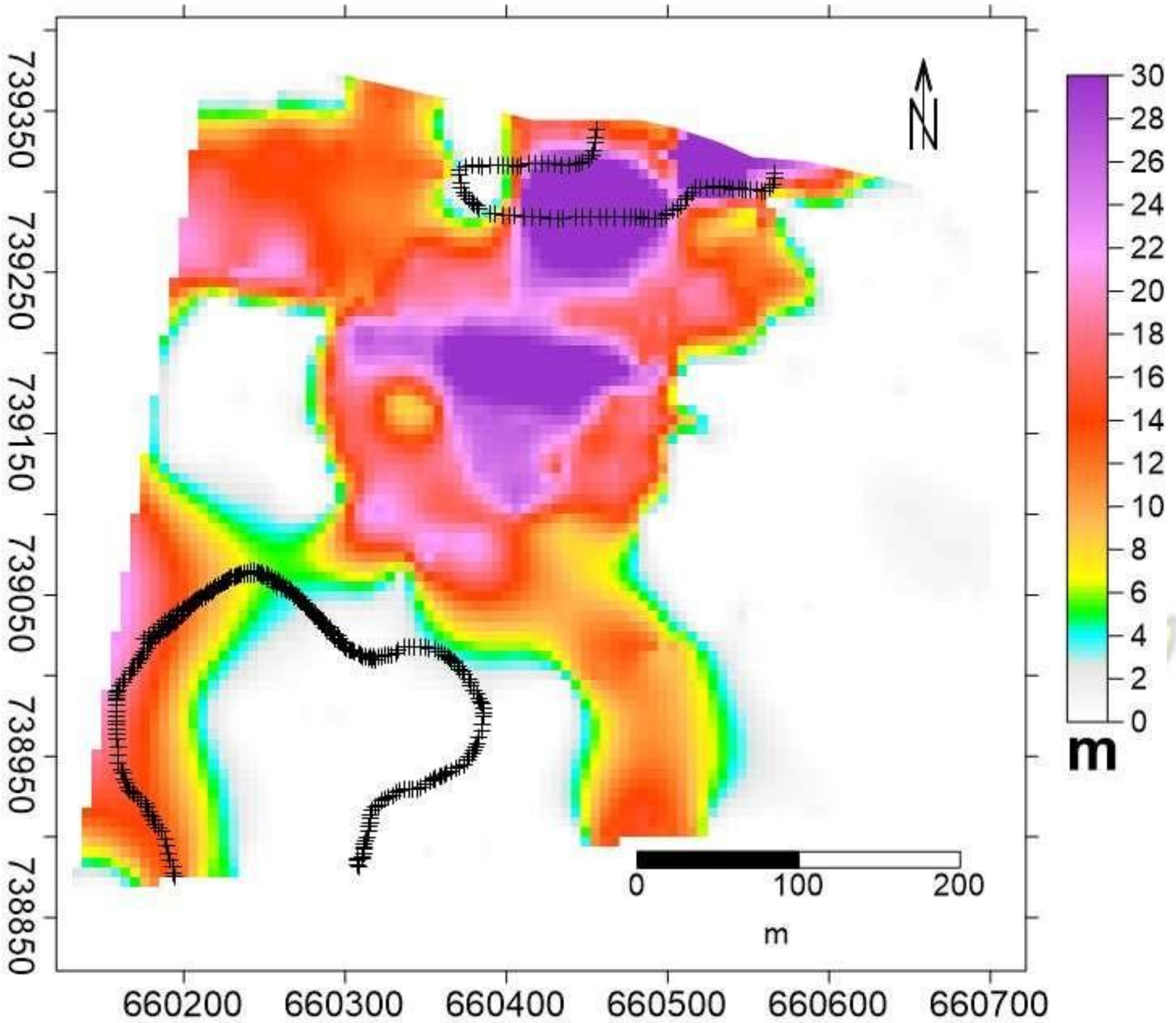

Figure 6.12 Plume thickness map with superimposed position of fractured zones (black lines) mapped in the granitic bedrock.

The superimposed fracture zones on the plume thickness map (black line, Figure 6.12) provide an insight into the vulnerability of the groundwater system to contamination from the waste. The fracture zones in the impermeable granitic bedrock serve as the mean of groundwater recharge in this formation (Kortatsi, 1994), hence a potential conduit for leachate when connected. The fracture zone in the northern part of the site is beneath the waste body (Figure 6.8 and Figure 6.10), forming a conduit for leachate infiltration. This poses a high risk of groundwater contamination and endangers the quality of water supply to the school and the hospital, which depend on the groundwater as a means of potable water supply.

6.5 Summary

Municipal solid waste monitoring and mapping has played an important role in controlling the effect of waste on the ecosystem. The full characterization of the waste framework and its impact have helped greatly in redesigning, pollution control and in some cases complete removal and relocation of the waste due to the hazard it poses to public health. In order to determine the impact of solid waste in the Kumasi Metropolis, combined time-domain DC/IP 2-D Cole-Cole parameter tomography and magnetic datasets were used in characterizing a decommissioned unengineered municipal waste deposit site situated on part of the Kwame University of Science Technological land in the Kumasi Metropolis of Ghana. High magnetic signature and low chargeability signatures aided in the mapping of the waste while low resistivity signature and normalized chargeability aided in the mapping of the plume and developing geological model of the area respectively. Resistivity is considered not to be the suitable parameter for mapping the size of the waste in geological environment like the KNUST waste site. The low resistivity signature associated with the waste could not help in mapping it but rather help in mapping the plume as it extends beyond the waste position as observed in the drilled logs. The magnetic data was used to map the lateral extent of the waste deposit. Also observed from this data is the erratic distribution of the high magnetic signature which mapped the waste. This is attributed to the inhomogeneous distribution of ferrous metals which form part of the waste. The DC/IP investigations and magnetic data helped the full characterization of the KNUST waste deposit. The KNUST waste deposit is seen to have threat to the quality of the groundwater around the KNUST SHS. The quality of groundwater in this area is at high risk from the pollutant from the deposited waste since the waste is deposited on a delineated fracture which is a potential aquifer within the area. The developed lithological model of the site can serves as an input into future hydrological model of the site.

CHAPTER 7: OHWIM MUNICIPAL SOLID WASTE DISPOSAL SITE

7.1 Introduction

The Ohwim solid waste disposal site is located in the Batama Submetropolitan area in northern part of the Kumasi Metropolis. It is about 20 km from the KNUST campus. The waste deposit was used to reclaim a valley that happened to be a head of river (Figure 4.1 and Figure 7.2) in the period, 2004 to 2009. The waste deposited at the area is mainly domestic and consists mainly of organic waste, plastic rubbers and container, ferrous metal debris and hospital waste. The only industrial waste deposited at the site is waste truck tyres used by a road constructor during road construction in the metropolis. Currently there is high development of residence settlement in the catchment area of the site. The satellite map of the site showing the position of the waste in red, the course of river (blue line) and IP surveyed profiles in yellow in the catchment area of the waste are shown in Figure 7.1.

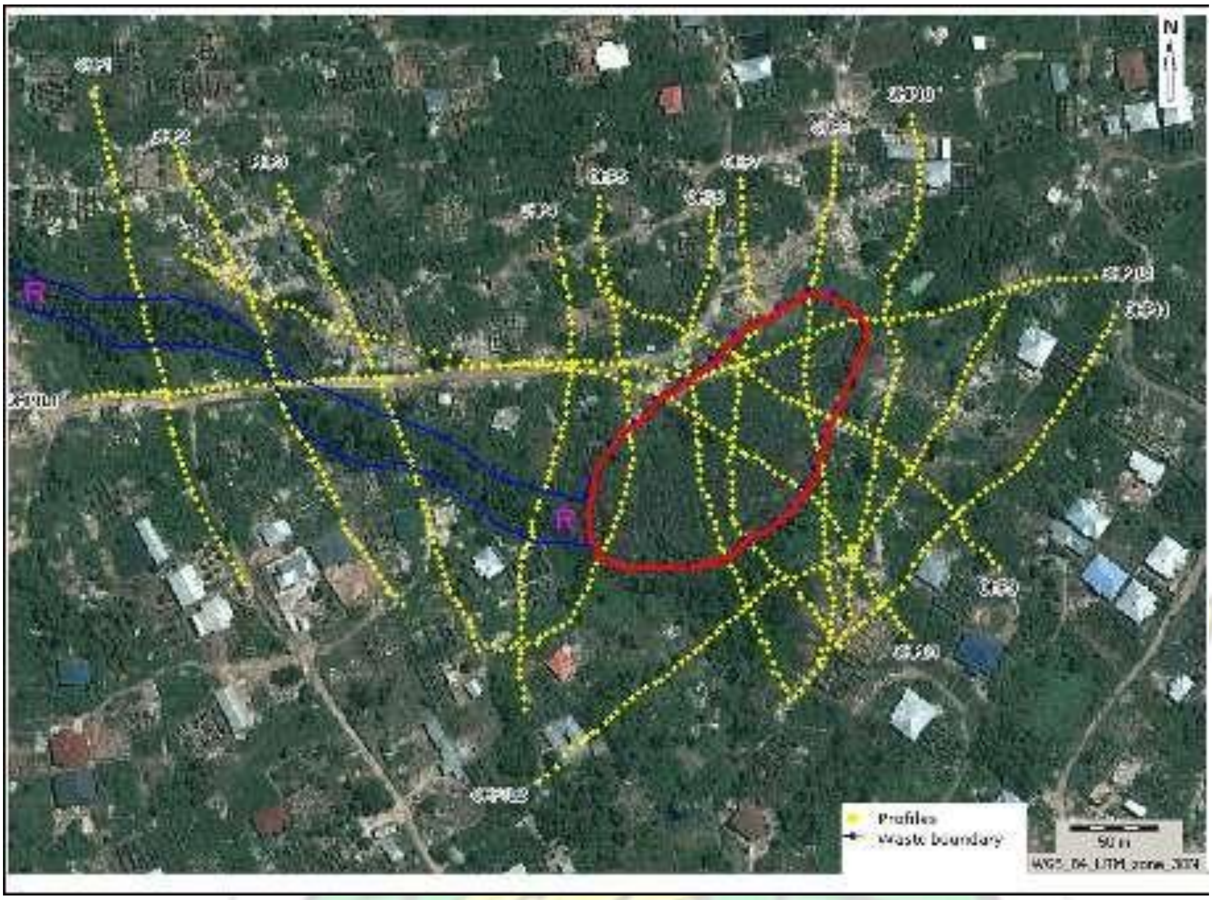

Figure 7.1 Satellite image of the Ohwim solid waste disposal site showing the position of waste deposit (red line), IP profiles (yellow lines) and the river channel (blue line, R-R).

Figure 7.1 is the satellite image of the study site superimposed on by the DCIP profiles (yellow). The red line shows the outline of the waste deposit. Also noted in this image is a river channel (blue line RR) trending in the north-western direction and covered with vegetation. The development of residential buildings in the catchment area of the waste disposal site can also be noted (Figure 7.1).

Spectral time-domain induced polarization, magnetic susceptibility and ground magnetic surveys were used in the mapping and characterization of the Ohwim municipality solid waste disposal site. These geophysical methods have aided in the full characterization of the site by mapping both the lateral and vertical extent of the waste. Waste model of the area which included the waste thickness and plume thickness maps were also developed.

Furthermore, geological model of the site which included saprolite granitic bedrock interface and the saprolite thickness hence the depth of bedrock was also produced using the IP data.

7.2 Location of the Ohwim Waste Deposit Site

The Ohwim MSW Disposal site is situated in the Bantaman Submetropolitan area of the Kumasi Metropolis of the Ashanti Region in south-western Ghana. The location of the site is defined in the UTM WGS84 zone 30 coordinate system by 646900 E to 647400 E and 747500 N to 747900 N. The site is unengineered waste disposal site with no protective under layer. The site was used for waste disposal from 2002 to 2009. Geologically, the area consists of a thick sandy-clay saprolite layer with thickness in the range of 5 to 25 m underlain by basin type granitoid.

7.2.1 Digital Elevation Map (DEM)

Figure 7.2 is the digital elevation map of the site showing the variation in topography of the area. The eastern part of the area is having the higher elevation with topographical value above 266 m above mean sea level. The lowest elevation area as depicted in the image shows N-W direction. This direction controls the hydrology of the area with the surface water flowing in the north-western direction (R-R). This channel which carried the leachate from the waste is the head or river Anomakosa which is a tributary of river Owabi waterworks from which water is extracted and treated for the Kumasi Metropolis by the Ghana Waters Company.

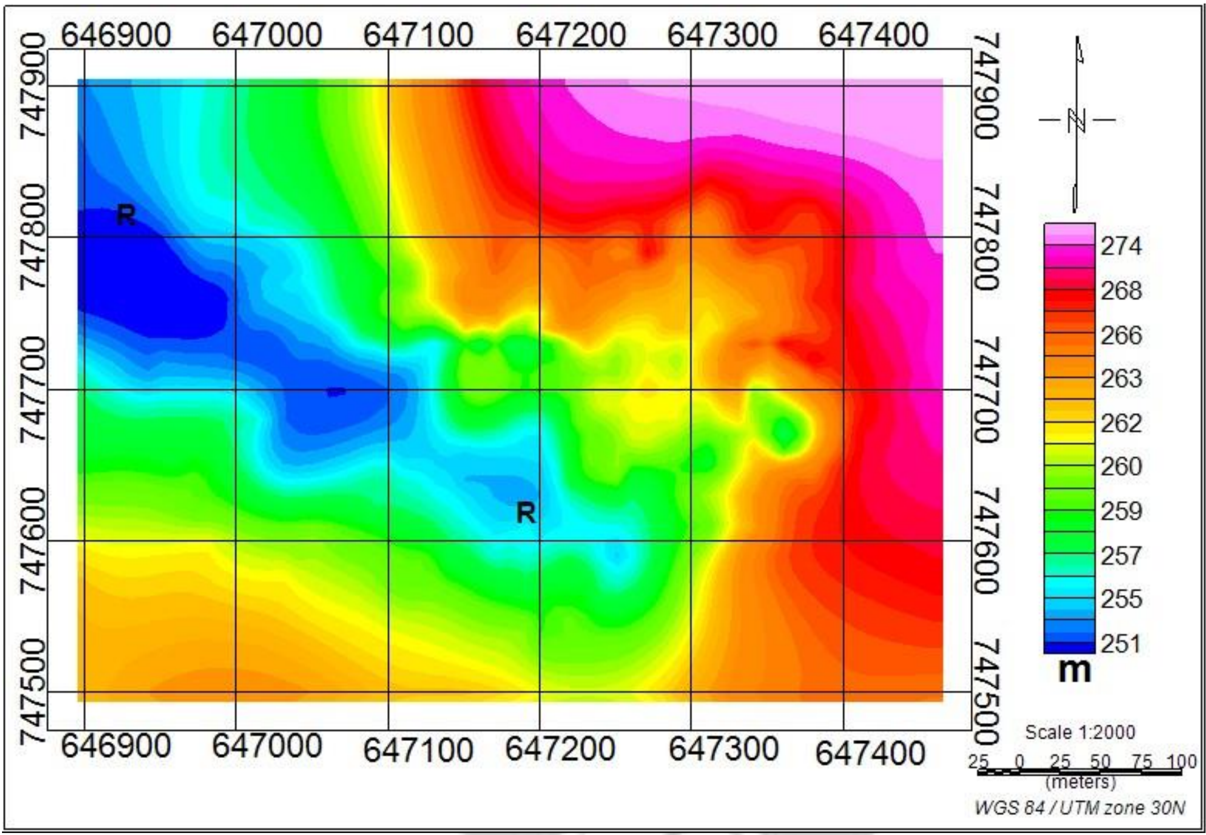

Figure 7.2 Digital elevation map of the Ohwim disposal site.

7.3 Survey Design

The spectral induced polarization were acquired with Iris SYSCAL-PRO instrument using 4 s current turn on-and-off with 20 time windows. Five metres electrode spacing was used in the surveying. The profiles were placed mainly in NW-SE direction in order to fully traverse the waste which is distributed in the NE-SW direction (Figure 7.1). The waste was estimated to have approximate width of 100 m. Fifteen (15) profiles with total lengths of 4.8 km ranging from 300 m to 600 m were surveyed in the catchment area to help in mapping the waste and its associated plumes.

The magnetic data (magnetic gradiometry and total magnetic intensity) were acquired on approximately 15 x 5 m grids. The surveys were conducted on 28 profiles with lengths ranging between 50 to 300 m. The total length of profiles surveyed was 5.7 km. The base station for diurnal correction was set at a point devoid of magnetic influence at (660436 E,

739098 N). The processing of the diurnally corrected data was carried out using the Oasis Montaj Software package. The gridding of the data was done using minimum curvature algorithm at one-quarter (1/4) the profile spacing. Furthermore, enhancement filters were applied to mainly reduce the data to the pole an important magnetic data processing techniques to help locate the observed magnetic anomalies directly over the magnetic source (e.g. Li, 2008).

Similarly, magnetic susceptibility survey was conducted on 26 profiles using approximately 15 x 5 m grid. A total of 5.7 km profile lengths were surveyed, with length of individual profiles ranging between 50 - 300 m. The data was imported into the Oasis Montaj Software package and gridding using minimum curvature algorithm at one-quarter (1/4) the profile spacing.

7.4 Results and Discussion

7.4.1 Magnetic Susceptibility Result

This section discusses the gridded magnetic susceptibility result of the Ohwim. It helps in the determination of the distribution of magnetic susceptibility signature in the area under study. It provides the potential of this method in the mapping of the lateral extent of the waste. The use of this method was based on the fact that ferrous metal which is a major component of the waste produces a strong magnetic susceptibility signature.

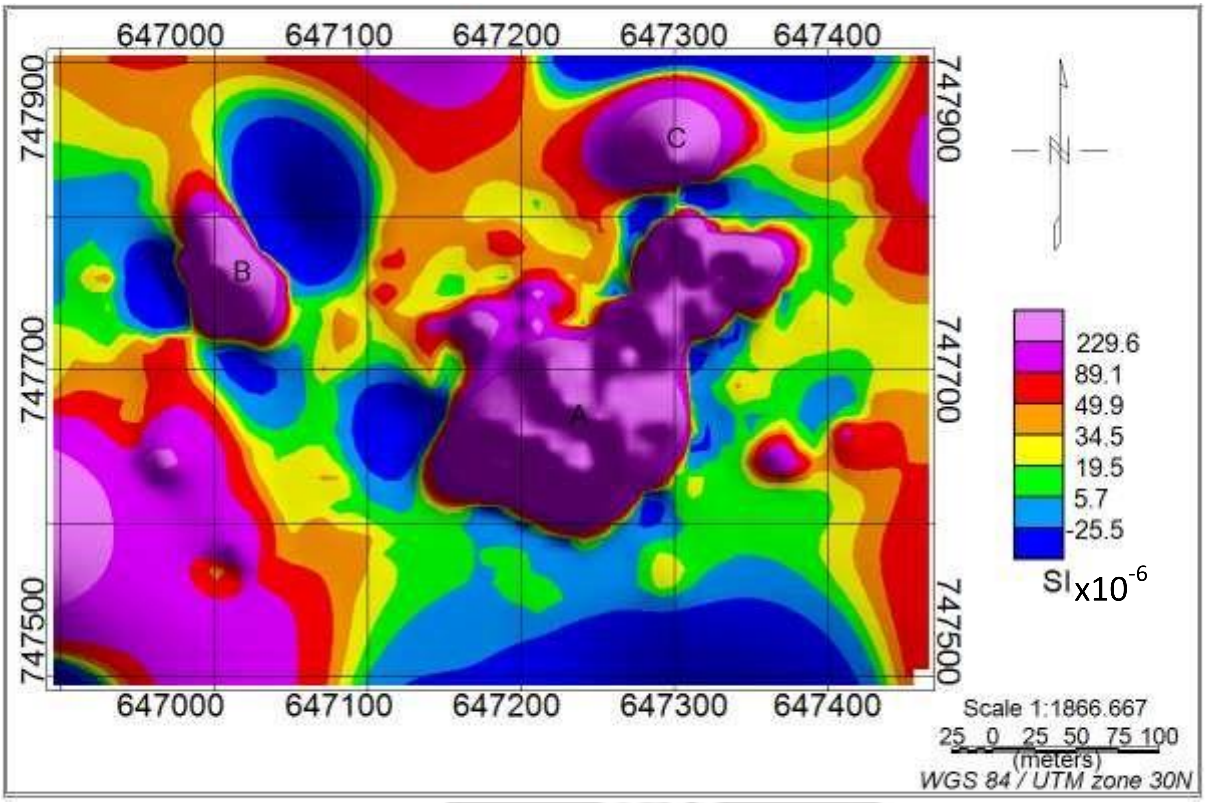

Figure 7.3 Magnetic susceptibility map of the area.

Figure 7.3 is the magnetic susceptibility anomaly map of the catchment area of the Ohwim Municipal Solid Waste Deposit Site. Three main magnetic susceptibility signatures can be identified on the map. These are the low magnetic susceptibility signature, the intermediate signature and the high signature which is attributed to the waste. Three main anomalous high magnetic susceptibility signatures (A, B and C) which are attributed to the ferrous metal composition of the waste (Wemegah *et al*., 2014) were identify. These regions produced magnetic susceptibility values greater than 89.1 x10^{-6} SI. The region A (Figure 7.3) is the main position of the waste. From this image the lateral extent of the waste is estimated as 150 m by 150 m at it broader part (southern part of the waste, A) and 90 m by 80 m at the northern part of the waste (A).

Furthermore, signature (B) shows a position where used tyres were burnt. This position is depicted with high magnetic susceptibility signature due to the remains of the rusted metal wire used in the manufacture of the tyres. Other anomalous high magnetic susceptibility signature (C, D) are due to the erratic distribution of waste in the area attributed to uncontrolled dumping of waste at the site. Despite the site having been closed since 2009, people leaving around the catchment area of the site still indiscriminately dispose off waste around the area as shown in the image.

7.4.2 Total Magnetic Intensity (TMI) Result

A total magnetic intensity survey that exhibit magnetic properties that result from the presence of iron oxides in different forms and quantities was conducted on the Ohwim disposal site. The residual magnetic data obtained in magnetic survey in geological environment measures the composition of the magnetic minerals mainly ferrimagnetic minerals such as magnetite and maghemite in the rock formation (MacLeod *et al*., 1993). It serves as a means of distinguishing between different rock types based on their magnetic content. In case of waste mapping, the magnetic data produces anomaly that consists of the result of magnetic data of the waste due to it ferrous metal content superimposed on the signature produced by the geological environment.

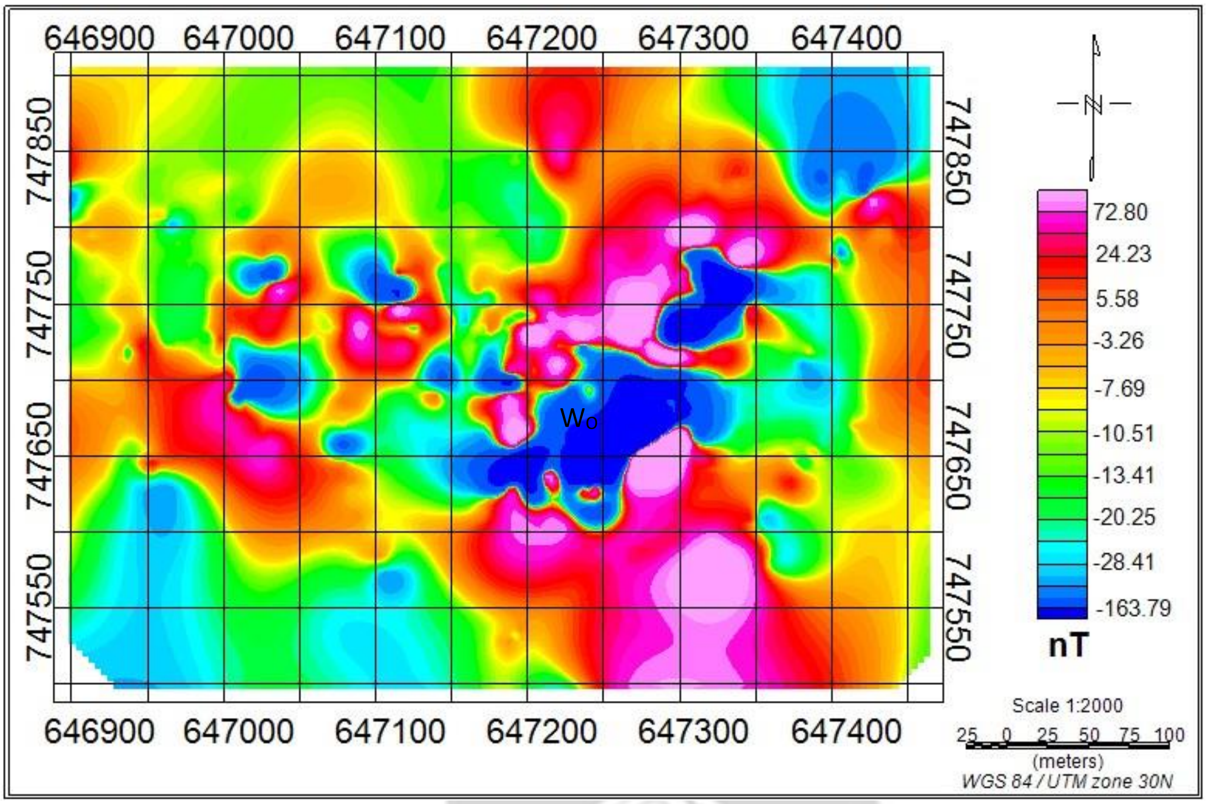

Figure 7.4 Total magnetic intensity map.

Figure 7.4 is the total magnetic intensity map of the study area. The ambient magnetic field in the location is 32,000 nT and the measured values range from 31742.2 to 32904.6 nT, with the anomalous residual field ranges from -615.86 to 3432 nT. The position of the waste is depicted with low magnetic value (W_o) which corresponds to area of high magnetic susceptibility (Figure 7.3). This reversal of magnetic signature is due to the effect of the geomagnetic field on the data since the data is collected at low magnetic latitude region. This area is surrounded by high magnetic signature (low magnetic susceptibility). In order to produce the observed magnetic anomaly directly above the source analytical signal filter was applied on the data to produce Figure 7.5.

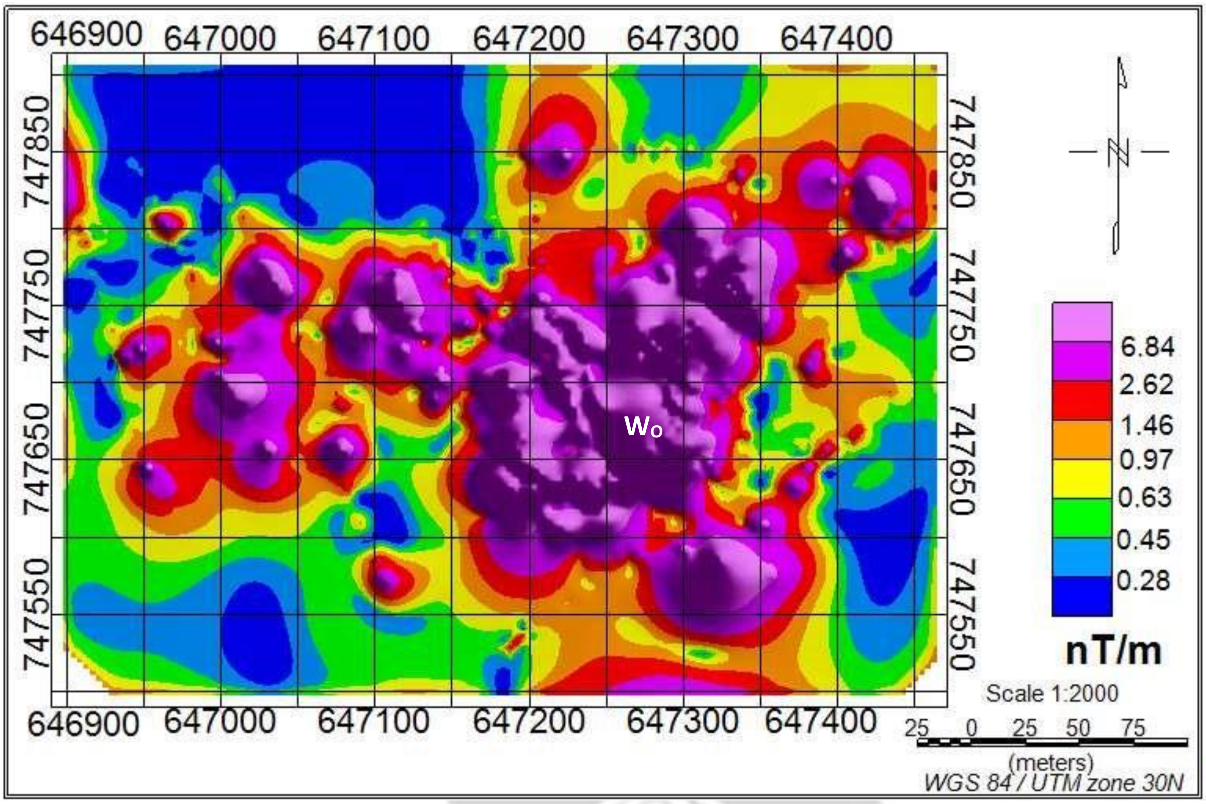

Figure 7.5 Analytical signal derivative map of the total magnetic intensity data.

The analytical signal image of the research area (Figure 7.5) mapped the wastes lateral extent with high magnetic signature. The main waste (W_o) is mapped at the central part of the site with a dimension of 150 x 250 m, western parts of the site also recorded significant anomalous magnetic signature attributed to the burnt tyre position. This high magnetic signature is attributed to the ferrous metal composition of the waste, mainly from domestic food cane and ferrous metal. Intermediate magnetic signature halo around the main waste can also be identified. The uncontrolled nature of the waste deposition at the site is also evident in the form of various spot of high magnetic anomaly as observed in the various part of the area.

7.4.3 Magnetic Gradiometry Result

The magnetic gradiometry which is said to be more sensitive to near surface magnetic features was conducted on the study area. This was done in order to aid in the mapping of small waste bodies in the area which were indiscriminately disposed in the area due to the uncontrolled nature of the waste disposal in the site. Figure 7.6 is the gridded magnetic gradiometric data over the catchment area of the Ohwim MSW, showing the distribution of the magnetic signature in the area. The total magnetic intensity values measured by the lower sensor ranges from 31680.96 to 33139.75 nT. Similarly, the measured magnetic gradiometric field values of the area ranges from -230.51 to 386.57 nT/m. The position of the waste is depicted with low magnetic value which corresponds to area of high magnetic susceptibility.

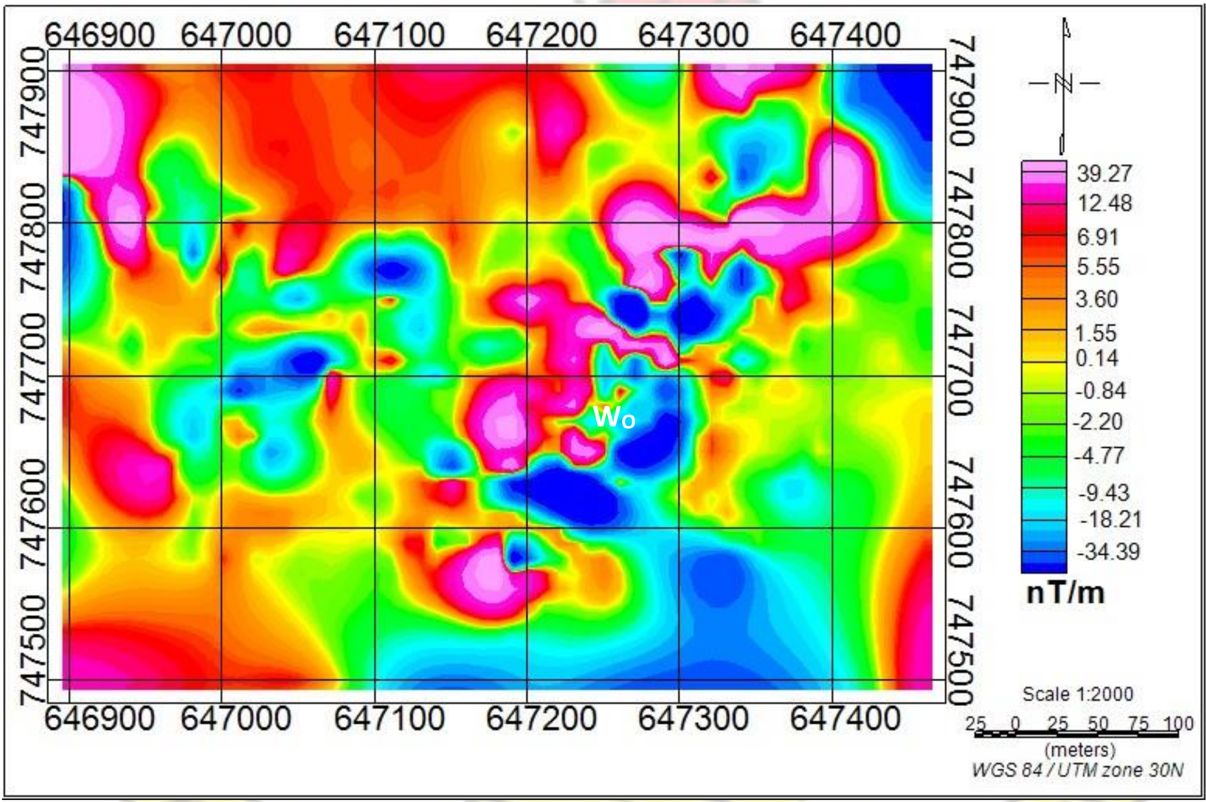

Figure 7.6 Magnetic gradiometry map.

The analytic signal transforms the magnetic datasets (Nabighian, 1972, 1984) on the other hand is the reduced to the pole map of the total magnetic intensity map of the area. Three main distinct anomalous zones are observed on this map. These are the high magnetic signature in the eastern corner of the map, low halo of magnetic signature separated by a medium magnetic signature. Comparing Figure 7.1 and Figure 7.7, it is observed that the main disposal site is delineated with high magnetic signature. This high signature is attributed to the presence of ferrous metal in the waste. Like the KNUST waste disposal site (Figure 6.4 and Figure 6.6) erratic distribution of the signature may be attributed to the inhomogeneity in the distribution of the ferrous metal in the waste and uncontrolled disposal of waste at the site.

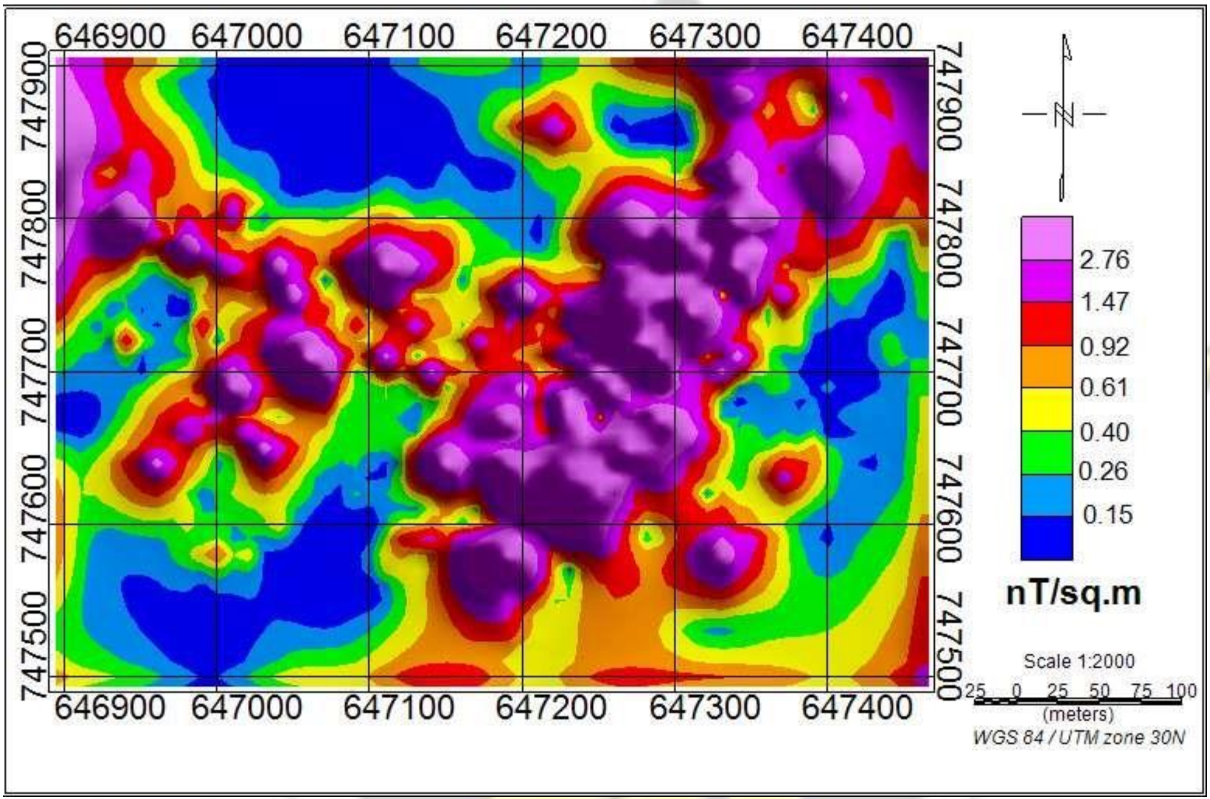

Figure 7.7 Analytical signal derivative map of the magnetic gradiometry data.

The analytical derivative map from both the magnetic gradiometry (Figure 7.7) and the TMI (Figure 7.5) surveys show similar magnetic signature over the study area except at the northeastern corner of the images where the gradiometry data shows high magnetic signature compared with the TMI. This area is closer to the community hence the difference could be attributed to the influence of the power lines and building since the magnetic gradiometry is more sensitivity to near noise sources. The lateral extent of the waste as mapped by the two datasets is 150 m by 250 m wide.

7.4.4 Spectral Time Domain Induced Polarization

Figure 7.8 presents the inversion results of two representative profiles which were surveyed on the main waste, in terms of the Col-Cole parameters (ρ, m_0, τ and C) and normalized chargeability. The resistivity section (Figure 7.8a) shows a low-resistivity anomaly (below 20 Ωm) that coincides with the waste deposit and the plume between 80 and 150 m profile length (profile 7) and 130 and 240 m profile lengths (profile 8). Furthermore, a moderate decrease in resistivity is observed in the northern part of the profile 7, below 10 m in depth. The chargeability sections (Figure 7.8b) also show relatively intermediate signature at the position of the waste. This chargeability anomaly does not correlate well with the waste. Also noted in this image is the high chargeability signature at the northern part of the sections attributed to the leachate plume. The normalized chargeability sections show high signature (Figure 7.8e) that is associated with the waste. This signature was used in mapping the waste thickness in the area. The frequency factor sections (Figure 7.8c) do not produce any signature that can help in mapping anything of interest. The relaxation time sections (Figure 7.8d) produced a low signature that is associated with the saprolite at the top 10 to 30 m depth of the section but are distorted beneath the waste due to the increase in pore fluid conductivity below the waste.

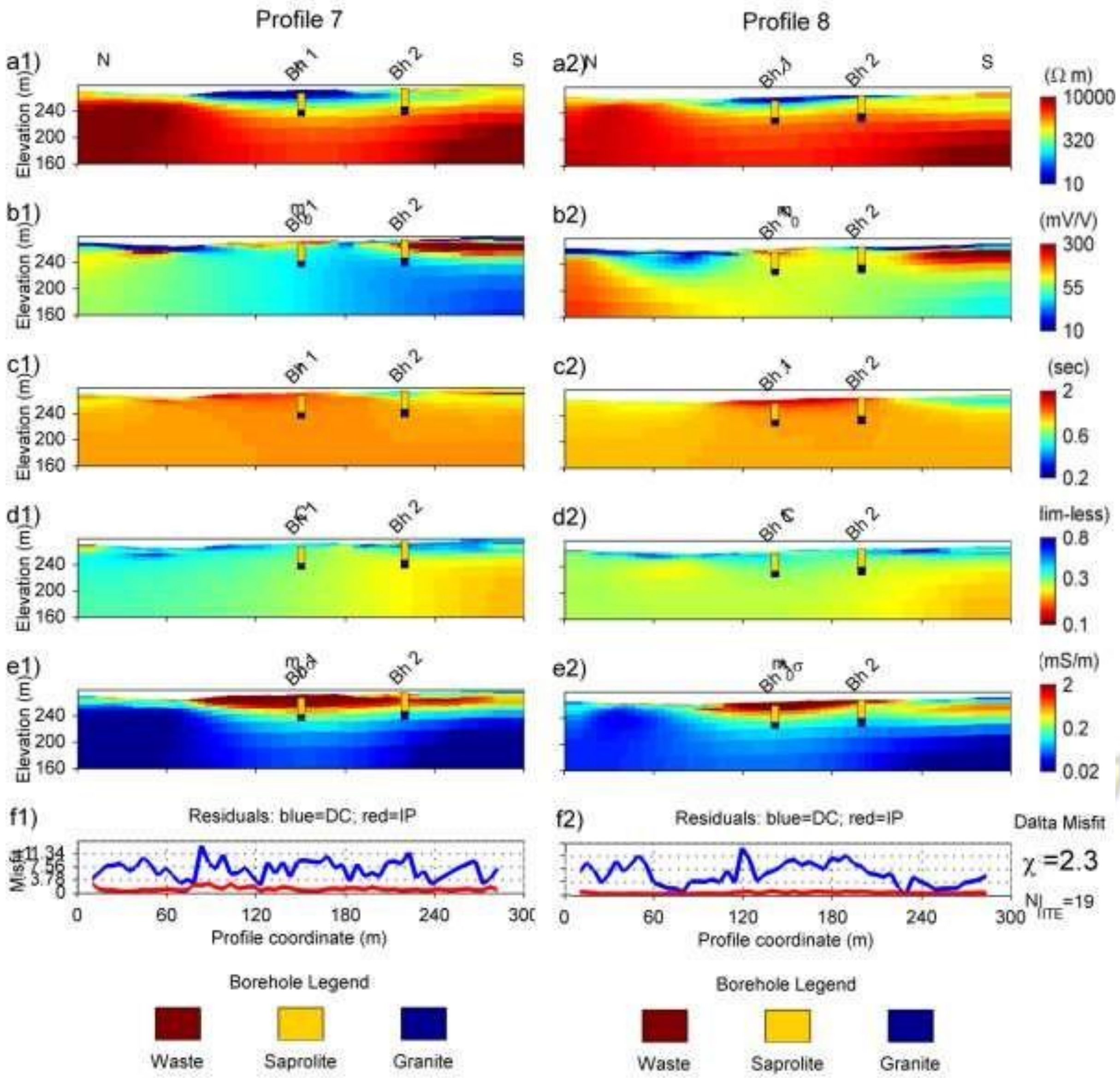

Figure 7.8 Cole-Cole DCIP parameters of profiles 7 (sections 1) and 8 (sections 2) that traverse the waste a) resistivity section b) chargeability section c) frequency factor section d) relaxation time e) normalized chargeability section showing f) misfit of the inversion results.

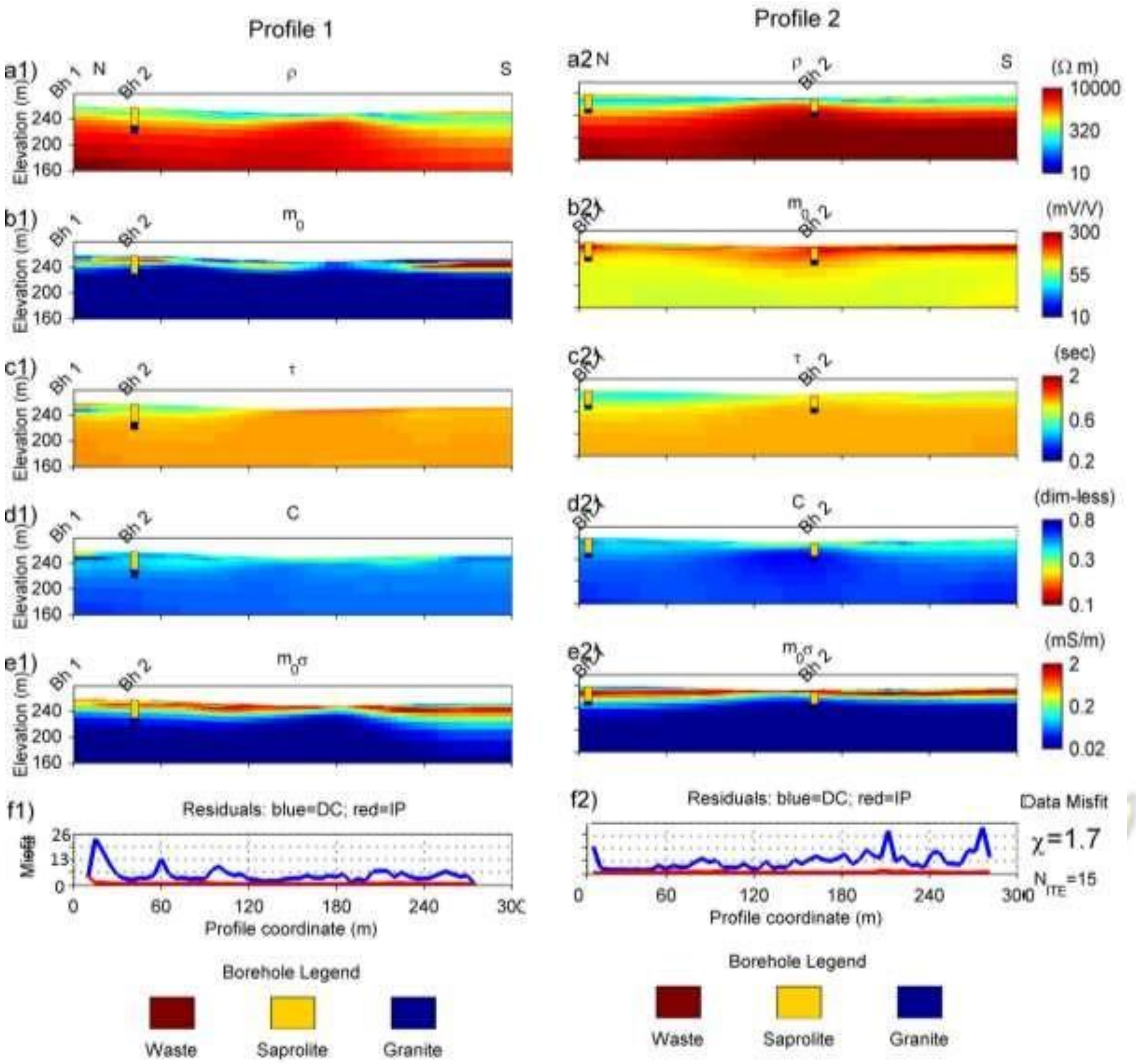

Figure 7.**9** present profiles 1 and 2 that traverse the river channel that carries leachate from the waste. It can be observed from this map that the top 25 m depth of the sections have low moderately low resistivity that is attributed to the pollution plume caused by the effluent from the waste deposit. This zone also presented a relatively moderate chargeability signature and normalized chargeability. The southern part of the sections which are not, much affected by the increasing conductivity by the plume recorded relatively low normalised relaxation time. The normalized chargeability section produced a high signature that coincided well with the saprolite thickness from the drilled log.

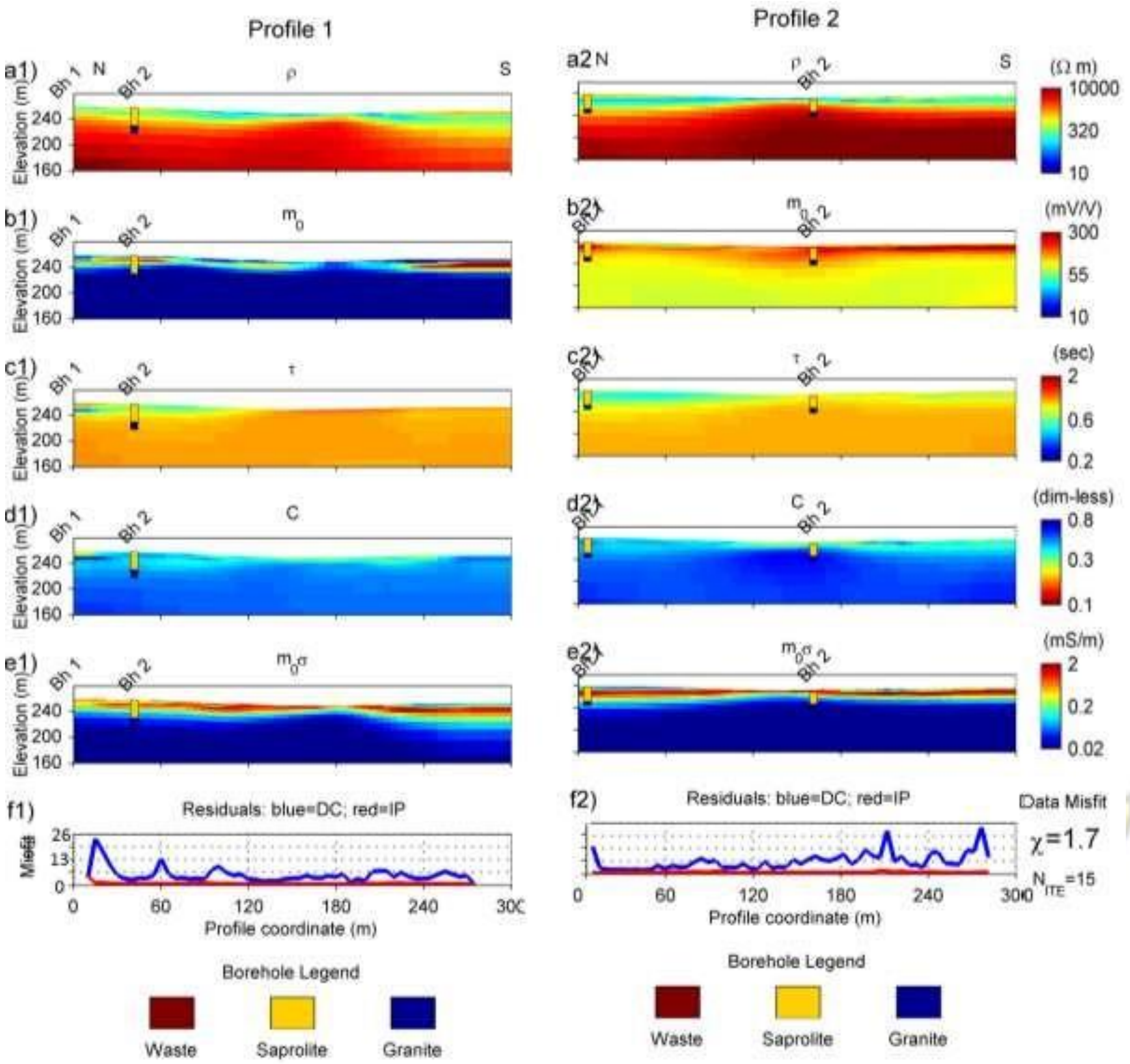

Figure 7.9 Cole-Cole DCIP parameters of profiles 1 (sections 1) and 2 (sections 2) that traverse the river channel waste a) resistivity section b) chargeability section c) frequency factor section d) relaxation time e) normalized chargeability section showing f) misfit of the inversion results.

Figure 7.10 shows result of profile 12 and 11 which do not traverse the waste. The resistivity sections recorded moderate resistivity signature at the upper part of the section with thickness varying from 3 to 30 m. The high resistivity signature observed at the top of the section between profile length 80 to 90 m on profile 11 (Figure 7.10a1) and 80 to 100 m on profile 12 (Figure 7.10a2) show the section of the profiles that traverse the batholitic granite outcrop. The chargeability sections (Figure 7.10b) and normalized chargeability sections (Figure

7.10e) also show signatures that are associated with the saprolite and the granite bedrock. The saprolite layer produced a high chargeability signature at depth (<30 m thick) with low chargeability at the surface (<5 m thick) corresponding to loose surface sandy soil. The granitic bedrock on the other hand recorded a general low signature in chargeability and normalized chargeability due to its less clay content. General reduction in the thickness of the high normalized chargeability signature over the position of the granitic outcrop is also noted. Similarly, the saprolite zones recorded a low τ values with thickness in the range of 3 to 30 m and granitic bedrock recording high anomalous τ values. It is therefore deduced from this result that the top 3 to 30 m depth of these sections represent the position of the saprolite.

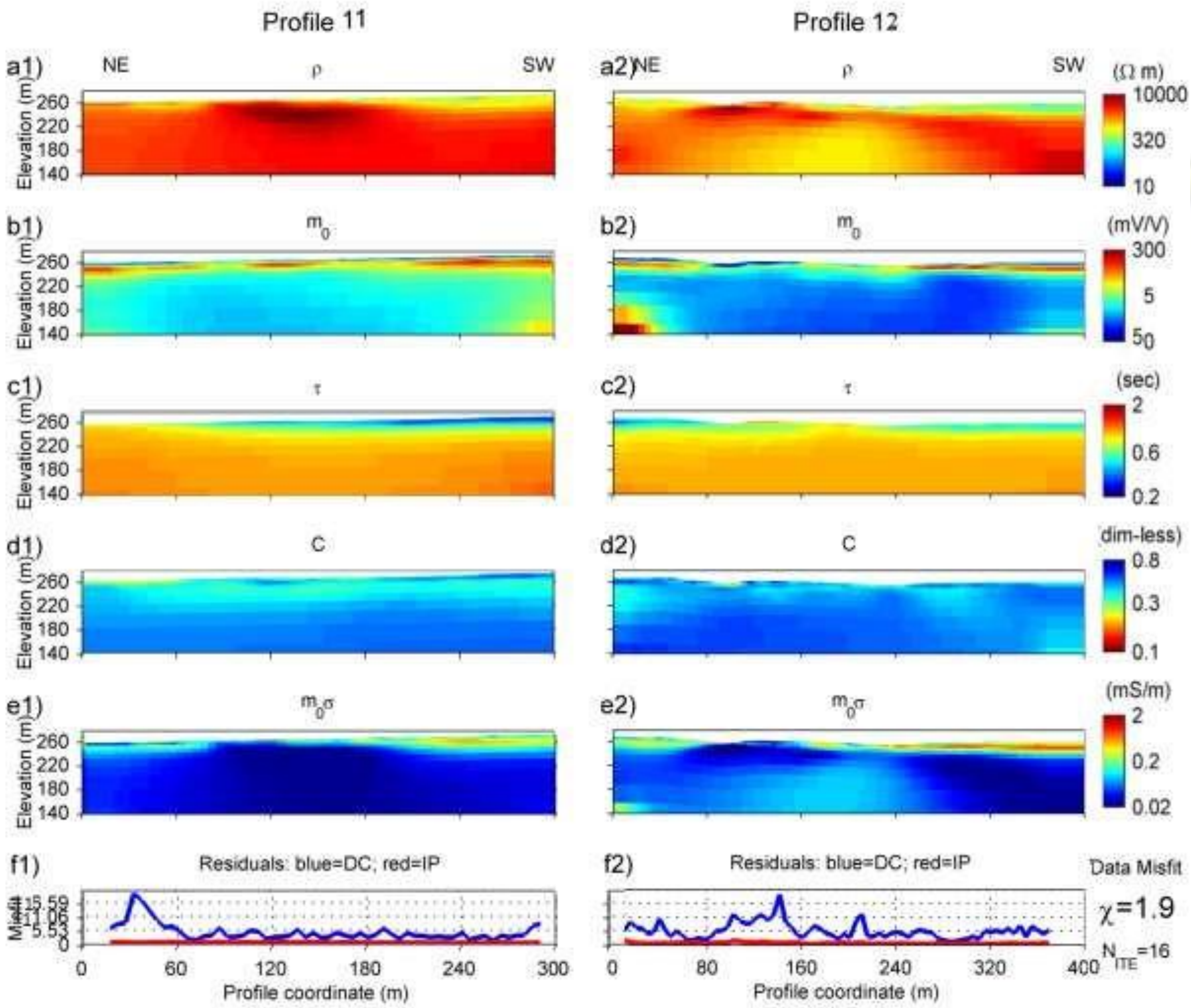

Figure 7.10 Cole-Cole DCIP parameters of profiles 11 (sections 1) and 12 (sections 2) surveyed outside the waste a) resistivity section b) chargeability section c) frequency factor section d) relaxation time e) normalized chargeability section f) misfit of the inversion results.

7.4.5 3D View of Time Domain Induced Polarization Result

In order to view the spectral IP results of the profiles in 3D, the images were transformed into a „vkt files" and imported into a ParaView. Figure 7.1a is a 3D resistivity pseudosection of the 13 surveyed profiles. The signatures coincided well from all the crossing profiles showing the reliability of the data. The 3D image shows three distinct signatures that are associated with the waste, the plume, the saprolite and the granitic bedrock. The low resistivity zone with value less than 10 Ωm (kw) corresponds to the position of the waste deposit. The zone with resistivity values in the range 10-100 Ωm observed on profiles 1, 2, 3 and the edge of 4 correspond to the associated plume within the river channel that carries the leachate from the site. The zone with resistivity values in the range of 200-1000 Ωm and with thickness in the range of 10 to 30 m corresponds to the weathered saprolite layer. It is also noted that below the waste this zone extends to greater depth than observed on the profiles that do not traverse the waste. This is attributed to the infiltration of the leachate from the waste into the lower granitic rock beneath the waste thereby reducing it resistivity. The high resistivity zone (> 4000 Ωm) at depth greater than 25 m corresponds to the granitic bedrock.

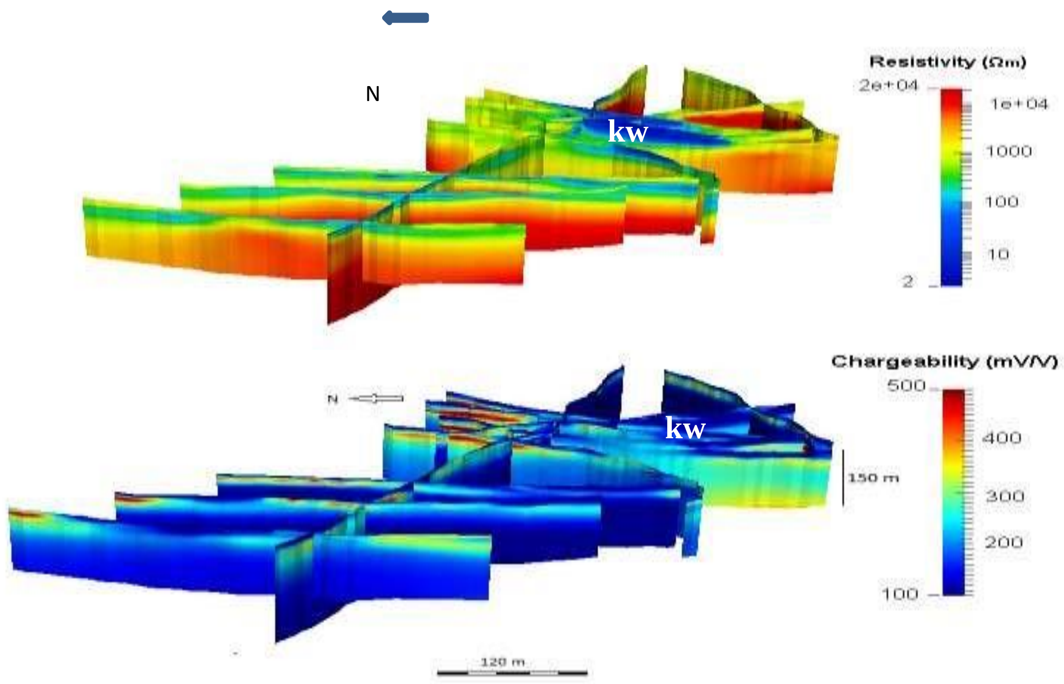

Figure 7.11 Representative 3D view of a) resistivity section b) chargeability sections of the surveyed profiles

Figure 7.11b is the 3D display of the chargeability sections of the profiles surveyed in the site. The high to moderate chargeability signature that is observed on the surface of the profiles, extending to a depth of 25 m at most parts of the sections corresponds to the saprolite layer. The m_0 section shows moderately low signature in the south-eastern, part of the area (kw) corresponding to the waste deposit, where the high conductivity of the waste may have suppressed the IP effect. In order to decouple the IP phenomenon from the conductivity of the pore fluid, the normalized chargeability sections were produced (e.g. Figure 7.12e).

7.4.6 Models from IP Inversion Results

The results of the IP inversion of the Cole-Cole parameters were used to produce various models namely, waste thickness and plume thickness as well as geological model of the site. These provided insight into the extent of pollution and its potential impact on the quality of groundwater and the soil in the catchment area of the waste.

7.4.6.1 Modelled Waste Thickness

One of the major aims of this study is to determine the waste distribution in this area. In order to achieve this, normalised chargeability sections which have high signature association with the waste were used. Figure 7.13 is the mapped waste thickness delineated using the high normalised chargeability zone of the inversion models. The main waste was mapped in the south-eastern corner (w1, Figure 7.13). This waste has a lateral extent of 120 by 200 m with thickness ranging from 3 to 12 m. The waste (w2) that is mapped in the north-western corner with dimension of 150 x 50 m is associated with the position of deposition and burning of used tyre.

The lateral extent of the waste mapped from the IP data is in agreement with the magnetic results (Figure 7.5 and Figure 7.7), but with a smaller extension in the zone in the magnetic data. The smaller lateral extension of the waste mapped by IP is probably due to the different sensitivity of the two methods to thin waste layers. The IP inversions cannot resolve waste thickness significantly smaller than the electrode spacing which can be determined by the magnetic methods.

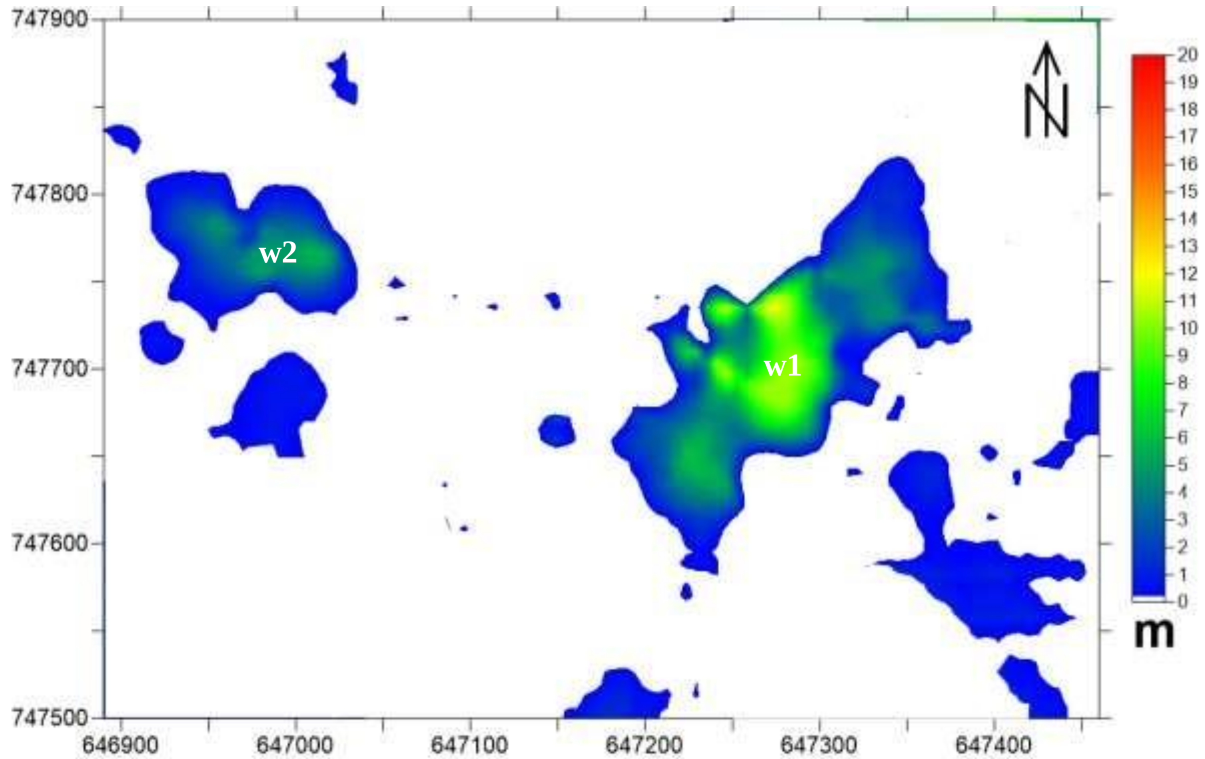

Figure 7.13 Modelled waste thickness.

7.4.6.2 Modelled Pollution Plume Thickness

Resistivity sections were used in mapping the pollution plume associated with the waste. Low resistivity signature which extends to depth beyond the waste (Figure 7.8a2) was attributed to the plume. This is because the infiltration of the leachate from the site into the soil leads to an increase in ion overload in the pore fluid of the hosting rock or soil leading to a reduction in the overall apparent resistivity. The elevation corresponding to the bottom of layer with resistivity less than 140 Ωm were picked using the surface picking tool of the Aarhus Workbench. These picked elevations were gridded to form the basement surface of the pollution plume. The plume thickness (Figure 7.14) is obtained by subtracting the plume basement surface from the digital elevation map of the study area.

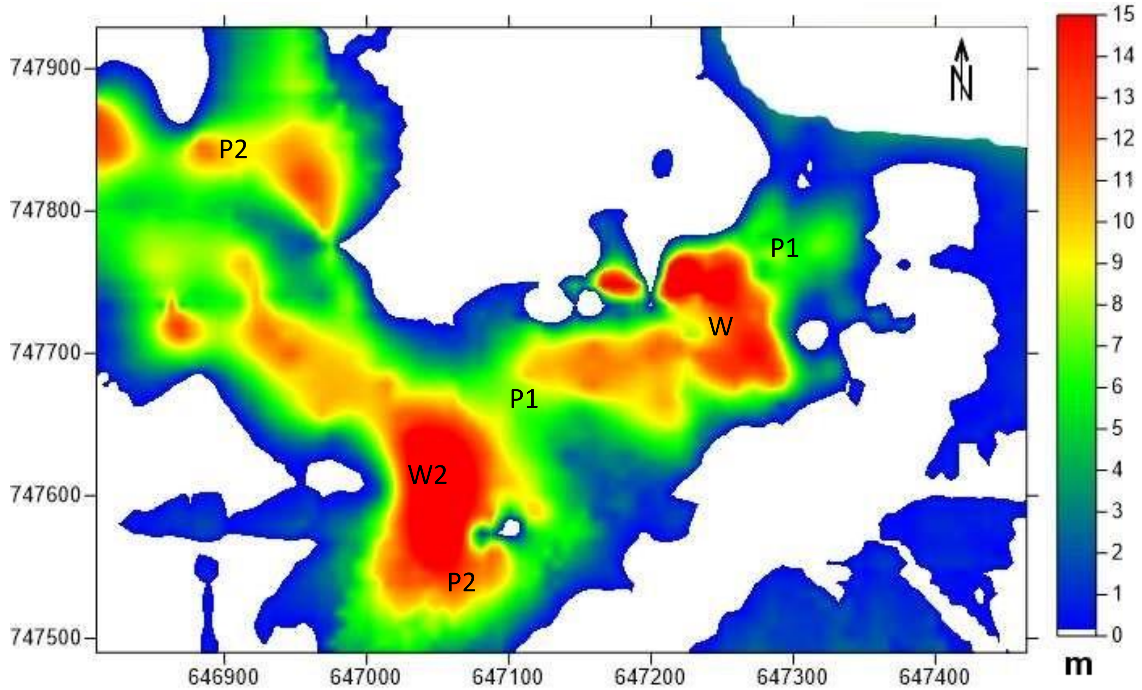

Figure 7.14 Modelled pollution plume thickness.

Figure 7.14 is the plume thickness map of the study area, showing the position of pollution plume that is associated with the waste. Two main trends of pollution plume can be identified on the image, (P1-P1) trending in NE direction which is associated with the position of the waste (Figure 7.13, Figure 7.5 and Figure 7.7). The thicker plume along this position is located beneath the waste around W (Figure 7.14). Also noted is the NW trending plume (P2P2) along which a thick plume (W2) with thickness greater than 12 m is recorded. From the map of the study area (Figure 4.1) and the DEM map (Figure 7.2), it can be observed that the position of P2-P2 corresponds with the position of the river which flows at the foot of the waste. The thick plume observed in this direction is an indication that most of the leachate from the waste flow through the river. The plume along this direction is also observed to be broader than the river channel showing a possible infiltration of the leachate into the surrounding porous saprolite. This shows the vulnerability of the groundwater system to pollution from the effluent.

7.4.6.3 Modelled Saprolite Thickness

The understanding of the lithostratigraphic sequence of the area of waste deposition site provides insight into the understanding of the potential and the possible risk of the leachate in polluting the soil and the groundwater. Therefore the geological model of the study area was developed using the chargeability and normalized chargeability sections. The saprolite layer produces strong IP effect attributed to its relatively high clay content which enables the mapping of the saprolitic oxide zone using the chargeability section. Despite this, there is a distortion in the signature below the waste attributed to the increasing pore fluid salinity (e.g. Olorunfemi and Griffiths, 1985; Barker, 1990). The normalized chargeability which is not affected by the fluid conductivity (bulk conductivity of the medium) (e.g. Pelton *et al*., 1978; Lesmes and Frye, 2001) produced signature that is related to the lithostratigraphic sequence of the area. This is evident in the correlation between the normalized chargeability results and the drilled geological log from the two boreholes (Figure 7.8 and Figure 7.9). The normalized chargeability therefore provides a good result beneath the waste and proved valuable in the development of the lithological section of the area.

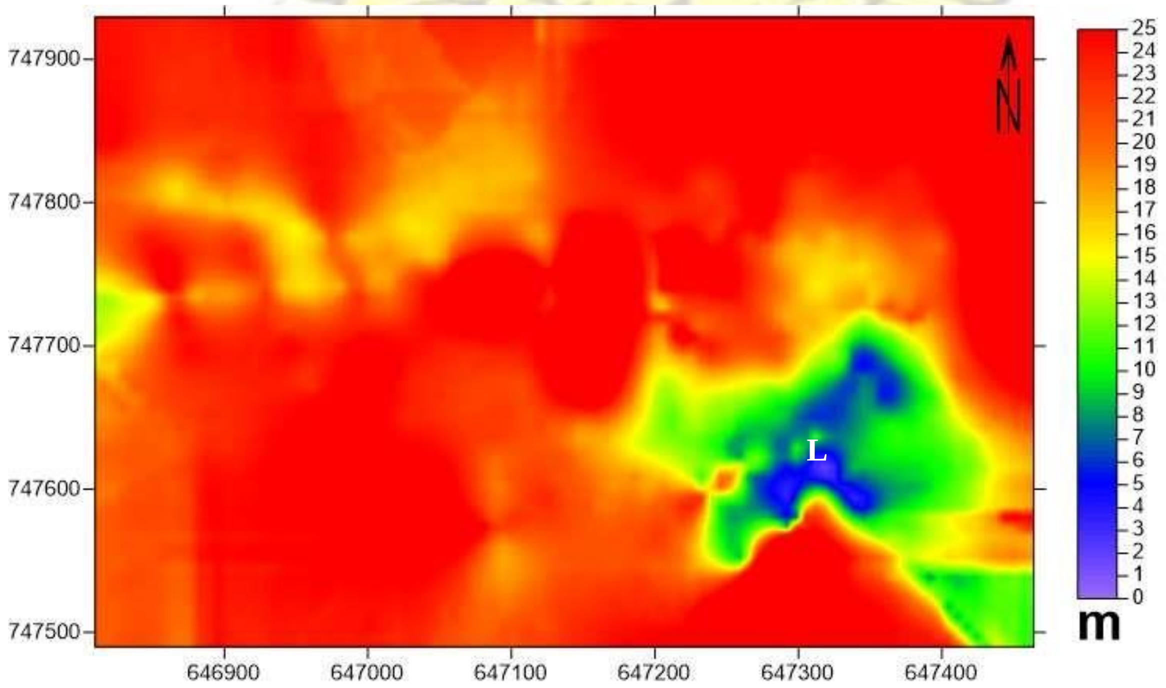

Figure 7.15 Modelled Saprolite thickness.

Figure 7.15 is the mapped saprolite thickness map of the study area showing the variation of saprolite thickness over the catchment area, hence the variation of depth to bedrock. The area has saprolite thickness in most parts of the site in the range of 23 to 35 m. A major deviation from this is observed around point (L) where the saprolite thickness is less than 11 m. This region is observed to have a batholitic outcrop of granite characteristic of the basin granitoids (Leube *et al.*, 1990; Sylvester and Attoh, 1992; Griffis *et al*., 2002) with some granitic boulders with diameter in the range of 3 to 7 m in the area.

The position of the granitic outcrop affected the plume pattern in the area. As can be noticed in Figure 7.14, there is no plume association with the area around (L), this is because the nonporous granitic outcrop forms a hydraulic barrier to the infiltrating leachate from the waste thereby preventing infiltration into the subsurface system. The absence of fracture within the granitic outcrop aided in the protection of the subsurface water system in this area. The high elevation and the impermeable nature of the granite creates a hydraulic gradient causing the leachate flow into the low elevation area (Figure 7.2) behind the outcrop leading to the high pollution plume (W2) at this point (Figure 7.14).

7.5 Summary

Combined time-domain DC/IP 2-D tomography, magnetic and magnetic susceptibility surveying results were used to characterized the Ohwim municipal solid waste disposal site. The high magnetic and magnetic susceptibility signatures that are associated with the waste helped in mapping the lateral extent (150 m by 250 m) of the waste deposit. Also observed from these results is the erratic distribution of the high magnetic signature in the catchment area. This is attributed to the inhomogeneous distribution of ferrous metals within the waste and the erratic distribution of the waste in the area. The resistivity aided in the mapping of the plume while the normalized chargeability mapped both the waste thickness and the lithological units of the catchment area. These results provide an insight into the success of integrated geophysical methods in the mapping of unprotected solid waste disposal sites in developing worlds like Ghana.

CHAPTER 8: DOMPOASE MUNICIPAL SOLID WASTE DISPOSAL SITE

8.1 Introduction

The Dompoase Landfill is the first MSW engineered landfill to be constructed in Ghana in 2003, the only landfill disposal site in the Kumasi Metropolis. The landfill became operation in 2004. It has both a solid waste deposit site and liquid waste deposit and treatment site. The site currently has two operational waste disposal cells. The first cell for waste disposal is expected to have a lifespan of 15 years (Mensah *et al.*, 2003). The second cell which is constructed adjacent to the old cell is currently used when the old cell become too wet (water saturated) and difficult for the refuse trucks to climb over. The initial design of the cell has the installation of vertical gas-outlets which were continuously extended as the waste amount increases but was left at the later stage of the site development. Although there is a plan to collect the methane gas produced from the waste for domestic use, this is not done at present.

The state of the landfill poses some level of environmental changes. Prominent among them is the danger posed by the released effluent from the sewage treatment pond that ends up in the Oda River. This poses serious health challenges to communities leaving around the stream that depends on this water as their means of potable water supply. Another major problem is the stench emanating from the site which can be sensed up to about 1 km away from the site. The site is also serving as a major breeding ground for mosquitoes as no regular spraying is carried out to reduce the production of these insects on the site. Also the newly constructed cell for waste disposal which is to be used when the current waste disposal cell is closed at end of it proposed 15 years lifetime (Mensah *et al.*, 2003) is constructed without protective underlying impermeable layer. This was done on the basis that there is high clay content in the underlying saprolite layer to prevent the seepage of leachate into the groundwater system.

8.2 Study Area

8.2.1 Location of Dompoase Landfill

The Dompoase Landfill is located in the Asokwa Submetropolitan area of the Kumasi Metropolis. It is located about 9 km from the KNUST Campus and 6 km from the Kumasi city centre. The site is situated on one hundred acre of land with the area defined by 655200 to 656200 E and 731790 to 732810 N coordinates in the UTM WGS84 zone 30N coordinate system. As observed around most of the MSW disposal site in the metropolis, there are development of residential accommodation in the catchment area of the waste (Figure 8. 1). Some of these structures are built on the flow path of the effluent from the site without consideration of the health risk it poses.

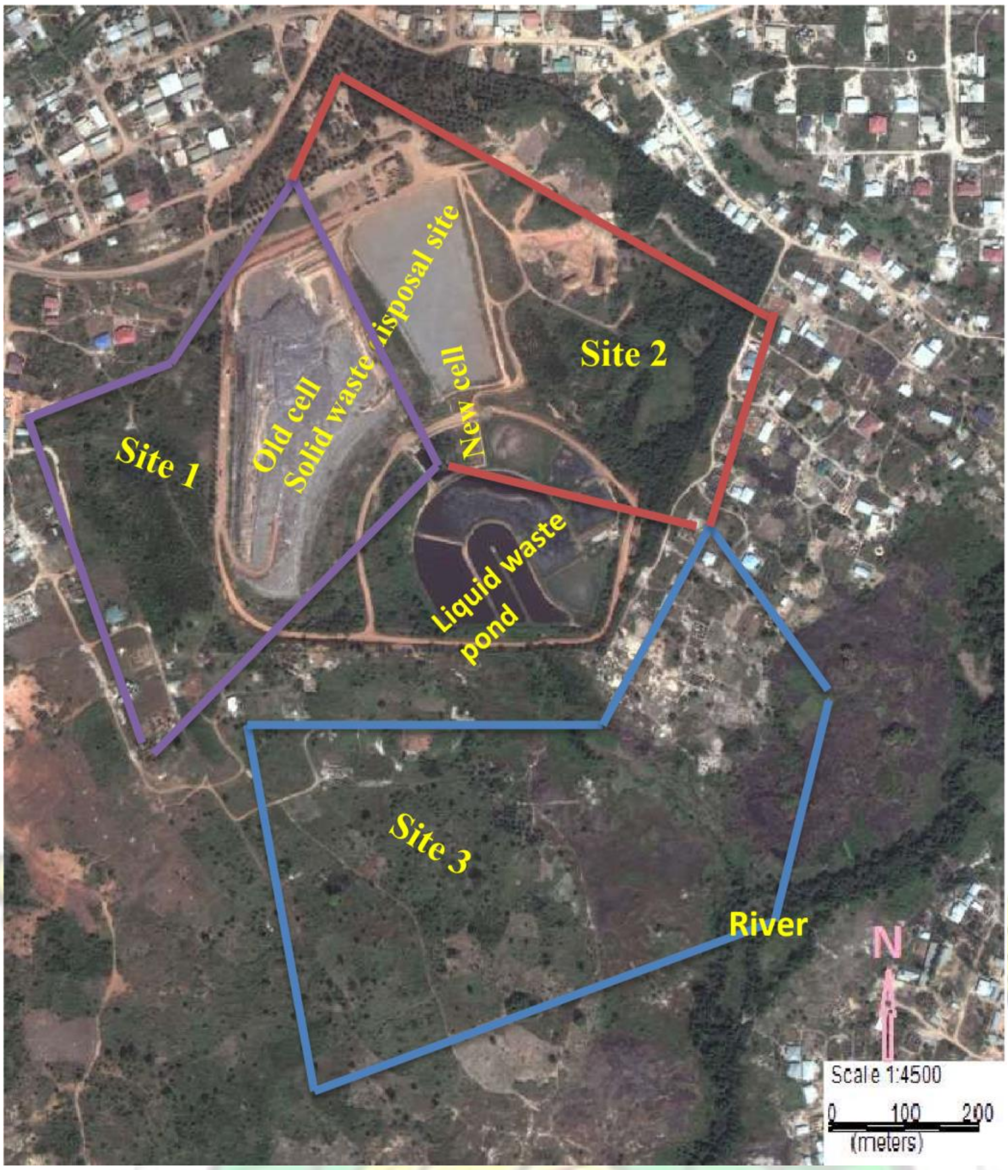

Figure 8. 1 Satellite image of the Dompoase Landfill site.

Geologically, the formation in the area consists of top layer weathered saprolite layer of thickness in the range of 25 to 30 m underlain by the basin type granitic bedrock.

8.2.2 Digital Elevation Map (DEM)

Figure 8.2 is the digital elevation map of the catchment area of the landfill site. The topography of the area varies from 228 to 278 m with the area with topography greater than

262 m, W (Figure 8.2) representing the waste. It is noted that the waste was deposited to a height of around 10 to 20 m from its surrounding environment. The general topography of the area decreases from north-west to south-east, direction that controls the drainage in the area. The channel that carries the effluent from the site also flows in this direction into river Oda (Figure 8. 1 and Figure 8.2). Most parts of the low-lying south-eastern corner of the site are mostly flooded with the effluent during the raining season. This makes the area vulnerable to pollution from the leachate from the landfill.

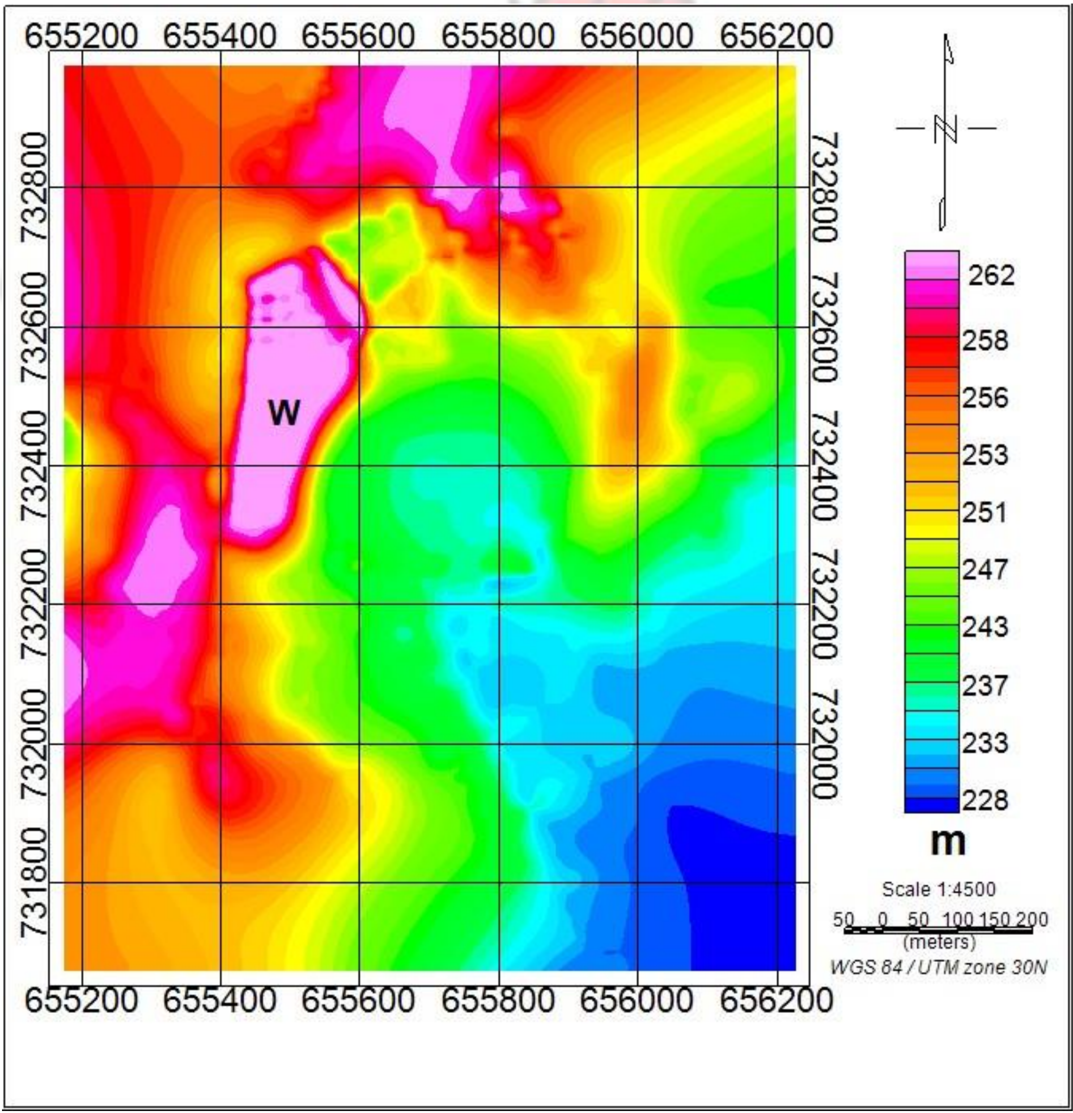

Figure 8.2 The digital elevation map of Dompoase Landfill site.

8.3 Survey Design

The time domain spectral induced polarization data were acquired on 35 profiles in the catchment area of the landfill using 5 m electrode spacing. The length of the profiles ranges from 300 to 600 m with total profile length surveyed been 15 km. The surveys were designed to monitor any possible infiltration of the leachate into the underground system and also to determine the extent of pollution caused in the low topographic wetland by the released effluent from the site.

The magnetic data (the gradiometry and the total magnetic intensity) were acquired on approximately 15 x 5 m grids. The surveys were conducted on 45 profiles with lengths ranging between 100 to 1000 m. The total length of profiles surveyed was 20.5 km. The base station for diurnal correction was set at the point (656090E, 732700N). The processing of the diurnally corrected data was carried out using the Oasis Montaj Software package. Similarly, magnetic susceptibility survey was conducted on 45 profiles using approximately 15 x 5 m grid. A total of 17.2 km profile lengths were surveyed, with length of individual profiles ranging between 100-800 m. The profile layout of the survey profiles are shown in Figure 8.3.

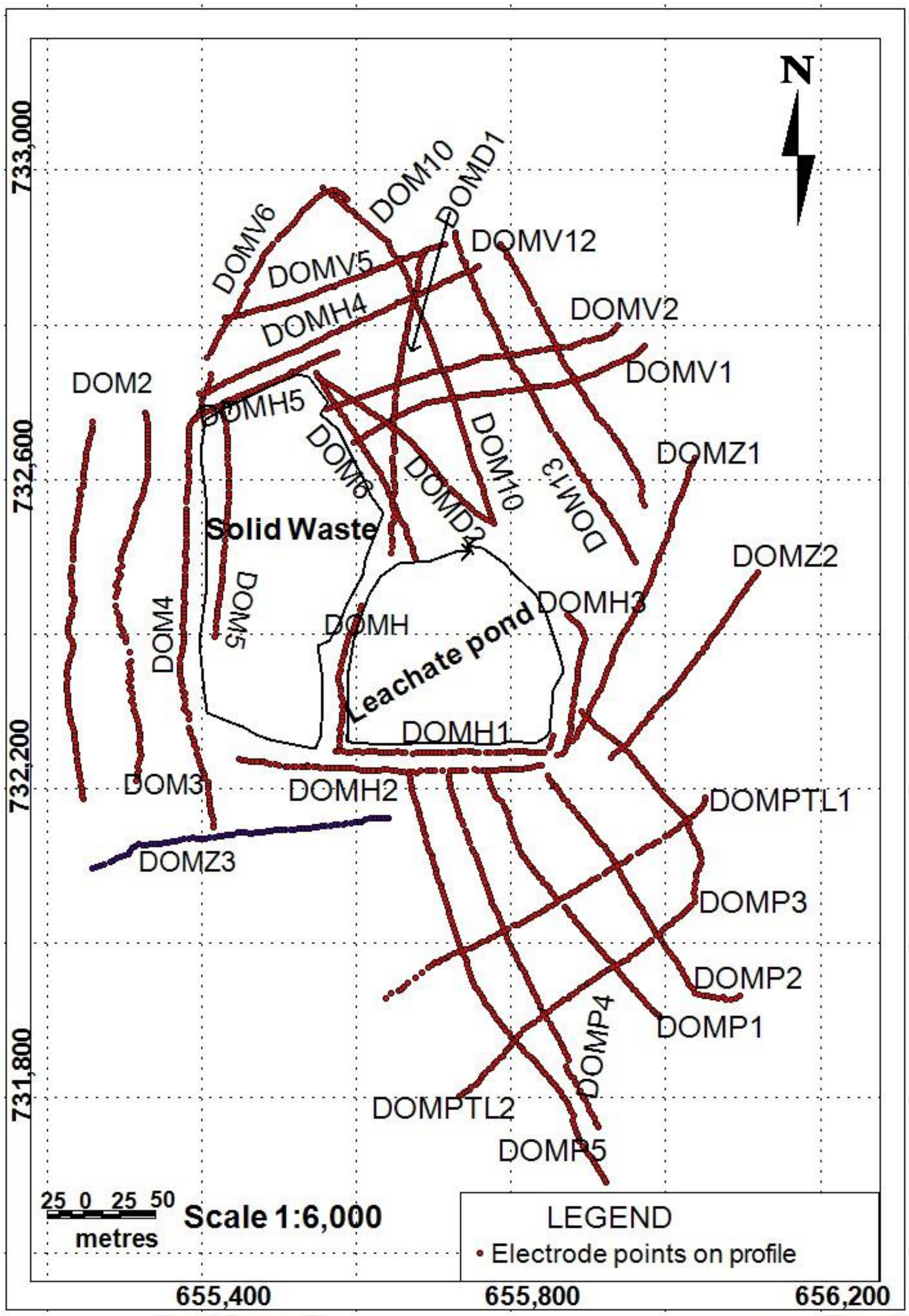

Figure 8.3 The surveyed profiles layout at the Dompoase site.

The survey was designed by dividing the site into three sections (Figure 8. 4), each with a specific goal as follows:

Section 1: Determine the level of pollution in the new cell as the waste from the old cell was observed to extend beyond the defined boundaries into the new cell which is not having a protective underlying cover to prevent infiltration of the leachate.

Section 2: Map possible plumes around the solid waste disposal site.

Section 3: Determine the level of pollution of the discharge effluent in the surrounding wetland.

8.4 Results and Discussion

The results from the magnetic, magnetic susceptibility and the time domain spectral induced polarization surveys conducted in the catchment area of the Dompoase Landfill have helped to provide full insight into the state of the landfill. The magnetic and magnetic susceptibility results helped in mapping the lateral extent of the waste deposit and showed the controlled nature of waste deposition at the site. The magnetic data mapped the flow path of the released treated effluent from the sewage pond showing high ferromagnetic and heavy metal composition of the leachate. The IP result also mapped leachate flow positions from the landfill into the environment. The profile surveyed on the waste shows a high conductivity zone below waste bringing the integrity of the underlying impermeably layer to prevent the infiltration of leachate into question.

8.4.1 Magnetic Susceptibility Result

The magnetic susceptibility map of the Dompoase Municipal Solid Waste Landfill is shown in Figure 8.4. The magnetic susceptibility values measured are in the range of (-2 to 13923)x10^{-6} SI. The gridded image shows the position of waste mapped with high magnetic susceptibility signature. The lateral extent of the mapped waste deposit is 400 x 500 m. The high magnetic susceptibility signatures observed at points in the catchment away from the main waste deposit is attributed mainly to the scrap metals which were picked by scavengers from the waste and left on the roads to be compressed by passing trucks to reduce its volume. Also mapped on this image is the position of the new cell with the extent of the waste deposition in its southern section.

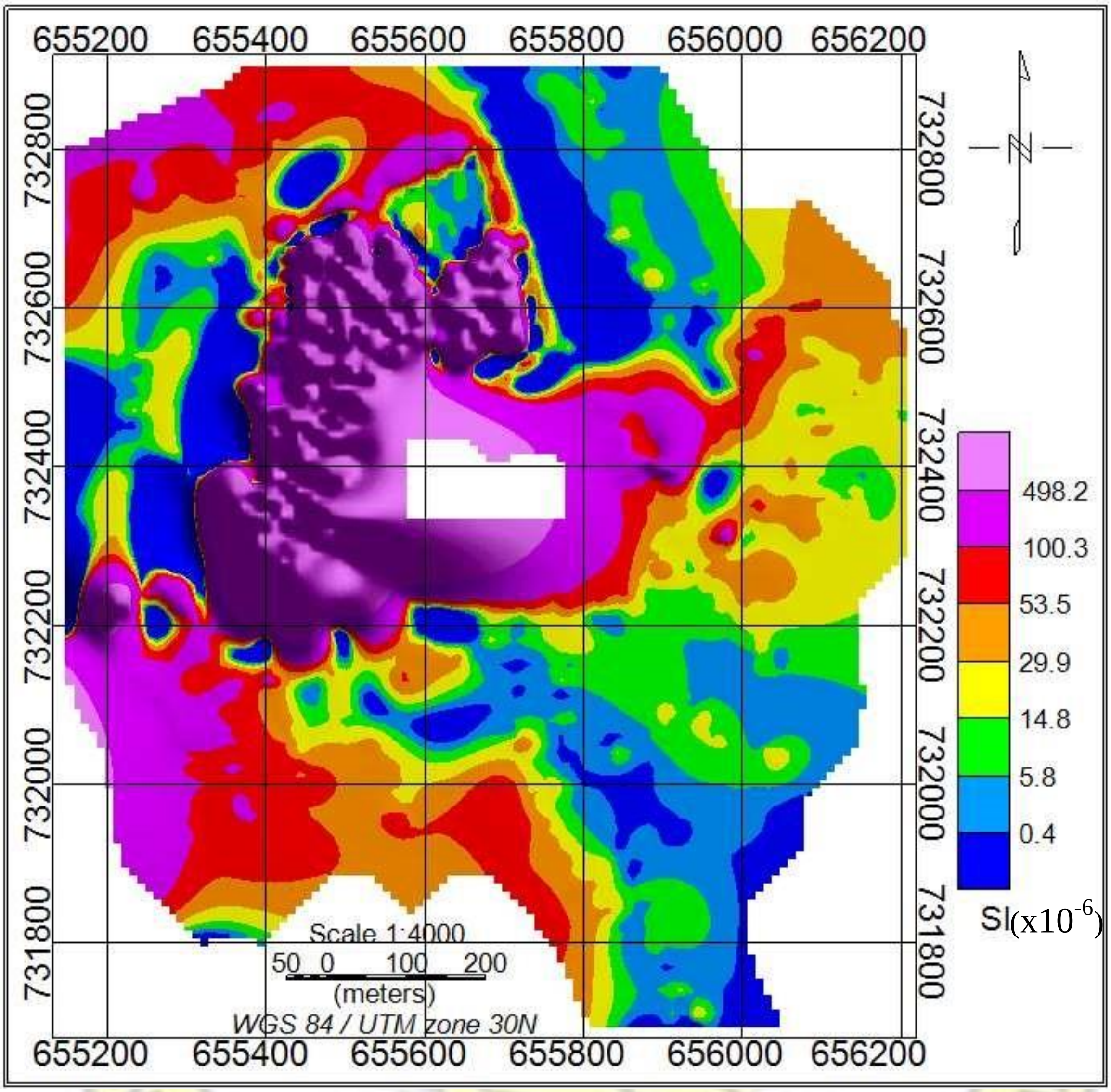

Figure 8.4 Magnetic susceptibility map of the Dompoase Landfill site.

8.4.2 Total Magnetic Intensity (TMI) Result

Figure 8.5 shows the total magnetic intensity map of the study area. The measured total magnetic field values in the area range from 30863.8 to 33524.5 nT. The residual total magnetic field data obtained in this survey ranges from -1505.62 to 1120.46 nT. The position of the waste is depicted with low magnetic value which corresponds to area of high magnetic susceptibility.

This reversal of magnetic signature was due to the low latitude region where the data is collected.

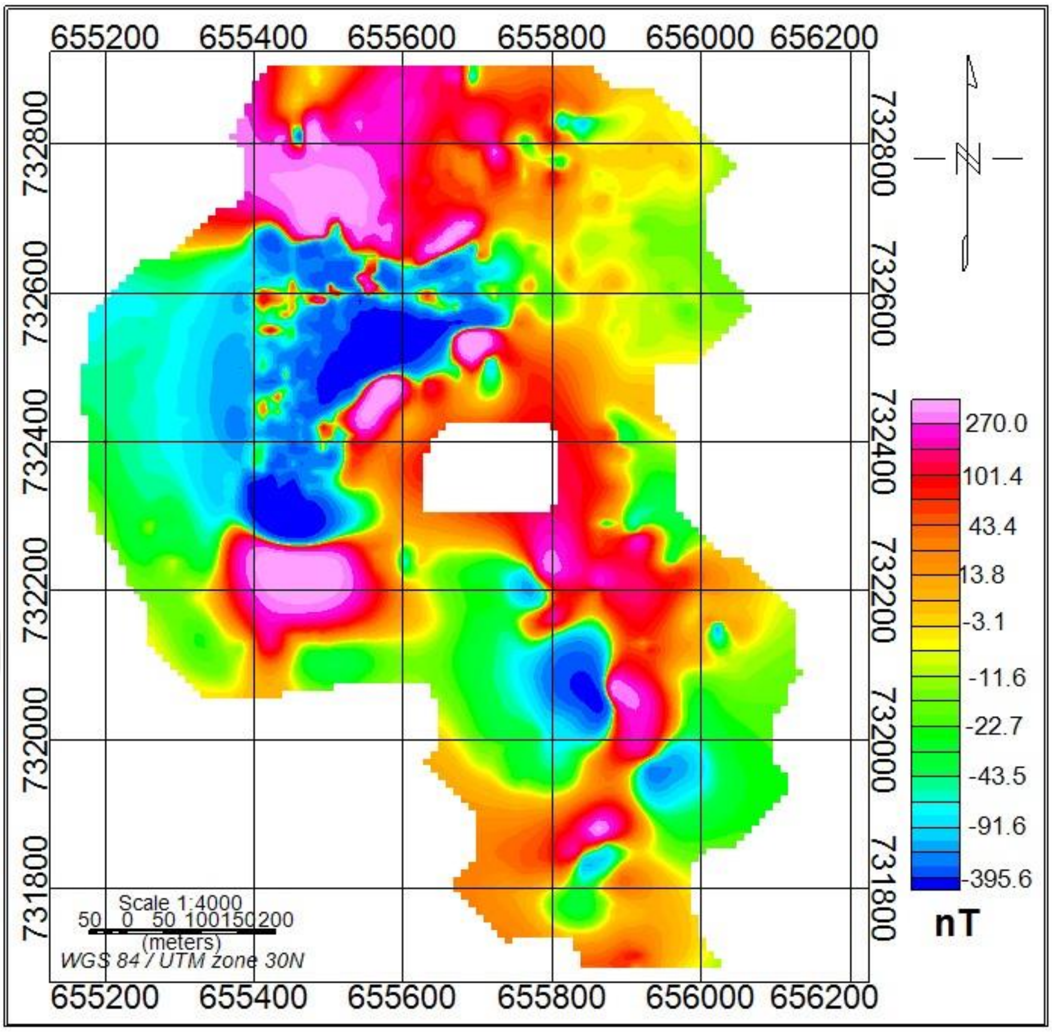

Figure 8.5 Total magnetic intensity map of the Dompoase Landfill site.

Figure 8.6 is the analytical signal derivative of the total magnetic intensity map of the Dompoase Landfill site. From the result it can be seen that the main waste is delineated with high magnetic feature within the analytical signal image with value greater 6.19 nT/m. From this image (Figure 8.6) two main anomalous magnetic zones can be identified, zone 1 (Z1) and zone 2 (Z2). The Z1 corresponds to the position of the landfill which covers an approximate area of 300 m by 200 m at its southern section and 500 m by 300 m at its northern section. Similarly, zone 2 (Z2) magnetic feature at the southern part of the site covers approximate area of 50 m by 500 m. It was observed that no municipal solid waste was deposited in zone 2 (Z2). This position contains the channel within which the treated effluent from the landfill is released into the environment and flows into river Oda (Figure 4.1 and Figure 8. 1). The high magnetic signature of this zone is an indication of high dissolved ferrimagnetic and heavy metal composition of the efluent. This could pose serious health risk as this area is used for growing food crops which could be contanminated with the heavy metals.

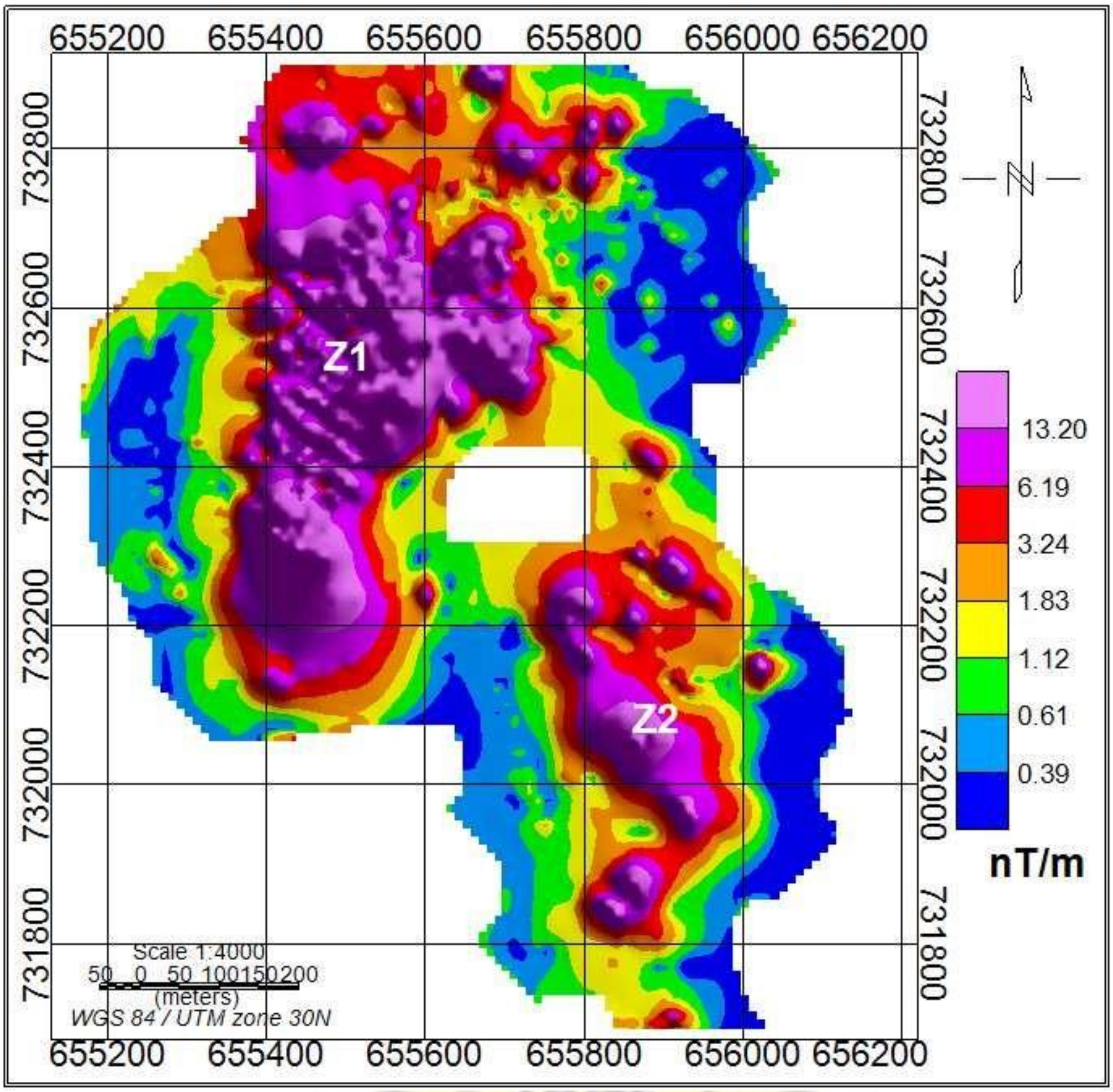

Figure 8.6 Analytical signal of the total intensity magnetic map.

8.4.3 Magnetic Gradiometry Result

Figure 8.5 is the magnetic gradiomtric map of the Dompoase Municipal Solid Waste Landfill site. The magnetic gradiometric field measured on the area is in the range of -482.87 to 668.19 nT/m. The main waste position as observed in Figure 8. 1 and Figure 8.2 is depicted with a general low magnetic value showing the effect of geomagnetic field on the result.

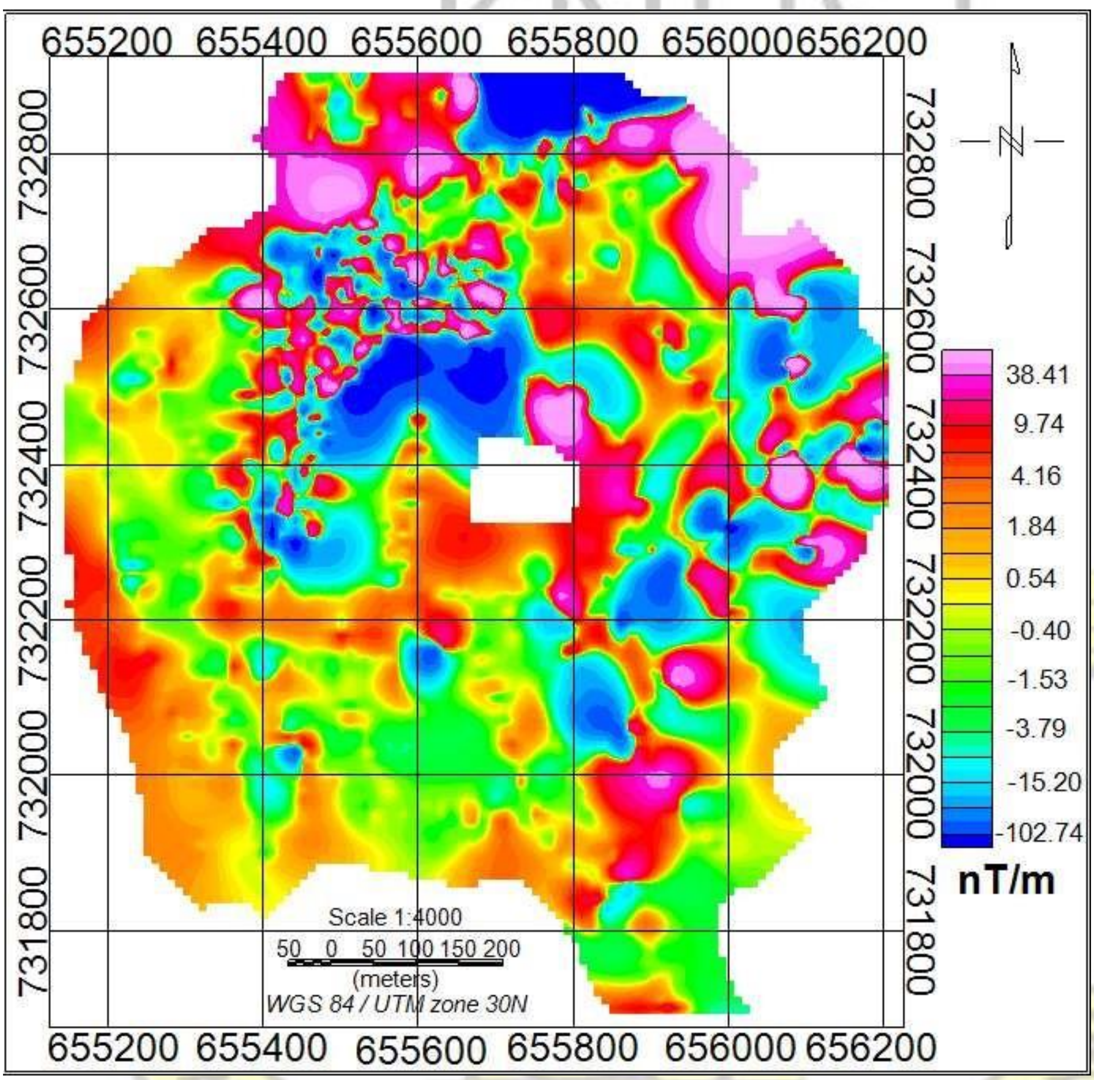

Figure 8.7 Magnetic gradiometry map of the Dompoase Landfill.

Figure 8.8 is the analytical signal derivative of the magnetic gradiometry data showing varying magnetic signature of the study area. The signature as observed in this map is low in magnitude as compared with the analytical signal derivative of the total magnetic intensity map. This is attributed to the double derivative of this data with distance since the magnetic gradiometry data is said to be approximately equal to the vertical derivative of the magnetic data (Rucker, 2010) provided the distance between the consoles are small. It is noticed that the position of the waste in the magnetic gradiometry is also mapped with high magnetic signature in the area labelled Z¨1 (Figure 8.8). Similarly, the position of the drainage channel of the supposed treated effluent is also mapped by high magnetic signature at Z¨2. Also noted is a high magnetic signature at the north-eastern part of the area (Figure 8.8). This area produced relatively lower magnetic signature in Figure 8.6. The difference in the two magnetic results is attributed to the influence on the magnetic gradiometry data by nearby residential facilities around the area as well as the high tension power line in that area since the magnetic gradiometry survey is more sensitive to near surface magnetic features (Kearey *et al*., 2002; Rucker, 2010).

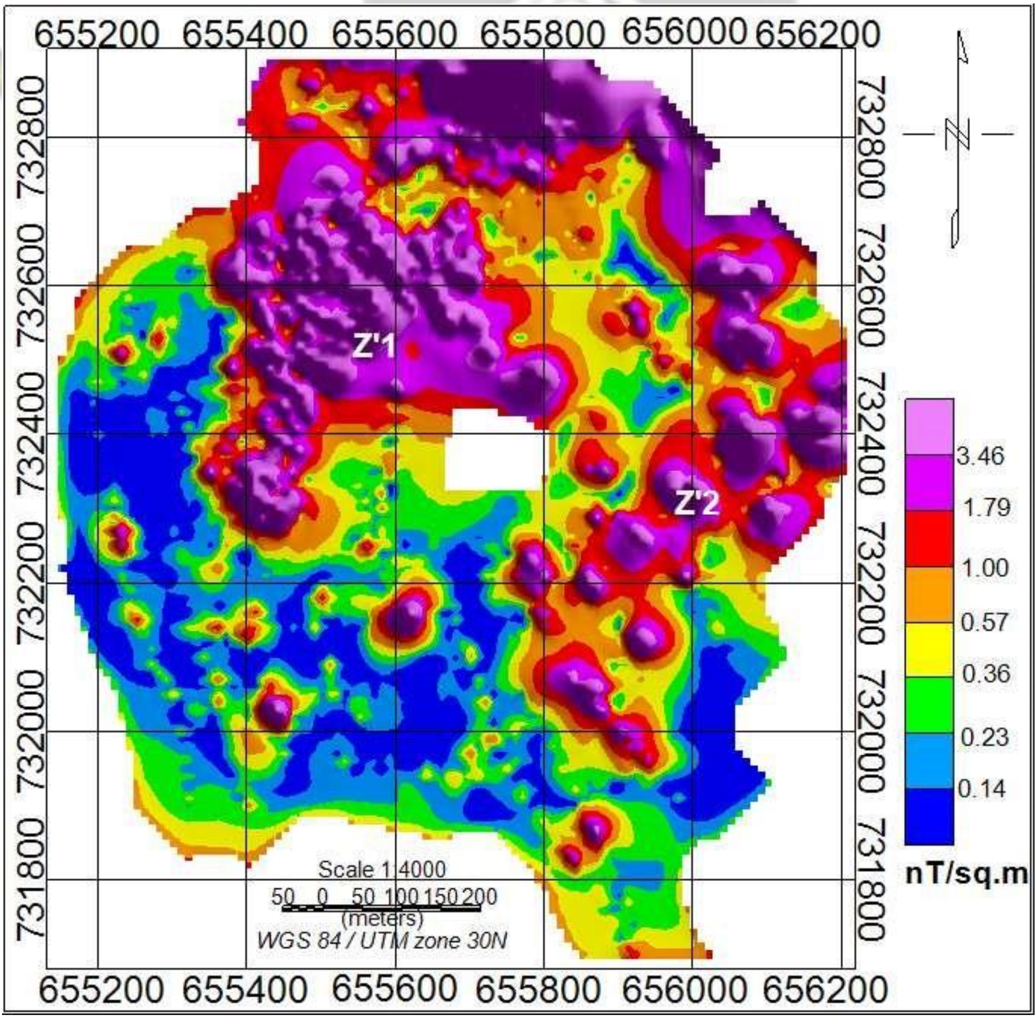

Figure 8.8 Analytical signal derivative of the magnetic gradiometry data.

The magnetic survey helped in the mapping of the Dompoase Landfill and its associated leachate and effluent. The high magnetic signature defines the portion of lateral extent of the main solid waste in both TMI and gradiometry data which is attributed to the high ferrous metal composition of the waste (Wemegah *et al*., 2014, 2015). The high magnetic anomaly along the path of the effluent shows a possible high content of heavy metals mainly from roasted and decay ferrous metals in the leachate from the waste. The broader extension of this anomalous zone Z2 (Figure 8.6) and $Z''2$ (Figure 8.8) is attributed to the overflow of the effluent into the surrounding farming field during the raining season. This poses a great environmental and health risk to the people who farm around the area and the quality of food they produced. Similarly, the ever increasing residence accommodation in the area calls for concern since these people depend on groundwater as their source of potable water which is at risk of possible heavy metal poison.

There is a general localization of the magnetic anomaly in the area (Figure 8.6 and Figure 8.8). This is an indication of controlled nature of the waste deposition at the Dompoase MSW landfill site as compared with the other solid disposal sites considered in this work. The few localised magnetic high identify in the western part of the magnetic gradiometric image (Figure 8.8) is due to the pile of ferrous metal by people who collect these metals for scrap. The ability of the gradiometry to map this position is due to it sensitivity to near surface magnetic materials.

8.5 Time Domain Spectral Induced Polarization

The results of some IP profiles surveyed in the area were presented and discussed in this section. The areas of infiltration of leachate from the landfill into the ground (pollution plumes) were mapped with low resistivity signatures due to the high ion overload in the interstitial pore fluids of the soil. The plumes were also observed to have strong IP effect as observed in the normalized chargeability results attributed mainly to the high microbial activities and ferrous iron components within the leachate. Various researchers have identified the production of biofilm during bioremediation to be a major contributor to IP effect (e.g. Atekwana *et al*., 2000; 2004a; Atekwana and Slater, 2009; Abdel Aal *et al*., 2010; Flores Orozco *et al*., 2011). Similarly, the strong IP effect associated with the waste can be attributed to the high ferrous oxide composition of the waste and the leachate mapped by the magnetic (Figure 8.6 and Figure 8.8) and magnetic susceptibility (Figure 8.4) results (e.g. Chen *et al.*, 2012). Flores Orozco *et al*. (2011) and Chen *et al.* (2012) reported a strong correlation between IP response and ferrous iron content of a soil ferrous mixture. Other researchers also identified the phenomenon of a strong association of phase response in spectral induced polarization to changes in groundwater geochemistry accompanying stimulated iron (Williams *et al*., 2009, 2011; Flores Orozco *et al*., 2011). The distortion of Cole-Cole IP parameters due to the high conductivity of the pore fluid was also observed.

8.5.1 IP Results of Section 1

Figure 8.9 presents sections of Cole-Cole IP parameters of profile 5 acquired on the main waste. This profile was surveyed in other to determine the integrity of the underlying impermeable membrane layer in preventing the seepage of leachate from the waste into the soil and eventually, the groundwater system. The result shows low resistivity signature with value less than 20 Ωm in the top 10 to 25 m of the resistivity section (Figure 8.9a). This zone also produced high normalized chargeability signature (Figure 8.9e) and therefore considered to map the waste. Below this zone is a zone of resistivity value in the range of 20 to 250 Ωm. This zone which is considered to be a leachate plume beneath the waste extends down to a depth greater than 50 m. The chargeability section produced some level of signature at the top part of the section that is associated with the waste and the leachate saturated top lateritic soil cover of the landfill. There is no signature in the other IP parameters (τ and C) attributed mainly to the high conductivity of the soil which leads to the distortion of these parameters (e.g. Wemegah *et al.*, 2015).

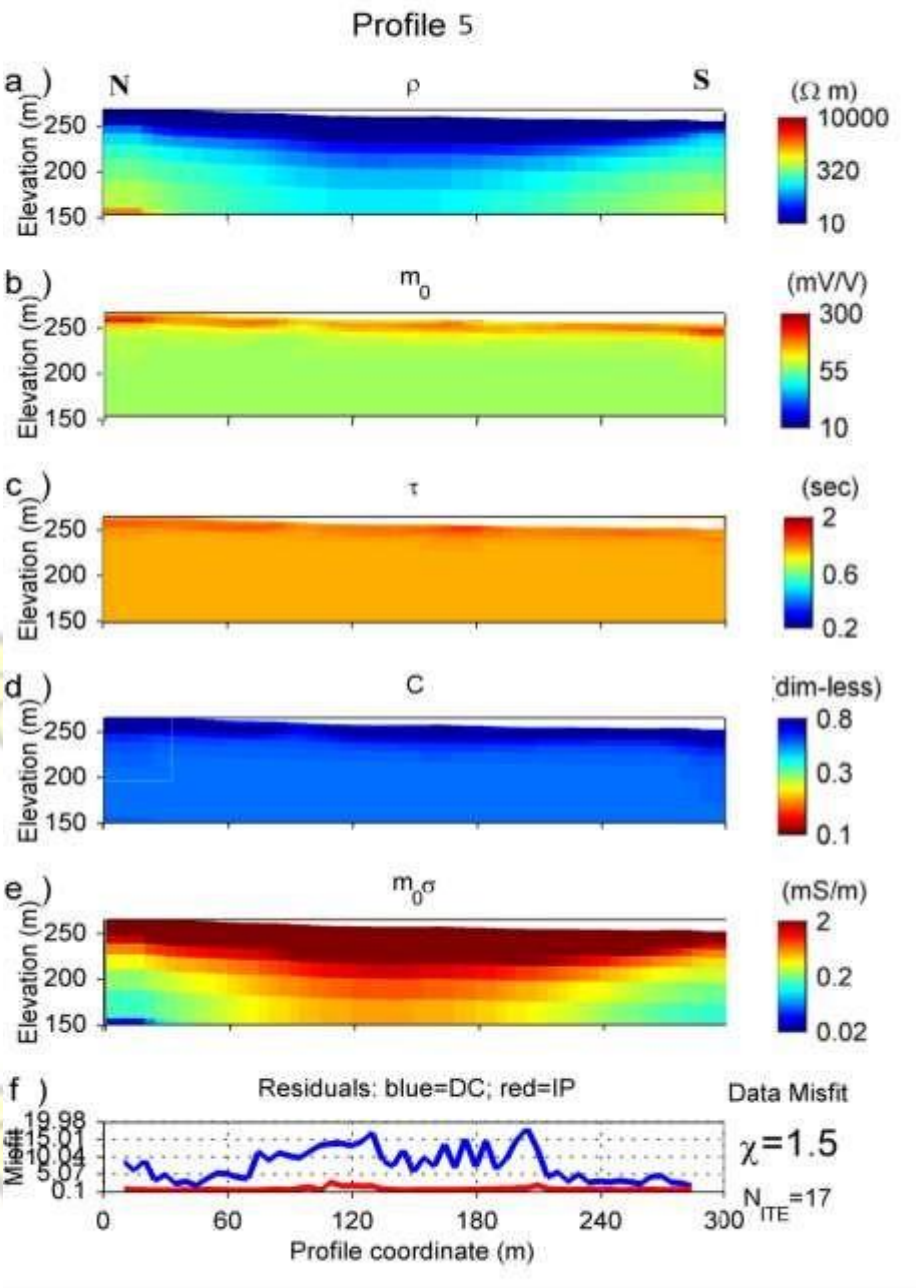

Figure 8.9 Cole-Cole spectral IP parameters of profiles 5 (a-d), e) normalized chargeability and f) Misfit of the inversion results.

Figure 8.10 presents Profiles 4 and 3 which were surveyed 30 m and 70 m from the waste deposit. Notably on profile 4 is a down dipping relatively low resistivity region at 0 to 240 m and 360 to 460 length of the resistivity section (Figure 8.10a1) with corresponding high chargeability (Figure 8.10e1). Similar anomaly trend in resistivity and normalized chargeability with lower magnitude is observed on profile 3 (Figure 8.10a2 and e2). These profiles are parallel to the deposit hence the signatures are indication of possible leachate plume from the landfill. The two vertical plumes mapped on these sections were caused by out flow of leachate from the landfill. This occurred between May and July 2013 when the waste became saturated with water after a long period of heavy rainfall in the metropolis.

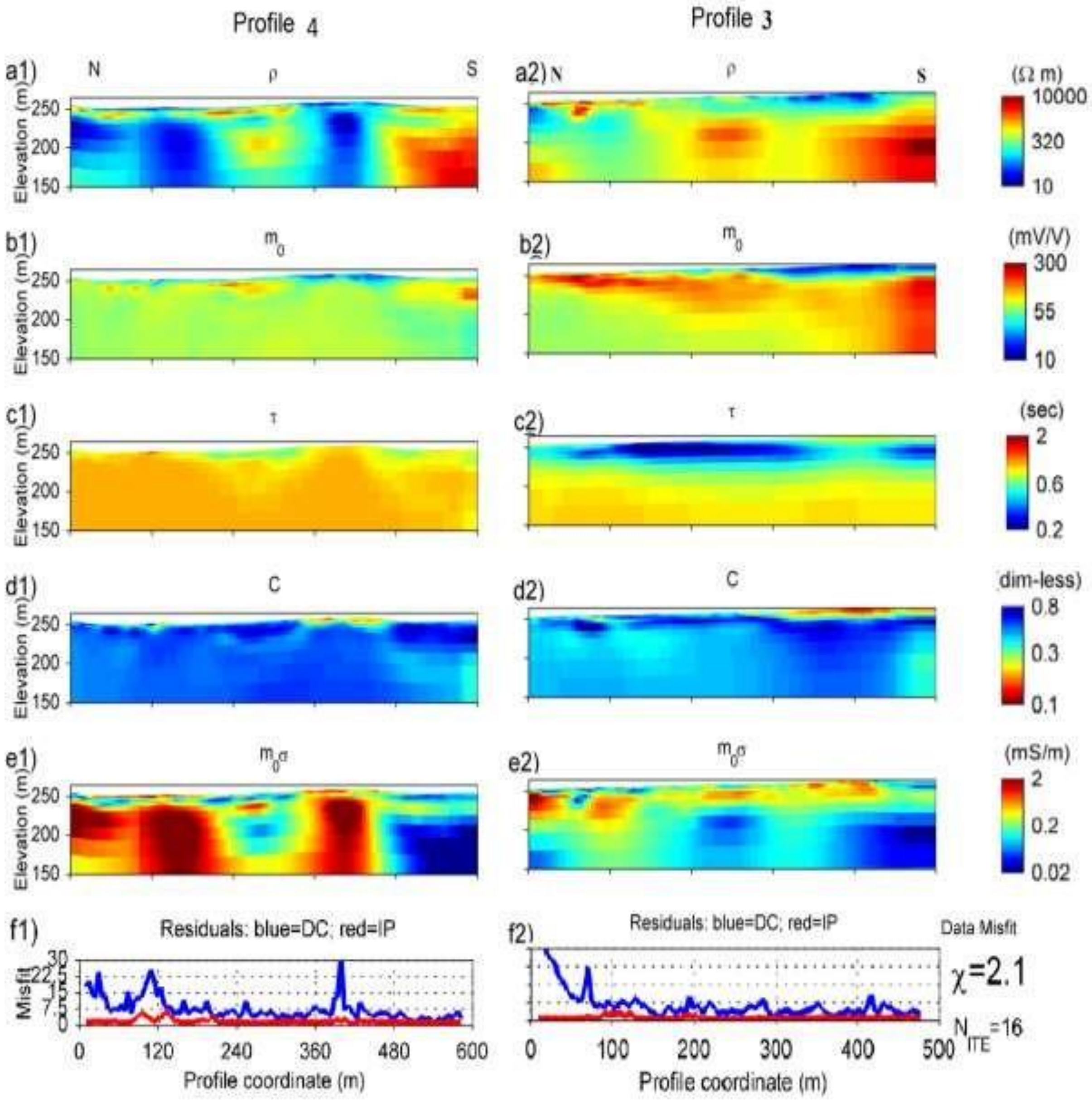

Figure 8.10 Cole-Cole spectral IP parameters of profiles 3 and 4 (a-d), e) normalized chargeability and f) Misfit of the inversion results.

The high normalised chargeability signature (Figure 8.10e) recorded by the plume is attributed to high biochemical process within the waste as well as its high ferromagnetic mineral composition. There is a high chargeability signature (Figure 8.10b) and a low relaxation time signature (Figure 8.10e) at the top layer of profile 4. These signatures are related to the position of the clayey highly porous saprolite layer. The saprolite which is generally clayey produces a strong chargeability. The low tau value recorded in this zone is due to the high porosity of the saprolite which has inverse relationship with tau (Vanhala, 1997; Slater and Lesmes, 2002; Binley *et al*., 2005). The distortion of the IP signatures due to increasing pore fluid conductivity is also evident in these sections (e.g. Wemegah *et al*., 2014, 2015). According to Olorunfemi and Griffiths (1985) and Barker (1990), the chargeability will increase as the salinity of the groundwater increases to value depending on the soil type and decrease with further increasing in concentration.

8.5.2 IP Results of Section 2

Surveys conducted in section 2 of the area aimed at determining any possible pollution plume from the waste in the north-eastern end of the site. This was deemed necessary because of the extension of the waste in recent times from the old cell into the new cell which was created without underground impermeable protective layer to prevent percolation of leachate into the soil.

Figure 8.11 was surveyed in the new cell parallel to the old cell. It can be seen from the resistivity section (Figure 8.11a) that the whole profile is represented with a very low resistivity signature with a corresponding high normalized chargeability (Figure 8.11e). This signature runs through the whole length of the profile showing possible pollution plume from the waste from the old cell. Inspection of the site revealed outflow of effluent from the waste into the new cell. The overflow of the leachate into the new cell was observed after the waste from the old cell was extended over the leachate collecting gutter at the boundary of the two cells.

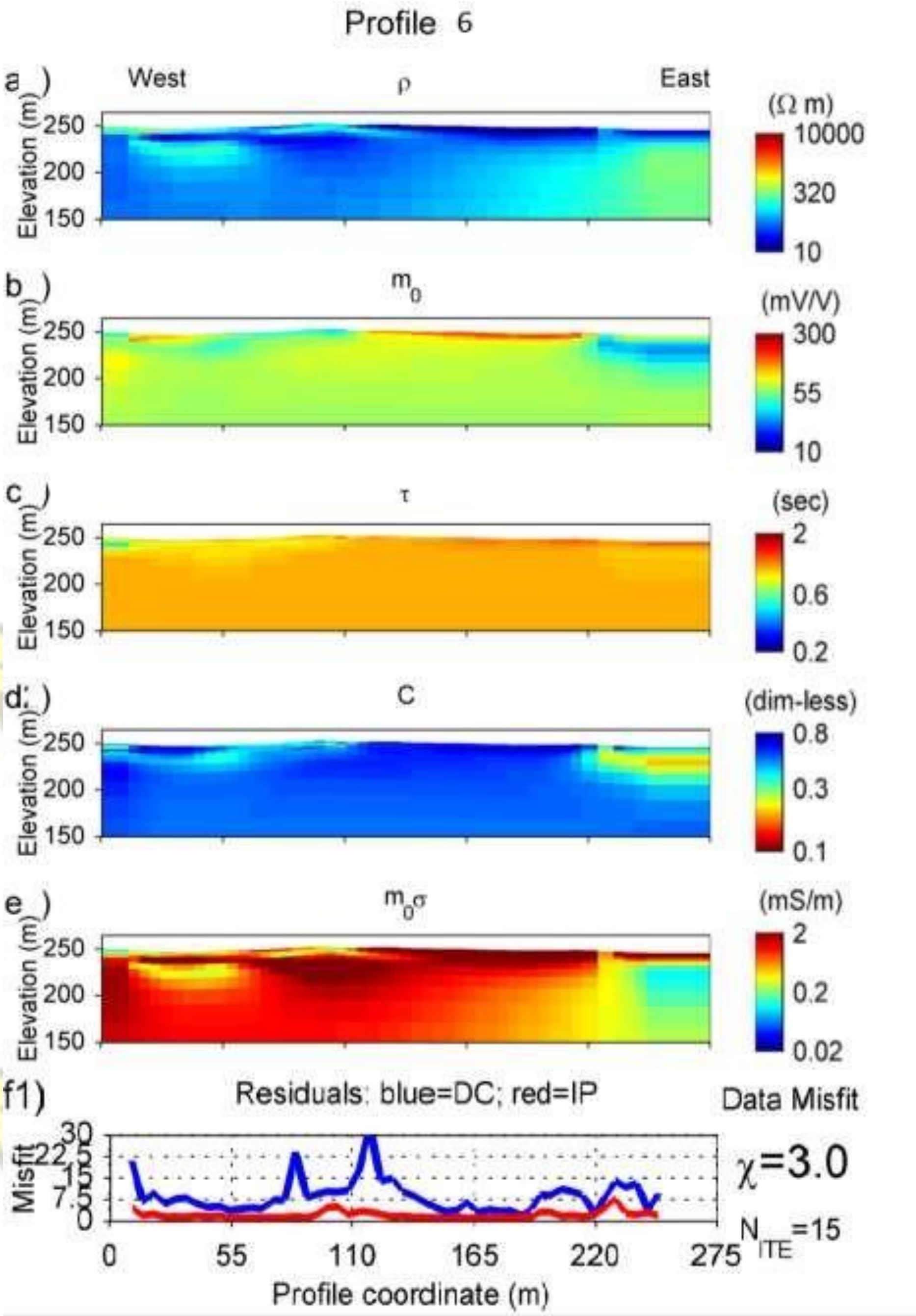

Figure 8.11 Cole-Cole spectral IP parameters of profiles 5 (a-d), e) normalized chargeability and f) Misfit of the inversion results.

Figure 8.12 presents two profiles that were surveyed perpendicular to the old cell through the new cell. This is to help determine the extent of the leachate plume as noticed at the edge of the waste (Figure 8.11) into the new cell. From these results, a general low resistivity and high normalized chargeability signatures were observed along the 100 m length of the profiles. This represents the extent of the leachate plume from the waste into the ground system. The big extension of the plume in this cell could mainly be attributed to the high topographic gradient created by excavation of the soil during the construction of the new cell. This created hydraulic gradient between the water saturated waste that is about 25 m high and the new cell (Figure 8.2) thereby aiding the flow of the leachate into the new cell. The depth extent of the plume in this cell is an indication of high porosity of the sandy clay top saprolite lithological unit. The lithological set up obtained from drilled log show depth of bedrock at 31 m with an aquifer zone within the saprolite at the 27.5 m. Consequently, the vertical extent of the plume zone to a depth of 30 m (Figure 8.11 a1 and e1) and a depth of 50 m (Figure 8.11 a2 and e2) show the vulnerability of the groundwater system to possible contamination form the leachate.

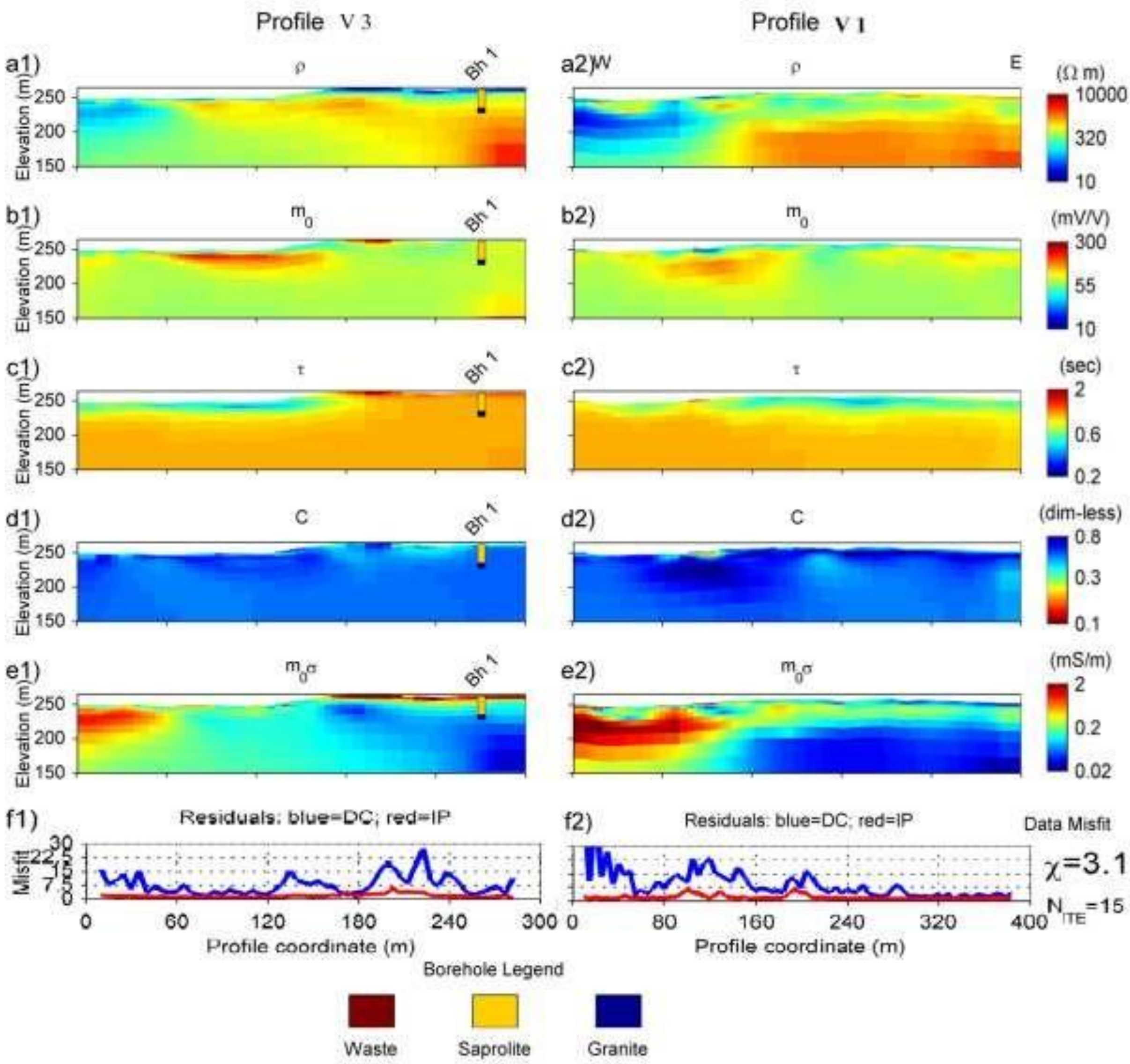

Figure 8.12 Cole-Cole spectral IP parameters of profiles V3 and V1 (a-d), e) normalized chargeability and f) Misfit of the inversion results.

8.5.3 IP Results of Section 3

Lastly, the survey in this area of the site is to help determine the impact of the released effluent from the treatment pond on the surrounding catchment area. The magnetic datasets (Figure 8.4 and Figure 8.6) mapped the flow channel of the effluent with high signatures attributed to the high amount of dissolved ferrous iron and heavy metal in the leachate. The plume at this area was mapped at the top 5 to 35 m depth. The greatest plume mapped between 350 to 450 m profile lengths (Figure 8.5a) corresponds to the position where the profile crosses the flow channel of the effluent. The presence of pollution plume on profile P2 (Figure 8.13a2) which is at a high elevation from the flow path is an indication of overflow of the leachate in that area. This occurs during the raining season when there is a high volume of effluent from the landfill and high volume of surface water runoff. This poses great health risk to the people putting up residential accommodation in this area. The area is also used for farming therefore an overflow of effluent with high heavy metal content could lead to heavy metal contamination of the food produce in this area.

The high resistivity signature (> 8000 Ωm) at depths range of 20 to 35 m (Figure 8.12a1 and a2), is associated with the granitic bedrock. These results therefore provide the means for the development of lithostratigraphic model of the site, which can be used as geological model for the development of a hydrological model of the catchment area. This can provide insight into the potential impact of the landfill in the long term.

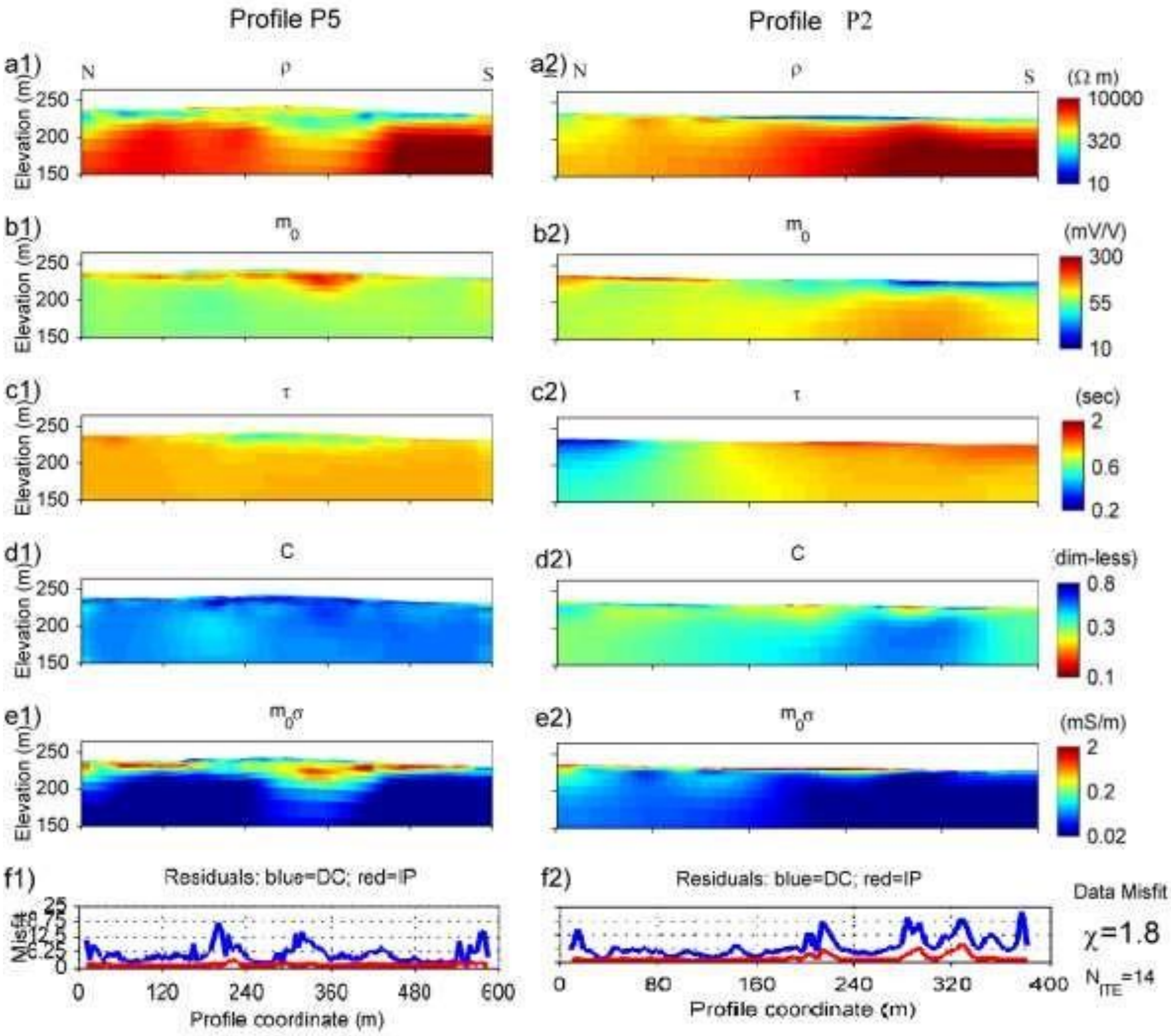

Figure 8.13 Cole-Cole spectral IP parameters of profiles P5 and P2 (a-d), e) normalized chargeability and f) Misfit of the inversion results.

8.5.4 3D Display of the Chargeability and resistivity sections

Figure 8.14 presents a 3D display of chargeability (a) and resistivity (a) sections of the surveyed profiles. The signatures in the crossing profiles were noted to correlate very well with each other showing the effectiveness of the data. The resistivity sections show low signatures within the area around the position off the main waste and its associated pollution plumes. The pollution plumes also produced strong chargeability signature attributed to high microbial activities in the leachate.

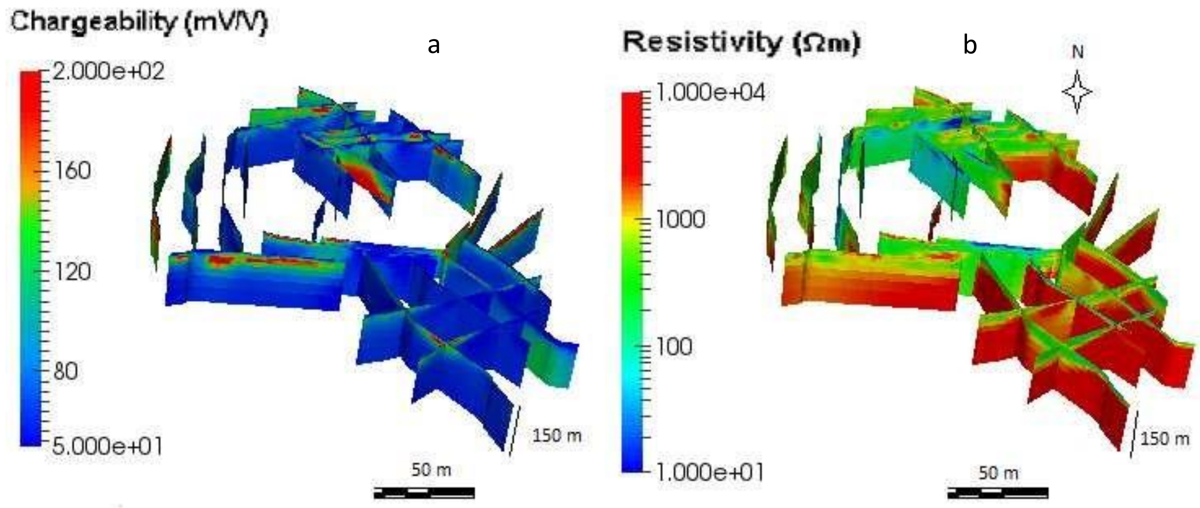

Figure 8.14 3D display of a) Chargeability sections b) Resistivity sections of surveyed profiles.

8.6 Summary

The result from the geophysical datasets acquired on the Dompoase Landfill helped in the mapping of municipal solid waste and its associated pollution plume at the Dompoase Landfill site. The magnetic data and the full wave IP result produced distinctive signatures that help in the mapping of both the lateral extent and the depth of the waste. The possible pollution plumes from the solid waste, leachate pond and the treated effluent channel were also mapped. The spectral IP parameters such as resistivity, relaxation time as well as the normalized chargeability aided in the mapping of the base of the waste plume in most of the sections.

Magnetic data mapped the main solid waste area with high magnetic signature attributed to the high composition of ferrous iron in the waste. The main waste position mapped by the magnetic data has approximate dimension of 300 m by 400 m. The effluent flow channel from the landfill was mapped with high magnetic signature which is an indication of heavy metal and ferromagnetic iron composition of the leachate. The IP parameters aided in the mapping of the pollution plumes in the catchment area of the landfill. The mapped plume of the catchment of the Dompoase Landfill shows the infiltration of leachate into the underground soil and water system posing a great risk to the quality of groundwater in the area.

CHAPTER 9: CONCLUSIONS AND RECOMMENDATIONS

9.1 Conclusions

Integrated geophysical methods namely, time-domain spectral induced polarization tomography in terms of the Cole-Cole parameters and magnetic data (collected in both total magnetic intensity and gradiometry mode) and magnetic susceptibility data were used to characterize the unengineered municipal solid waste disposal sites (KNUST and Ohwim disposal sites) and engineered municipal solid waste disposal site (Dompoase Landfill) located in the Kumasi Metropolis. The analytical signal derivative of the magnetic data and the magnetic susceptibility results depicted the lateral extent of the disposed waste, with high magnetic signature due to the high composition of ferrous metal in the waste, while the time domain Cole-Cole IP parameters helped in the delineation of the thickness of the waste deposit, the extent of the pollution plume and the site geology.

The IP inversion results show a general good misfit between the data and modelled DC resistivity and IP results at most parts of the profiles with some exception at points of very low conductivity at depth mainly attributed to 3D effect. This shows the quality and the soundness of data used in the interpretation.

At the KNUST waste disposal site, it was found that the waste deposit is characterized by a low-chargeability and low-resistivity signature, and that the area associated with the lowresistivity signature spreads out from the waste deposit into the permeable saprolite layer, indicating the presence of a leachate plume. The resistivity sections were therefore used to develop the plume model of the site while the normalized chargeability that is devoid of the effect of the pore fluid conductivity was used to develop the geological model. Similarly the low chargeability signature that is associated with the waste which was attributed to the lack of microbial activity in the waste was used to develop the waste model. The waste in the KNUST waste disposal site was mapped to cover an approximate area of 300 x 400 m and has thickness in the range of 0.5 to 10 m. Similarly, the pollution plume was mapped to cover an area of 400 x 400 m and has depth extension in range 1 to 30 m depth. Furthermore, the lithological setup of the site was developed, thanks to the contrast present in both the resistivity and IP parameters between the saprolite layer and the granite bedrock, the main lithological units of the area. A fracture zone within the granite bedrock at risk of leachate contamination was also outlined. The saprolite and the granite were also observed to have a strong signature (low and high respectively) in the relaxation time. This is attributed to the high and low porosity of the saprolite and the granitic bedrock respectively.

The MSW at the Ohwim disposal site on the other hand is associated with low resistivity signature, moderate chargeability values on some profiles and strong normalized chargeability anomaly. Similarly the waste has high magnetic signature which helps in mapping the lateral extent of the waste deposit. Some random magnetic anomaly attributed to uncontrolled and indiscriminate deposition of waste in the area was also mapped. Comparing the drilled logs to the sections, the waste model was developed using the normalized chargeability result. From the integrated geophysical result, the waste deposit was mapped to cover an area of 150 x 250 m and has thickness in the range of 5 to 12 m on the main waste site. The resistivity was used to map the pollution plume in the area which covered most part of the western and central parts of the site with depth of the plume at the main waste and the river channel reaching between 5 to 15 m. The geological model of the site was developed using the chargeability signature that distinguish the highly clayey saprolite to layer from the granitic bedrock. The saprolite thickness hence the depth of granitic bedrock, was mapped to be in arrange of 23 to 35 m. The thick plume mapped in the area shows that the groundwater is vulnerable to pollution from the leachate.

The survey at the Dompoase Landfill was designed to monitor the catchment of the landfill for any possible pollution threat from landfill. The magnetic data mapped the waste in the area to be covering an approximate area of 300 m by 200 m at its southern part and 500 m by 300 m at its northern part. The time-domain spectral induced polarization Cole-Cole parameters namely resistivity and chargeability as well as normalized chargeability help in the mapping of the plume. The high IP effect as identified with the waste and the plume is attributed to the high iron content as well as high microbial activity in the waste and the leachate. The result shows that the Landfill poses high risk to the soil and groundwater in the catchment area. Despite this, the controlled nature of the waste disposal at the Dompoase landfill makes it a possible good resource for the production of natural gas.

The outcome of this work shows that areas around municipal solid waste disposal sites in the Kumasi Municipalities are at risk of pollution from the waste. The groundwater quality which is the source of potable water source to people living around the catchment area of these waste disposal sites has its quality endangered by the waste thereby posing health risk to the populace. The data from this work can be used as starting model for the development of full hydrological model to help in the understanding of the future impact of the waste in the whole catchment area.

9.2 Recommendations

- The encroachment and the building of residential accommodation around old and current municipal waste disposal sites should be monitored due to the health risk that this site poses to people living in these environments.
- There is the need for the enactment of strong and adequate legislation both at the national and city levels to guide waste management decisions and strategies in the municipality.
- There is the need for steps to be taken to extend the lifespan of the cities landfill through waste diversion such as compositing since the wastes have high organic matter content.
- The high porosity of the saprolite makes it ineffective in preventing infiltration of leachate into the soil. Attempt should therefore be made to prevent further development of the Dompoase Landfill without a protective impermeable layer.

- There is the need for monitoring well networks at these sites to help detect any leakage plumes.
- Development of future landfills should be carried out after full impact assessments to provide a complete picture of the potential risks of the landfill site for the environment.
- There is the need for site remediation of most of these waste disposal sites to reduce the impact on the populace.
- Periodic geophysical surveys (DCIP, magnetic and magnetic susceptibility) are recommended at the sites to help in the understanding of the dynamics of the pollution in the sites.

References

Abdel Aal, G.Z., Atekwana, E.A., Slater, L.D. and Atekwana, E.A., 2004. Effects of microbial processes on electrolytic and interfacial electrical properties of unconsolidated sediments, Geophysical Research Letters **31**, L12505.

Abdel Aal, G.Z., Atekwana, E.A. and Atekwana, E.A., 2010. Effect of bioclogging in porous media on complex conductivity signatures. Journal of Geophysical Research **115**, G00G07,

Adriano, D., 1986. *Trace Elements in the Terrestrial Environment*. Springer - Verlag, New York, 46-59.

Allibone, A.H., McCuaig, T.C., Harris, D., Etheridge, M., Munroe, S., Byrne, D., Amanor, J. and Gyapong, W., 2002. Structural controls on gold mineralisation at the Ashanti Deposit, Obuasi, Ghana. Society of Economic Geologists, Special Publication **9**, 65-93.

Angoran, Y.E., Fitterman, D.V. and Marshall, D.J., 1974. Induced Polarization: A Geophysical Method for Locating Cultural Metallic Refuse. Science, New Series, **184**(4143), 1287-1288.

Ansari, A.H. and Alamdar, K., 2009. Reduction to the pole of magnetic anomalies using analytic signal. World Applied Sciences Journal **7**, 405-409.

Asase, M., Yanful, E.K., Mensah, M. and Stanford, J. 2009. Comparison of municipal solid waste management systems in Canada and Ghana: A case study of the cities of London, Ontario and Kumasi, Ghana. Waste Management **29**(10), 2779-2786.

Atekwana, E.A., Sauck, W.A. and Werkema, D.D. Jr., 2000. Investigations of geoelectrical signatures at a hydrocarbon contaminated site. Journal of Applied Geophysics **44**, 167-180.

Atekwana, E.A. and Slater, L.D., 2009. Biogeophysics: A new frontier in Earth science research. Reviews of Geophysics **47**, RG4004.

Atekwana, E.A., Atekwana, E.A., Legall, F.D. and Krishnamurthy, R.V., 2004a. Field evidence for geophysical detection of microbial activity. Geophysical Research Letters **31**, L23603.

Atekwana, E.A., Atekwana, E.A., Rowe, R.S., Werkema, D.D. and Legall, F.D., 2004b. Total dissolved solids in groundwater and its relationship to bulk conductivity of soils contaminated with hydrocarbon. Journal of Applied Geophysics **56**, 281-294.

Auken, E., Christiansen A.V., Kirkegaard, C., Fiandaca, G., Schamper, C., Behroozmand, A.A., Binley, A., Nielsen, E., Effersø, F., Christensen, N.B., Sørensen, K., Foged, N. and Vignoli, G., 2014. An overview of a highly versatile forward and stable inverse algorithm for airborne, ground-based and borehole electromagnetic and electric data. Exploration geophysics, A-M.

Auken, E., Viezzoli, A. and Christiansen A.V., 2009. A single software for processing, inverting, and presentation of AEM data of different system: The Aarhus Workbench.

Australian Society of Exploration Geophysics Geophysicist (ASEG) 2009, Sydney, Australia, Expanded Abstract, 1-5.

Awortwi, N., 2004. Getting the fundamentals wrong: Woes of public–private partnerships in solid waste collection in three Ghanaian cities. Public Administration and Development **224**, 213-224.

Aziz, A.M., Sauck, W.A., Shendi, E.H., Rashed, M.A. and El-Maksoud, M.A., 2013. Application of analytic signal and Euler Deconvolution in archaeo-magnetic prospection for buried ruins. Surveys in Geophysics **34**, 395-411.

Bagchi, A., 1994. *Design, construction, and monitoring of landfills*. Willey, Canada, 357.

Banton, O., Seguin, M.K. and Cimon, M.A., 1997. Mapping field scale physical properties of soil with electrical resistivity. Soil Sci. Soc. Am. J. **61**, 1010-1017.

Barker, R.D., 1990. Investigation of groundwater salinity by geophysical methods. In: S.H. Ward, (ed.) Geotechnical and environmental geophysics, vol. II: SEG Investigations in Geophysics **5**, 201-211.

Barrows, L. and Rocchio, J.E., 1990. Magnetic surveying for buried metallic objects, Ground Water Monit. Rev. **10**, 204-211.

Barthiban, S., Lloyd B.J. and Maier, M., 2012. Microbial quality of open dug wells in the Maldives Islands. Journal of Water Resource and Protection **4**, 474486.

Beatriz, A.H., Vega, M., Barrado, E., Pardo, R. and Fernandez, L., 1998. A case of hydrochemical characterization of an alluvial aquifer influenced by human activities. Water, Air and Soil Pollution **112**, 365-387.

Binley, A., Slater, L.D., Fukes, M. and Cassiani, G., 2005. Relationship between spectral induced polarization and hydraulic properties of saturated and unsaturated sandstone, Water Resource. Res. **41**, W12417.

Blasting, J.F., 1987. Characterization of an abandoned waste site using proton magnetometry and computer graphics. Restoration, Ground Water Monitoring and Geophysical Methods. Las Vegas, NWWA, 573-584.

Boadi, B., Wemegah, D.D. and Preko, K., 2013. Geological and structural interpretation of the Konongo Area of the Ashanti Gold Belt of Ghana from aeromagnetic and radiometric data. International Research Journal of Geology and Mining (IRJGM). **3**(3), 124-135.

Boadu, E.K., 2000. Hydraulic conductivity of soils from grain size distribution: New models. J. of Geotechnical and Geo-environmental Engineering **126**, 739-745.

Boadu, F.K. and Seabrook, B., 2000. Estimating hydraulic conductivity and porosity of soils from spectral electrical response measurement. JEEG **5**(4), 1-9.

Bolt, G.H. and Bruggenwert, M.G. (ed.s), 1978. *Soil Chemistry. Part A, Basic Elements*. Elsevier Science Publishing Co.

Bomer, E.D., Schopper, I.R. and Weller, A., 1996. Evaluation of transport and storage properties in soil and groundwater zone from induced polarization measurements. Geophysical Prospecting **44**, 583-601.

Buselli, G. and Lu, K. 2001. Groundwater contamination monitoring with multichannel electrical and electromagnetic methods. Journal of Applied Geophysics **48**, 11-23.

Butt, T.E., Lockley, E. and Oduyemi, K.O.K., 2008. Risk assessment of landfill disposal sites - State of the art. Waste Management **28**, 952-964.

Canbay, M., 2008. Magnetic susceptibility and magnetic anisotropy studies in the Armutlu Peninsula, The 18th International Geophysical Congress and Exhibition of Turkey.

Canbay, M., 2010. Investigation of the relation between heavy metal contamination of soil and its magnetic susceptibility. International Joural of Physical sciences **5**(5), 393-400.

Carlson, N.R., Hare, J.L. and Zonge, K.L., 2001. Buried landfill delineation with induced polarization: Progress and problems. Proceedings of the 2001 Symposium on the Application of Geophysics to Engineering and Environmental Problems (SAGEEP), Denver, Colorado, March 4-7.

Carlson, N.R., and Mayerle C.M., 2009. Changes in IP effects over time resulting from accelerated degradation processes at a landfill, international workshop on induced polarization in Near Surface Geophysics, Bonn University, Germany, 30 Sept - 1 Oct.

Chen, J., Hubbard, S.S., Williams, K.H., Flore-Orozco, A. and Kemna, A., 2012. Estimating the spatiotemporal distribution of geochemical parameters associated with biostimulation using spectral induced polarization data and hierarchical Bayesian models, Water Resour. Res. **48**, W05555.

Christiansen, V.A., Foged, N. and Auken, E., 2014. A concept for calculating accumulated clay thickness from borehole lithological logs and resistivity models for nitrate vulnerability assessment. Journal of Applied Geophysics **108**, 69-77.

Christensen, T.H., Kjeldsen, P., Albrechtsen, H.J., Heron, G., Nielsen, P.H., Bjerg, P.L. and Holm, P.E., 1993. Attenuation of landfill leachate pollutants in aquifers. Critical Reviews in Environmental Science and Technology **24**, 119-202.

Christensen, T.H., Kjeldsen, P., Bjerg, P.L., Jensen, D.L., Christensen, J.B. and Baun, A., 2001. Review: Biogeochemistry of landfill leachate plumes. Applied Geochemistry **16**, 659-718.

Cofie, O., Drechsel, P., Obuobie, E., Danso, G. and Keraita, B., 2003. Environmental sanitation and urban agriculture in Ghana, in Towards the Millennium Development Goals. Nigeria, Abuja, WEDC, 2003, 9-12.

Cole, K.S. and Cole, R.H., 1941. Dispersion and absorption in dielectrics. Journal of Chemistry and Physics **9**, 341-351.

Dahlin, T.R., Hakan, R.L. and Virginie, M.X., 2010. Resistivity-IP mapping for landfill applications. First Break **28**(8), 101-105.

Dahlin, T., Leroux, V. and Nissen, J., 2002. Measuring techniques in induced polarisation imaging. Journal of Applied Geophysics **50**, 279-298.

Dahlin, T. and Zhou, B., 2004. A numerical comparison of 2D resistivity imaging with 10 electrode arrays. Geophysics Prospecting **52**, 379-398.

Dahlin T. and Zhou B., 2006. Multiple-gradient array measurements for multi-channel 2D resistivity imaging. Near Surface Geophysics **4**, 113-123.

Daniels, J.J., Roberts, R. and Vendl, M., 1995. Ground penetrating radar for the detection of liquid contaminants. Journal of Applied Geophysics **33**(1-3), 195-207.

Davis, D.W., Hirdes, W., Schaltegger, E. and Nunoo, E.A., 1994. U/Pb age constraints on deposition and provenance of Birimian and gold-bearing Tarkwaian Sediments in Ghana, West Africa. Precambrian Research **67**, 89-107.

Dearing, J., 1999. *Report on environmental magnetic susceptibility*: Using the Bartington *MS2* System. Kenilworth, Chi Publishing, 1-54.

Denutsui, D., Akiti, T.T., Osae, S., Tutu, A.O., Blankson-Arthur, S., Ayivor, J.E., AduKwame, F.N. and Egbi, C., 2012. Leachate characterization and assessment of unsaturated zone pollution near municipal solid waste landfill site at Oblogo, AccraGhana. Research Journal of Environmental and Earth Sciences **4**(1), 134-141.

Dias, C., 2000. Developments in a model to describe low-frequency electrical polarization in rocks. Geophysics **65**, 437-451.

Dolk, H. and Vrijheid, M., 2003. The impact of environmental pollution on congenital anomalies. Br Med Bull **68**, 25-45.

Erdelyi, M., 2010. The Hydrogeology of Ghana. International Association of Scientific Hydrology Bulletin **10**(1), 37-41.

Fedi, M. and Florio, G., 2001. Detection of potential fields source boundaries by enhanced horizontal derivative method. Geophysics Prospecting **49**, 40-58.

Ferre, E.C., Wilson, L.J. and Gleizes, G., 1999. Magnetic susceptibility and AMS of the Bushveld alkaline granites, South Africa. Tectonophysics **307**, 113-133.

Fiandaca, G., Auken, E., Christiansen, A.V. and Gazoty, A., 2012. Time-domain polarization: Full-decay forward modelling and 1-D laterally constrained inversion of Cole-Cole parameters. Geophysics **77**(33), E213-E225.

Fiandaca, G., Ramm, J., Binley, A., Gazoty, A., Christiansen, A.V. and Auken, E., 2013. Resolving spectral information from time domain induced polarization data through 2D inversion. Geophysics Journal International **192**, 631-646.

Flores Orozco, A., Kemna, A., Oberdörster, C., Zschornack, L., Leven, C., Dietrich, P. and Weiss, H., 2012. Delineation of subsurface hydrocarbon contamination at a former hydrogenation plant using spectral induced polarization imaging. Journal of Contaminant Hydrology **136/137**, 131-144.

Flores Orozco, A., Williams, K.H., Long, P.E., Hubbard, S.S. and Kemna, A., 2011. Using complex resistivity imaging to infer biogeochemical processes associated with bioremediation of an uranium-contaminated aquifer. Journal of Geophysical Research G: Biogeosciences **116** (3), G03001.

Fobil, J., May, J. and Kraemer, A., 2010. Assessing the relationship between socioeconomic conditions and urban environmental quality in Accra, Ghana. International Journal of Environmental Research and Public Health **7**(1), 125-145.

Gaffney, C., Gater, J.A. and Ovenden, S.M., 2002. The Use of Geophysical Techniques in Archaeological Evaluations. IFA Technical Paper 6. Reading, Institute of Field Archaeologists.

Gazoty, A., Fiandaca, G., Pedersen, E., Auken, E. and Christiansen, A.V., 2012a. Mapping of landfills using time-domain spectral induced polarization data: the Eskelund case study. Near Surface Geophysics **10**, 575-586.

Gazoty, A., Fiandaca, G., Pedersen, E., Auken, E., Christiansen, A.V. and Pedersen, J.K., 2012b. Application of time domain induced polarization to the mapping of lithotypes in a landfill site. Hydrol. Earth Syst. Science **16**, 1793-1804.

Gazoty, A., Fiandaca, G., Pedersen, J., Auken, E. and Christiansen, A.V., 2013. Data repeatability and acquisition techniques for time-domain spectral induced polarization. Near Surface Geophysics **11**, 391-406.

Geosoft Inc., 1996. Oasis Montaj user guide, Geosoft Incorperated, Toronto, USA.

Oasis Montaj, 2006. Oasis Montaj user guide, Geosoft Incorperated, Toronto, USA.

Gershman, B. and Bratton Inc., 1986. Small-scale municipal solid waste energy recovery systems.

Gibson, P.J., Lyle, P. and Gorge, D.M., 1996. Environmental applications of magnetometry, profiling. Environmental Geology **27**, 178-183.

Gilkeson, R.H., Heigold, P.C. and Laymon, D.E., 1986. Practical application of theoretical models to magnetometer surveys on hazardous waste disposal sites - A case his- tory, Ground Water Monit. Rev. **6**, 54-61.

Graham, M.K., Preko, K., Wemegah, D.D. and Boamah, D., 2014. Geological and structural interpretation of part of the Buem Formation, Ghana, using aerogeophysical data. Journal of Environment and Earth Sciences **4**(4), 17-31.

Grant, F.S. and Dodds, J., 1972. MAGMAP FFT processing system development notes, Paterson Grant and Watson Limited.

Griffis, R.J., Barning, K., Agezo, F.L. and Akosah, F.K., 2002. *Gold Deposits of Ghana*. Minerals Commission Report, 19-37, 163-169.

Ghana Statistical Service (GSS), 2002. *Population and housing census 2000: Summary of final results*; Ghana Statistical Service: Accra, Ghana.

GSS, 2012. *Population and housing census 2010: Summary of final results*; Ghana Statistical Service: Accra, Ghana.

Gyau-Boakye, P. and Dapaah-Siakwan, S., 2004. Groundwater as source of rural water supply in Ghana. Journal of Applied Science and Technology **5**(1), 77-86.

Hackworth, J.B., 1996. EM Induction and Magnetic Surveys at Large Landfill Sites Using GPS for Positional Control. Proceedings of SEG the Symposium on the Application of Geophysics to Enigineering and Environmental Problems. SEG, 1151-1171.

Hanesch, M. and Scholger, R., 2002. Mapping of heavy metal loadings in soils by means of magnetic susceptibility measurements. Environmental Geology **42**, 857-870.

Herman, R., 2001. An introduction to electrical resistivity in geophysics. American Journal of Physics **68**(9), 943-952.

Hirdes, W., Davis, D.W. and Eisenlohr, B.N., 1992. Reassessment of Proterozoic granitoid ages in Ghana on the basis U/Pb zircon and monazite dating. Precambrian Research **56**, 89-96.

Hirdes, W., Leube, R., Mauer, R. and Kesse, G.O., 1988. The Early Supergroup of Ghana: Depositional environment, tectono-thermal development and conceptual model of an early Proterozoic suite. Abstract, International conference and workshop on the geology of Ghana with special emphasis on gold-geology and exploration in Ghana and in selected other Precambrian terrains, October, Accra, Ghana.

Hottin, G. and Quedraogo, O.F., 1975. Notice explicative de la carte geologique a 1:1,000,000 de la Republique de Haute-Volta. Direction de la Geologie et des Mines, Rpublique de Haute-Volta, Quagadougou, 58.

Johannessen, L.M. and Boyer, G., 1999. Observations of solid waste landfills in developing Countries: Africa, Asia, and Latin America. Urban Development Division, Waste Management Anchor Team, The World Bank.

Johansson, S., Fiandaca, G. and Dahlin, T., 2014. Field application of resistivity and spectral time domain IP to investigate geoelectrical signatures of free-phase PCE. Near Surface Geoscience 2014, Athens, Greece, Extended Abstract.

Jordanova, N., Jordanova, D. and Tsacheva, T., 2008. Application of magnetometry for delineation of anthropogenic pollution in areas covered by various soil types. Geoderma **144**, 557-571.

Jørgensen, F., Lykke-Andersen, H., Sandersen, P.B.E., Auken, E. and Nørmark, E., 2003. Geophysical investigations of buried Quaternary valleys in Denmark: An integrated application of transient electromagnetic soundings, reflection seismic surveys and exploratory drillings. J. Appl. Geophysics **53**, 215-228.

Kankam-yeboah, K., Dapaah-siakwan, S. and Nishigaki, M., 2003. The hydrogeological setting of Ghana and the potential for underground dams. Journal of the Faculty of Environmental Science and Technology **8**(1), 39-52.

Kearey, P., Brooks, M. and Hill, I., 2002. *An Introduction to Geophysical Exploration*. TJ International Publishing, Padstow, Cornwall, 164.

Keller, G.V., 1959. Analysis of some electrical transient measurements on igneous, sedimentary and metamorphic rocks, in: Wait, J.R., (Ed.) Overvoltage research and geophysical applications, Pergamon Press; 92-111.

Kemna, A., Binley, A., Cassiani, G., Niederleithinger, E., Revil, A., Slater, L., Williams, K., Orozco, A., Haegel, F.-H., Hördt, A., Kruschwitz, S., Leroux, V., Titov, K. and Zimmermann, E., 2012. An overview of the spectral induced polarization method for near-surface applications. Near Surface Geophysics **10**, 453-468.

Kemna, A., Binley, A. and Slater, L., 2004. Crosshole IP imaging for engineering and environmental applications. Geophysics **69**, 97-107.

Kesse, G.O., 1969. The geology of Sheet 128, Kumasi, NE. Ghana. Geol. Surv. Bull. No. **39**.

Kesse, G.O., 1972. The geology of Sheet 165, Sekodumasi SW. Ghana. Geol. Surv. Bull. No. **41**.

Kesse, G.O., 1985. *The mineral and rock resources of Ghana*. A.A. Balkema, Rotterdam, 610.

Ketibuah, E., Asase, M., Yusif, S., Mensah, M., and Fischer, K., 2005. Comparative analyzes of household waste in the cities of Stuttgart and Kumasi - Options for waste recycling and treatment in Kumasi. Stuttgart, Germany: WASTE, Universität Stuttgart.

Khanal, S.C., 2007. Post project environmental monitoring and impact assessment - a case of gokarna sanitary landfill site after operation and closure, Scientific World **5**(5), 60-66.

Kirsch, R. (ed.), 2006. *Groundwater Geophysics* – A tool for hydrogeology, 2nd Edition, Springer, Berlin, Germany, 1-20.

Kirsch, R., Sengpiel, K.P. and Voss, W., 2003. The use of electrical conductivity mapping in the definition of an aquifer vulnerability index. Near Surf. Geophysics **1**, 13-19.

Kjeldsen, P., Bjerg, P.L., Rugged, K., Christensen, T.H. and Pedersen, J.K., 1998a. Characterization of an old municipal landfill (Grinsted, Denmark) as a groundwater pollution source: Landfill hydrology and leachate migration. Waste Management & Research **16**(1), 14-22.

Kjeldsen, P., Grundtvig, A., Winther, P. and Andersen, J.S., 1998b. Characterization of an old municipal landfill (Grinstead, Denmark) as a groundwater pollution source: Landfill history and leachate composition. Waste Management & Research **16**(1), 3-13.

Klučiarová, D., Márton, P., Pichler, V., Márton, E. and Túnyi, I., 2008. Pollution detection by magnetic susceptibility measurements aided by the stemflow effect. Water, Air, and Soil Pollution **189**, 213-223.

Kumasi Metropolitan Assembly and Ministry of Local Government and Rural Development (KMA and MLGRD), 2006. Development Plan for the Kumasi Metropolitan Area (2006-2009) (Kumasi: Kumasi Metropolitan Assembly).

Kortatsi, B.K., 1994. Groundwater utilization in Ghana, Water Resources Research Institute, IAHS Publ. no. 222, Accra, Ghana, 151.

Lecoanet, H., Lévêque, F. and Seguna S., 1999. Magnetic susceptibility in environmental applications: comparison of field probes. Phys. Earth Planet. Inter. **115**, 191-204.

Leroux, V., Dahlin, T. and Rosqvist, H., 2010. Time-domain IP and Resistivity Sections Measured at Four Landfills with Different Contents. Near Surface Geophysics 2010, Zürich, Switzerland, Expanded Abstracts, P09.

Leroy, P. and Revil, A., 2009. A mechanistic model for the spectral induced polarization of clay materials. Journal of Geophysical Research **114**, B10202.

Lesmes, D.P. and Frye, K.M., 2001. Influence in pore fluid chemistry onthe complex conductivity and induced polarization responses of Berea sandstone. Journal of Geophysical Research **106**, 4079-4090.

Leube, A. and Hirdes, W., 1986, The Birimian Supergroup of Ghana: Depositional environment, structural development, and conceptual model of an Early Proterozoic suite: Hanover, Bundesanstalt für Geowissenschaften und Rohstoffe **99**, 529, 260.

Leube, A., Hirdes, W., Mauer, R. and Kesse, G.O., 1990. The early Proterozoic Birimian supergroup of Ghana and some aspects of its associated gold mineralization. Prec. Res. **46**, 139-165.

Li, X., 2008. *Magnetic reduction-to-the-pole at low latitudes.* Fugro Gravity and Magnetic Services. Houston, USA.

Luo, Y. and Zhang, G., 1998. Theory and application of spectral induced polarization. Geophysical Monograph Series, SEG.

MacLeod, I.N., Jones, K. and Dai, T.F., 1993. 3-D analytic signal in the interpretation of total magnetic field data at low magnetic latitudes. Exploration Geophysics **24**, 679-688.

Magiera, T., Strzyszcz, Z., Kapicka, A. and Petrovsky, E., 2006. Discrimination of lithogenic and anthropogenic influences on topsoil magnetic susceptibility in Central Europe. Geoderma **130**(3-4), 299-311.

Marchetti, M., 2000. Anomalie magnetiche in aree di discarica: una breve rassegna, In: Atti XIX Convegno Nazionale CNR-GNGTS.

Marchetti, M., Chiappini, M. and Meloni, A., 1998. A test site for magnetic detection of buried steel drums, Annuli di Geophysical **41**(3), 491-498.

Marchetti, M., Camarilla, L., Di Mauro, D. and Zirizzotti, A., 2002. Ground magnetometric surveys and integrated geophysical methods for solid buried waste detection: a case study. Annals of Geophysics **45**(3/4), 563-573.

Marchetti, M. and Settimi, A., 2011. Integrated geophysical measurements on a test site for detection of buried steel drums, Annals of Geophysics, **54**(1), 105-114.

Marshall, D.J. and Madden, T.R., 1959. Induced polarization, a study of its causes. Geophysics **24**, 790–816.

McDougall, F.R. and Hruska, J.P., 2000. The use of life cycle inventory tools to support an integrated approach to solid waste management. Waste Management and Research **18**, 590-594.

Mensah, A.E., Cofie, O. and Montangero, A., 2003. Lessons from a pilot co-composting plant in Kumasi, Ghana. 29th WEDC International Conference, 3, Abuja, Nigeria.

Mikac, N., Cosovic, B., Ahel, S.A. and Toncic, Z., 1998. Assessment of groundwater contamination in the vicinity of a municipal waste landfill (Zagreb, Croatia). Water Sciences Technology **37**(8), 37-44.

Milési, J.P., Ledru, P., Feybesse, J.L., Dommanget, A. and Marcoux, E., 1992. Early Proterozoic ore deposits and tectonics of the Birimian Orogenic Belt, West Africa. Precambrian Res. **58**, 305-344.

Moore, E., Matalon, E., Clary, J., Firestone, L. and Anda, S.D., 2011. The human costs of nitrate-contaminated drinking water in the San Joaquin Valley. 1st Edn., Pacific Institute for Studies in Development, Oakland, ISBN-10: 1893790312, 45.

Morris, J.W.F. and Barlaz, M.A., 2011. A performance-based system for the long-term management of municipal waste landfills. Waste Management **31**, 649–662.

Nabighian, M.N., 1972. The analytic signal of two-dimensional magnetic bodies with polygonal for automated cross-section: Its properties anomaly interpretation. Geophysics **37**(3), 507-517.

Nabighian, M.N., 1984. Toward a three-dimensional automatic interpretation of potential field data via generalised Hilbert transforms: Fundamental relations. Geophysics **49**, 780-789.

Nabighian, M.N., Grauch, V.J.S., Hansen, R.O. LaFehr, T.R., Li, Y., Peirce, J.W., Phillips, J.D. and Ruder, M.E., 2005. The historical development of the magnetic method in exploration. Geophysics **70**(6), 33ND-61ND.

Ministry of Local Government and Rural Development (MLGRD), 1999. Environmental Sanitation Policy. Government of Ghana. http://www.rspo-inghana.org/sitescene/custom/userfiles/file/ENVIRONMENTAL_SANITATION_POLICY.pdf, (Accessed: July 25, 2013).

Obeng, P.A, Donkor, A.E. and Mensah, A., 2009. Assessment of institutional structures for solid waste management in Kumasi", Management of Environmental Quality. An International Journal **20**(2), 106–120.

Okrah, C., Danuor, S.K., and Dapaah-Siakwan, S., 2013. Geophysical investigations for groundwater in the middle Precambrian province of Upper Denkyira District using electromagnetic and electrical resistivity methods. Journal of the Ghana Science Association **14**(1), 103-114.

Olhoeft, G.R., 1985. Low-frequency electrical properties. Geophysics 50, 2492-2503.

Olorunfemi, M.O. and Griffiths, D.H., 1985. A laboratory investigation of the induced polarization of the Triassic Sherwood Sandstone of Lancashire and its hydrogeological applications: Geophysical. Prospecting **33**, 110-127.

O"Reilly, W., 1984. *Rock and mineral magnetism*, Blackie, Glasgow.

Patel, P., Desai, M. and Desai, J., 2011. Geotechnical parameters impact on artificial ground water recharging technique for Urban Centers. Journal of Water Resource and Protection **3**, 275-282.

Pelton, W.H, Ward, S.H., Halof, P.G., Sill, W.R. and Nelson, P.H., 1978. Mineral discrimination and removal of inductive coupling with multi-frequency induced polarization. Geophysics **43**, 588-609.

Pettersson, J.K. and Nobes, D.C., 2003. Environmental geophysics at Scott Base: Ground penetrating radar and electromagnetic induction as tools for mapping contaminated ground at Antarctic research bases. Cold Regions Science and Technology **37**, 187195.

Post, J., 1999. The problem and potentials of privatising solid waste management in Kumasi, Ghana. Habitat International **23**(2), 201-216.

Poulsen, T.G., Moldroup P., Sørensen K. and Hansen, J.A., 2002. Linking landfill hydrology and leachate chemical composition at a controlled municipal landfill (Kåstrup, Denmark) using state-space analysis. Waste Management and Research **20**, 445-456.

Republic of Ghana, 1999. Environmental Sanitation Policy, Accra: Ministry of Local Government and Rural Development.

Reeve, C.V., 1989. Aeromagnetic interpretation and rock magnetism. First Break **7**, 275-286.

Revil, A. and Florsch, N., 2010. Determination of permeability from spectral induced polarization in granular media. Geophysical Journal International **181**, 1480-1498.

Reynolds, J.M., 1997. *An introduction to applied and environmental geophysics*, Wiley publication, New York.

Riediker, S., Suter, J.F.M. and Giger, W., 2000. Benzene and naphthalenesulfonates in leachates and plumes of landfills. Water Resources **34**(7), 2069-2079.

Roest, W.R., Verhoef, J. and Pilkington, M., 1992. Magnetic interpretation using the 3-D analytical signal. Geophysics **57**, 116-125.

Rucker, D.F., 2010. The application of magnetic gradiometry and electromagnetic induction at a former radioactive waste disposal site. Waste Management and Research **28**, 364-372.

Ruffet, C., Guenguen, Y. and Darot, M., 1991. Complex conductivity measurements and fractal nature of porosity. Geophysics **56**, 758-768.

Sandrin, A. and Elming, S., 2006. Geophysical and petrophysical study of an iron oxide copper gold deposit in northern Sweden. Ore Geology Reviews, **29**(1), 1-18.

Schmidt, A., Yarnold, R., Hill, M. and Ashmore, M., 2005. Magnetic susceptibility as proxy for heavy metal pollution: A site study. Journal of Geochemical Exploration **85**, 109117.

Schmutz, M., Revil, A., Vaudelet, P., Batzle, M., Viñao, P.F. and Werkema, D.D., 2010. Influence of oil saturation upon spectral induced polarization of oil-bearing sands. Geophysical Journal International **183**, 211-224.

Schön, J.H., 1996. *Physical properties of rocks: Fundamentals and principles of petrophysics. Handbook of geophysical exploration*. Sect. 1; Vol. 18. Elsevier Science Publishing Co., Pergamon Press.

Slater, L.D. and Lesmes, D.P., 2002. IP interpretation in environmental investigations. Geophysics **67**(1), 77-88.

Slater, L., Ntarlagiannis, D.D. and Wishart, D., 2006. On the relationship between induced polarization and surface area in metal-sand and clay-sand mixtures. Geophysics **71**(2), A1-A5.

Splajt, T. Ferrier, G. and Fro stick, L.E., 2003. Application of ground penetrating radar in mapping and monitoring landfill sites. Environmental Geology **44**(8), 963-967.

Sogade, J.A., Scira-Scappuzzo, F., Vichabian, Y., Shi, W., Rodi, W., Lesmes, D.P. and Morgan, F.D., 2006. Induced-polarization detection and mapping of contaminant plumes. Geophysics **71**, B75-B84.

Songsore, J., 1992. Review of household environmental problems in the Accra Metropolitan Area, Ghana; SEI: Stockholm, Sweden.

Songsore, J., 1998. Proxy indicators for rapid assessment of environmental health status of residential areas - The case of the Greater Accra Metropolitan Area (GAMA), Ghana; SEI and SIDA Publication: Stockholm, Sweden.

Sylvester, P.J. and Attoh, K., 1992. Lithostratigraphy and composition of 2.1 Ga belts of the West African Craton and their bearing on crustal evolution and the ArcheanProterozoic Boundary. Journal of Geology **100**, 377-393.

Tagini, B., 1971. *Esquisse structurale de la Cote D'Ivoire. Essai de geotectoniqu regionale*. These University Lausanne. Societe d"Estat pour kle devepement miniere de la Cote D"Ivoire.

Taylor, P.N., Moorbath, S., Leube, A. and Hirdes, W., 1992. Early Proterozoic crustal evolution in the Birimian of Ghana: Constraints from geochronology and isotope geochemistry. Precambrian Research **56**(1-2), 97-111.

Telford, W.M., Geldart, L.P. and Sheriff, R.E., 1990. *Applied Geophysics*, 2nd Edition, Press Syndicate of the University of Cambridge, Cambridge.

Tyagi, S., Lord, A.E., (Jr.) and Koerner, R.M., 1983. Use of a proton precession magnetometer to detect buried drums in sandy soil. J. Hazard. Mater. **8**, 11-23.

US EPA, 2006. MSW characterization methodology introduction, 1-12.

Van Overmeeren, R.A. and Ritsema, I.L., 1988. “Continuous vertical electrical sounding”. First Break **6**, 313-324.

Vanhala, H., 1997. Mapping oil-contaminated sand and till with the spectral induced polarization (SIP) method. Geophysical Prospecting **45**, 303-326.

Vanhala, H. and Peltoniemi, M., 1992. Spectral IP studies of Finnish ore prospects. Geophysics **57**, 1545 - 1555.

Verduzco, B., Fairhead, J.D., Green, C.M., MacKenzie, C., 2004. The meter reader - new insights into magnetic derivatives for structural mapping. The Leading Edge **23**, 116-119.

Viezzoli, A., Pedersen, J. and Pytlich, A., 2008, Quantitative appraisal of noise in time domain induced polarization data. An extended abstract presented at the 14th Near Surface European Meeting of Environmental and Engineering Geophysics. Kraków, Poland, 15-17 September.

Vinegar, H.J. and Waxman, M.H., 1984. Induced polarization of shaly sands, Geophysics **49**, 1267-1287.

Vodounhessi, A., 2006. Financial and institutional challenges to make faecal sludge management integrated part of ecosan approach in West Africa. Case study of Kumasi, Ghana. MSc Thesis WM 2006.05, UNESCO-IHE Institute for Water Education, Delft, The Netherlands.

Weller, A., Slater, L., Nordsiek, S. and Ntarlagiannis, D., 2010. On the estimation of specific surface per unit pore volume from induced polarization: A robust empirical relation fits multiple data sets. Geophysics 75(4). WA105-WA112.

Wemegah, D.D., Fiandaca, G., Auken, E., Menyeh, A. and Danuor, S.K., 2014. Spectral time-domain IP and magnetic for mapping municipal solid waste deposits in Ghana. Extend abstract submitted at the 20th European Meeting of Environmental and Engineering Geophyiscs, Athens, Greece, 14-18 September 2014.

Wemegah, D.D., Fiandaca, G., Auken, E., Menyeh, A. and Danuor, S.K., 2015. Spectral time-domain induced polarization and magnetic surveying – an efficient tool for characterization of solid waste deposits in developing countries. (Accepted for publication Near Surface Geophysics).

Wildung, R.E. and Zachara, J.M., 1981. Effects of oil shale solid waste disposal on water quality: Current knowledge, information requirement, and research strategy. Proceedings in International Symposium, Colorado.

Williams, P.T., 2005. *Waste treatment and disposal*. John Wiley and Sons Ltd. Chippenham, Wiltshire, Great Britain.

Williams, K.H., Kemna, A., Wilkins, M., Druhan, J., Arntzen, V., Guessan, L.N., Long, P.E. Hubbard, S.S. and Banfield, J.F., 2009. Geophysical monitoring of coupled microbial and geochemical processes during stimulated subsurface bioremediation, Environ. Sci. Technol. **43**(17), 6717-6723.

Wilson, D.C., 2007. Development drivers for waste management. Waste Management and Research **25**, 198–207.

WMD-KMA, 2008, 2010, 2012. Waste management department annual report. KMA-WMD: Kumasi, Ghana.

Wright, E.P. and Burgess, W.G., (ed.s) 1992. The hydrogeology of crystalline basement aquifers in Africa. Geological Society Special Publication **66**, 1-27.

Wrighte, J.B., Hastings, D.A., Jones, W.B. and Williams, H.R., 1985. *Geology and mineral resources of West Africa*. Allen and Urwin, London, 165.

Wynn, J.C. 1986. Archaeological prospection: An introduction to the special Issue. Geophysics **51**(3), 533-537.

Yenigü, N.B., Elfeki, A.M.M., Gehrels, J.C., van den Akker, C., Hensbergen, A.T. and Michel, D.F., 2005. Reliability assessment of groundwater monitoring networks at landfill sites. Journal of Hydrology **308**, 1-17.

Zanoni, E.A., 1972. Groundwater pollution and sanitary landfills - A Critical Review. Ground Water **10**(1), 3-16.

Zurbrügg, C. and Schertenleib, R., 1998. Main problems and issues of municipal solid waste management in developing countries with emphasis on problems related to disposal by landfill. Presented at Third Swedish Landfill Research Symposia, Luleå, Sweden, October 1998.

Zume, J., Tarhule, T.A. and Christenson, S., 2006. Subsurface imaging of an abandoned solid waste landfill site in Norman, Oklahoma. Groundwater Monitoring and Remediation **26**, 62-69.

Appendices

Appendix 1: Publications

1. Wemegah, D.D., Fiandaca, G., Auken, E., Menyeh, A. and Danuor, S.K., 2015. Spectral time-domain induced polarization and magnetic surveying – an efficient tool for characterization of solid waste deposits in developing countries. Accepted for publication, Near Surface Geophysics.

Appendix 2: Conference Presentations

1 Wemegah, D.D., Fiandaca, G., Auken, E., Menyeh, A. and Danuor, S.K., 2015. Spectral time-domain induced polarization and magnetic surveying for mapping the decommissioned KNUST municipal solid waste deposit, Kumasi. 4th Ghana Science Association One Day Seminar, KNUST, Kumasi, 15th April, 2015.

2 Wemegah, D.D., Fiandaca, G., Auken, E., Menyeh, A. and Danuor, S.K., 2015. Spectral time-domain IP and magnetic survey for mapping the Ohwim municipal solid waste deposit. 4th Ghana Science Association One Day Seminar, KNUST, Kumasi, 15th April, 2015.

3 Wemegah, D.D., Fiandaca, G., Auken, E., Menyeh, A. and Danuor, S.K., 2014. Spectral time-domain IP and magnetic for mapping municipal solid waste deposits in Ghana. Extended abstract submitted at the 20th European Meeting of Environmental and Engineering Geophyiscs, Athens, Greece, 14-18 September 2014.

4 Wemegah D.D., Menyeh, A. and Danuor S.K., 2014. Geophysical application in pollution studies. Presentation at the 2nd Africa Geosciences student conference, KNUST, Kumasi, 20th – 24th May, 2014.